LAKE-INDUCED SNOWFALL ASSOCIATED WITH LAKES ERIE AND ONTARIO IN CMIP5 GCMS

by

Zachary J. Suriano

A thesis submitted to the Faculty of the University of Delaware in partial fulfillment of the requirements for the degree of Master of Science in Geography

Spring 2014

LAKE-INDUCED SNOWFALL ASSOCIATED WITH

LAKES ERIE AND ONTARIO IN CMIP5 GCMS

by

Zachary J. Suriano

Approved: ____
Daniel J. Leathers, Ph.D.
Professor in charge of thesis on behalf of the Advisory Committee

Approved: ____
Tracy L. DeLiberty, Ph.D.
Chair of the Department of Geography

Approved: ____
Nancy M. Targett, Ph.D.
Dean of the College of Earth, Ocean, and Environment

Approved: ____
James G. Richards, Ph.D.
Vice Provost for Graduate and Professional Education

ACKNOWLEDGMENTS

I would first like to thank the University of Delaware, and the Department of Geography for providing me the opportunity and funding to earn my degree and conduct this research. I would like to thank my advisor, Dan Leathers, for his support, insight, and guidance throughout the last two years. He is an excellent mentor and has helped me in more ways than I can acknowledge. I would also like to thank my other committee members, Sara Rauscher and Drew Ellis, for sharing their expertise and assisting in the review process. I owe a thank you to all of the graduate students within the department for their constant motivation that kept me working. Finally, thank you to my family and Lindsey, whose love and support made all of this possible.

TABLE OF CONTENTS

LIST OF TABLES

LIST OF FIGURES

ABSTRACT

In this study, an analysis of simulated lake-induced snowfall from 2006-2100 is conducted, investigating the presence of a lake-induced snowfall signal to the lee of Lakes Erie and Ontario. Output from seven fully coupled global climate models (GCM) s are used from phase five of the Coupled Model Intercomparison Project (CMIP5). Snowfall trends over the entire study area and in the defined lake-induced Snowbelt are examined seasonally for two Representative Concentration Pathway (RCP) scenarios. In addition, physical mechanisms associated with these trends, such as lake lapse rates, surface temperatures and snow to total precipitation ratios are examined.

The models perform well when compared to derived and observed snowfall observations despite model difficulties in resolving small scale orographic and finite lake effect processes. Snowfall declines by 20 – 45% over the entire region, with snowfall actually increasing in the lake-induced region during the first quarter century before declining rapidly in RCP 8.5. An additional 1.7 cm snow-water-equivalent (SWE) signal of purely lake-induced snowfall is detected within the ensemble mean of the defined lake-induced Snowbelt to the lee of the two lakes that is not seen in the grid cells outside of the lake belt. Surface two-meter temperature is found to have the most significant impact on snowfall changes in the region, with impacts not on total precipitation, but on the percentage of precipitation falling as snow. Lake lapse rates were found to not provide enough evidence to draw useful conclusions on snowfall trends.

Chapter 1

INTRODUCTION

The Laurentian Great Lakes generate large quantities of lake effect snow where on average the lake effect contributes between 10 and 50 percent of the total regional winter precipitation in the surrounding region (Norton and Bolsenga 1993; Scott and Huff 1996). Over the past century, both overall and lake effect snowfall have increased across the region (Leathers et al. 1993; Norton and Bolsenga 1993; Leathers and Ellis 1996; Burnett et al. 2003; Ellis and Johnson 2004; Kunkel et al 2009). As the climate continues to change into the future, it is unclear if this trend will continue or if there will be a decline in lake effect snowfall associated with potential atmospheric warming. Due to the large impact this snowfall has on the economy and hydrology of the region, it is important to have a better understanding of the methods available for diagnosing the potential impact of changes into the future. The term "lake-induced snowfall" is used to encompass both lake effect snow along with lake-enhanced snow and is further explained within the methodology. This study seeks to identify a potential lake-induced snowfall signal to the lee of Lakes Erie and Ontario using Global Climate Model projections. If a signal is present, regional snowfall trends, and the mechanisms behind them will be examined into the 21st century.

1.1 Lake Effect Snow and its Impact

The Laurentian Great Lakes, and their total water surface area of over 240,000 km^2, exert a substantial influence on the climate of the surrounding region, particularly relating to snowfall. Due to their large thermal capacity and geographic location, the Great Lakes produce considerably higher amounts of lake-induced snowfall on their immediate leeward shores than in locations further inland. An inland site may receive upwards of half of the snowfall than a site within the lake's influence (Norton and Bolsenga 1993). The snow primarily forms during the late fall and winter months as the warm waters of the lake destabilize the boundary layer of wintertime arctic air masses moving over the lakes (Eichenlaub 1979). The height and strength of this destabilized boundary layer is proportional to the vertical extent of the convective cloud band development and downwind snowfall, with deeper and less stable layers resulting in stronger convection (Niziol et al. 1995).

The creation of the atmospheric instability is the most critical process in the formation of lake effect events (Kristovich et al. 2003). Typically, a temperature difference, or lapse rate, between the lake surface and 850hPa of at least 13°C is necessary to produce lake effect snow or closer to 10°C when synoptic situations, such as a mid-latitude cyclone, are supportive (Holroyd 1971; Niziol et al. 1995). This lapse rate is very important in the development of snow bands, and small differences of only 2°C can result in a 30-40 percent difference in snowfall totals (Topics in Lake Effect Forecasting 2005, https://www.meted.ucar.edu). The development of a lake lapse rate can be affected by the presence of ice on the lake surface. As more lake ice develops, there is a documented decline in the sensible and latent heat fluxes, and an associated decrease in lake effect snow band formation (Braham and Dungey 1984; Niziol et al. 1995). Sensible heat fluxes generally remain constant below 70% ice coverage, while there is a linear decrease in the latent heat flux with ice coverage, supporting the claim for higher fluxes of energy with less ice (Gerbush et al. 2008).

If there is boundary layer instability, a lifting mechanism also needs to be present along with winds suitable for the development of significant lake effect snowfall. Uplift can be achieved strictly through instability, but it is often enhanced through frictional and thermal convergence over the lake, or orographically on shore by the presence of topographic features such as the Allegheny and Tug Hill Plateaus in New York State. Uplift strength is associated with the winds over the lakes, specifically with regards to the steering wind's speed, shear, and fetch. Wind shear throughout the column of air has an optimal level of less than 30° of directional shear. When higher levels develop, the bands become less organized and can begin to decay (Niziol et al. 1995). Ideal wind speed falls within 15-20 m/s for maximizing parcel residence time along with sensible and latent heat fluxes over the lake (Topics in Lake Effect Snow Forecasting 2005, https://www.meted.ucar.edu). When speeds are too high, bands are unlikely to develop, while with speeds less than 5 m/s, land breezes tend to dominate and minimal snowfall develops (Niziol et al. 1995). The fetch, or distance the arctic air travels over the open water, is the final component of the wind that controls snowfall. Fetch can have substantial effects on the type of snow band that develops. It is typically determined by the wind direction at 850 hPa, with a minimum fetch threshold often set at 80km for snowfall (Topics in Lake Effect Snow Forecasting 2005, https://www.meted.ucar.edu). All else being equal, a larger fetch will produce stronger convergence and more snowfall than a smaller fetch.

Lake effect snow band(s) develop into long, thin structures that range from 5-50 km wide, by 20-200 km long depending on the specific formation (Hill 1971; Orlanski 1975). Hjelmfelt (1990) and Niziol et al. (1995) described five different types of snow bands that can develop downwind of the Great Lakes, with some bands capable of producing as much as 150-250 cm of snow in a single event downwind of the body of water (Niziol 1989) (Figure 1.1). Each of the different types produces different levels of snowfall intensity and often impact different parts of the lake's shore. Type I snow bands are observed when the winds are blowing parallel to the long axis of the lake and long fetches are achieved. These bands are the most convectively active and thus have the most intense precipitation, with snowfall rates exceeding 10 cm per hour (Moore and Orville 1990). Type I bands often extend far inland, upwards of 200 km, but with a narrow width often less than 50 km. Type II bands, or "multi-bands" are also parallel wind bands but develop under short-fetch conditions, such as perpendicular to the long axis of the lake. This shorter fetch limits the fluxes from the lake and changes the convergence strength such that multiple, less intense bands form via horizontal roll convection. The multiple bands can penetrate upwards of 50 km inland but bring less intense snowfall than Type I bands. Type III is a hybrid of the first two types that results from upwind connections to other lakes such as Huron or the Georgian Bay (Byrd et al. 1992). The Type I band develops upwind and propagates downstream to the Eastern Lakes and redevelops into Type II bands. The extent is similar to Type II bands with snowfall rates between those of Types I and II. The opposite can also occur with Type II transition into a Type I. Type IV bands are the result of land breezes and are shore-parallel bands that develop in slow wind conditions of less than 5 m/s. This type is associated with low intensity snowfall and do not move inland more than a few kilometers. Despite the low intensity of snowfall associated with this type, they can still lead to moderate accumulations due to their slow moving nature. Type V bands are referred to as "meso-scale vortices" and are the product of the lake shore geometry. The band develops into a vortex cloud structure with spiral armbands that typically produce low snowfall rates compared to the other lake effect types.

An additional consideration is the presence of lake-enhanced snowfall that occurs downwind of the lakes. Defined as snow falling in association with a synoptic scale system that is enhanced by the underlying lake fluxes, lake-enhanced snowfall can be difficult to differentiate from synoptic snowfall in some cases (Eichenlaub 1979; Tardy 2000). Such events have broad regions of snowfall with areas of higher totals located downwind of the lakes. Other instances of lake-enhancement can come from weak synoptic scale motions such as warm advection or positive vorticity advection aiding in uplift (Eichenlaub 1979; Tardy 2000; Chuang and Sousounis 2003). A situation like this will contribute to precipitation development and allow for less than favorable atmospheric conditions, such as a weak lapse rate, to become snow producing events.

Snowstorms influenced by the Great Lakes in any form are capable of causing significant damage to infrastructure in the surrounding region. Lake effect snow processes have strong negative impacts on automobile traffic patterns and accidents, air travel, snow-removal costs and injuries, disruption to local retail sales, along with destruction of personal property and residences (Norton and Bolsenga 1993;

Schmidlin 1993; Kunkel et al. 2002). Agriculture can also be strongly impacted during the winter months specifically the New York wine vineyards located within lake effect regions (Norton and Bolsenga 1993). When the snow begins to melt, extensive flooding can occur in regions of excess snow pack leading to loss of life and destruction of property (Changnon et al. 2006). Increased snowfall can, however, benefit specific sectors of the economy including winter season recreational businesses, winter product transactions, and even private snow removal companies (Schmidlin 1993; Kunkel et al. 2002).

1.2 Snowfall Trends

The behavior of Great Lakes snowfall in the last 75 years has been well documented in the literature, qualitatively outlined in Table 1.1 (Leathers et al 1993; Norton and Bolsenga 1993; Leathers and Ellis 1996; Burnett et al. 2003, Ellis and Johnson 2004; Kunkel et al. 2009). While not focusing on the Great Lakes region specifically, Leathers et al. (1993) found wintertime snowfall increased from 1945-1985 to the lee of Lakes Erie and Ontario. Norton and Bolsenga (1993) similarly found increases in snowfall from 1951-1980 across the entire Great Lakes basin including areas east of Lake Ontario.

Using a synoptic climatological approach, Leathers and Ellis (1996) found an increase in the frequency of winter circulation patterns most often associated with lake effect snow that can explain upwards of 60% of the increases in snowfall to the lee of Lakes Erie and Ontario. Burnett et al. (2003) followed a different approach by examining specific snowfall sites and comparing “lake effect sites” to “non-lake effect sites." They also concluded that east of Lake Erie and Lake Ontario; there has been an increase of lake effect snow for a longer period, ranging from 1931-2001. Ellis and Johnson (2004) saw increased snowfall at sites east of Lake Ontario, with rate increases between 1.5-3 cm per year from 1932-1971, followed by very little trend from 1972 to 2001. Kunkel et al. (2009) found varying trends depending on the period of analysis. For Lake Erie, from 1925 to 2007, there was a statistically significant increase in snowfall but for Lake Ontario, there was no statistically significant trend for the same period.

The factors that can greatly impact lake effect trends fall under three main categories: atmospheric temperatures, water temperatures, and lake ice. Increasing surface and atmospheric temperatures will conceptually result in a northerly shift in the rain/snow line. This potentially results in temperatures being too warm for snow to reach the surface and could cause an extension of the lake-effect rain season into the later fall months (Figure 1.2). By examining the newest Intergovernmental Panel on Climate Change (IPCC), Assessment Report Five (AR5), the average global surface temperature of 2003-2012 has increased by approximately 0.78°C from the 1850-1900 mean, with a similar trend in the Great Lakes region (Stocker et al. 2013). Looking into the future, the AR5 suggests with "likely" confidence (66-100%), a mean global temperature increase of 1.1°C to 4.8°C relative to the 1986-2005 mean, and a mean atmospheric temperature increase in the Great Lakes region of approximate 2°C to 5°C by the end of the century (Collins et al. 2013).

These temperature changes alone would likely lead to a decrease in future lake effect snowfall. However, as temperatures increase, lake waters warm with accompanying decreases in ice formation, which has been shown to increase lake effect snowfall (Burnett et al. 2003; Wright et al. 2013). Trumpickas et al. (2009) found a projected increase of lake surface temperatures of 0.9°C to 4.8°C for Lakes Erie and Ontario by the end of the century in their analysis of model data. The increase in lake and surface temperature directly determines the amount of ice formation that can occur on the lakes. Ice cover and thickness have decreased over the Great Lakes Region from 1963 through 2001 (Assel et al. 2003; Assel 2005).

Based on these observations and projections, it is reasonable to conclude lake effect snow may change in the future. A rational hypothesis is that lake effect snow will increase due to warmer lake waters and less ice formation until atmospheric temperatures become too warm for precipitation to consistently fall as snow.

1.3 Previous Methodologies

There have been a limited number of studies that have examined potential future changes in lake effect or lake-induced snowfall (Cohen and Allsopp 1988; Kunkel et al. 2002; Gula and Peltier 2012; Krasting et al. 2013). Cohen and Allsopp (1988) used an adaptation of the Goddard Institute for Space Studies (GISS) Global Climate Model (GCM) under a 2 x CO_2 scenario with a specific study region of Southern Canada. When the 2 x CO_2 scenario was compared to the 1 x CO_2 scenario, they found there was a mean winter snowfall decline of 60-70% along the northern shore of Lake Ontario and on the Niagara Peninsula, along with a 60-90% decline in southwestern Ontario. Kunkel et al. (2002) expanded on this work, examining the future lake effect potential for Lake Erie using downscaled data from two GCMs: the second-generation Hadley Centre model and the first generation Canadian Climate Centre coupled atmosphere-ocean model. Despite uncertainties involving the models' treatment of the lake, Kunkel et al. (2002) found a 50-90% decrease in the frequency of surface conditions associated with heavy lake effect snow by the late 21st century. In comparison, Gula and Peltier (2012) used the Weather Research and Forecasting model (WRF) as means to dynamically downscale global projections from the Community Climate System Model (CCSM) version 3. They found with this method, for the decade 2050-2060 there was an increase in snowfall compared to 1979-2001 in some areas to the lee of the lakes. However, there were also areas showing slight decreases or no change. Krasting et al. (2013) employed the use of 18 atmosphere-ocean coupled GCMs, part of the Coupled Model Intercomparison Project version 5 (CMIP5), to examine snowfall across the entire northern hemisphere. While Krasting et al. (2013) did not focus on the Great Lakes region specifically; general trends can be examined in their results. They projected a winter-season decline of approximately 3-6 cm per decade for the period 2006-2100.

1.4 Summary

While a number of studies have examined future snowfall trends over the Great Lakes, an analysis of lake-induced snowfall has not been conducted. This study investigates the potential presence of a snowfall signal to the lee of Lake Erie and Lake Ontario from 2006 to 2100 through the use of data from 7 different coupled GCMs from CMIP5. Grid cells within the models are classified as a lake-induced or as the non-lake-induced grids to determine if the models are capable of resolving any snowfall induced by the lakes. This information can then be used to examine snowfall trends for both the overall region and within the lake-induced belt. Finally, the physical mechanisms associated with these trends are examined including the lapse rate over the lakes and the ratio of snow to total precipitation over time.

Table 1.1. Summary of 20th century snowfall trends for Lakes Erie and Ontario.

Study	Time Period	Snowfall Trend
Leathers et al (1993)	1945-1985	Increase
Norton and Bolsenga (1993)	1951-1980	Increase
Leathers and Ellis (1996)	1951-1982	Increase
Burnett et al. (2003)	1931-2001	Increase
Ellis and Johnson (2004)	1932-1971	Increase
	1972-2001	No trend
Kunkel et al. (2009)	1925-2007	Increase

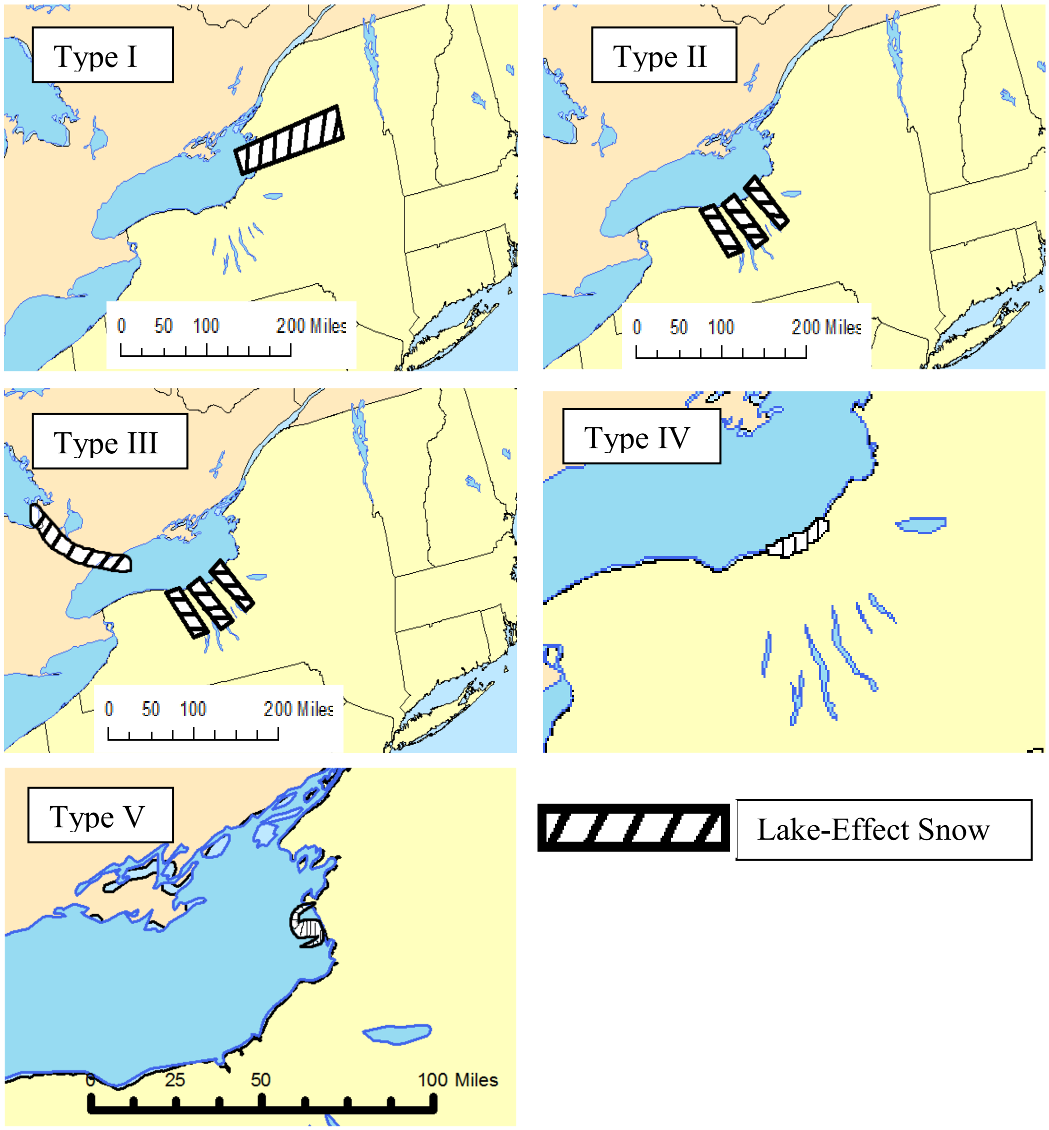

Figure 1.1. Lake effect snow bands as described in Niziol et al. (1995).

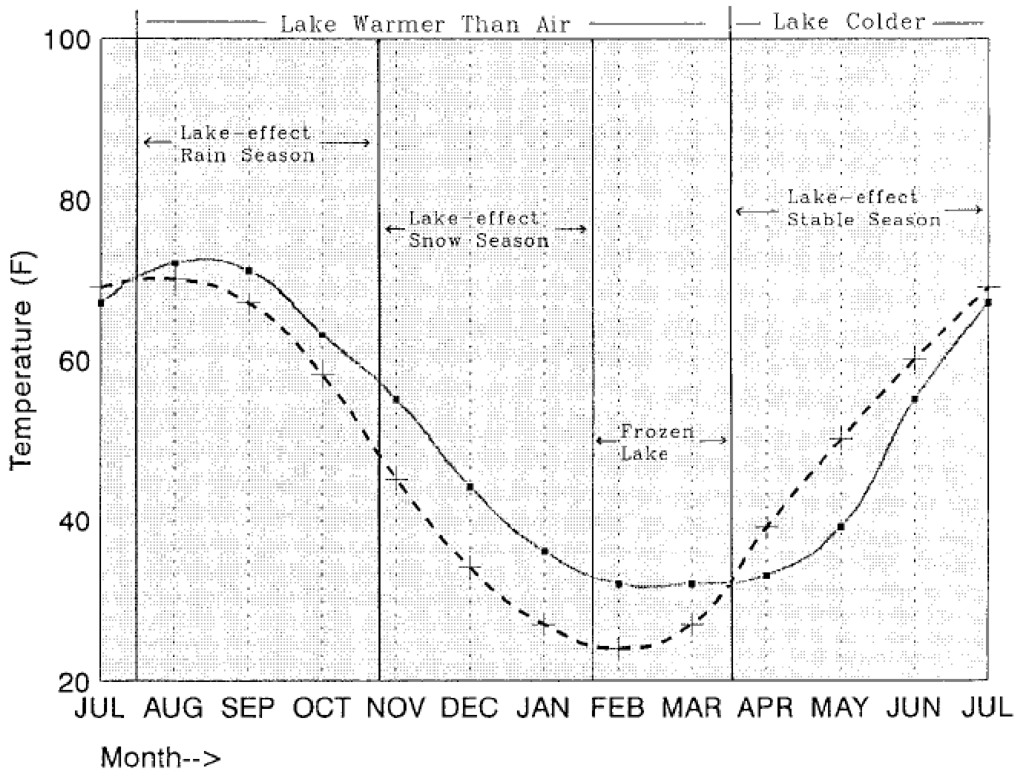

Figure 1.2. Lake effect seasons downwind of Lake Erie (NWS Buffalo, New York 1987; Miner and Fritsch 1997).

Chapter 2

DATA AND METHODS

2.1 Study Area

The study area is a rectangular region bounded approximately by 40 degrees north latitude, 45 degrees north latitude, 85 degrees west longitude, and 72.5 degrees west longitude (Figure 2.1). This area encompasses the eastern Great Lakes region including the entire states of New York and Pennsylvania, along with parts of Ohio, West Virginia, Indiana, Michigan, Ontario, and New England and stretches to the Atlantic coast of New Jersey. Coordinates are approximate due to the varying model resolutions. Model grid cells were chosen to best represent the above coordinates. The focal point of the gridded coordinates is the western most portion of New York State as to include both Lakes Erie and Ontario in the region while leaving a large number of grid cells downwind of the lakes for study.

2.2 The Models

The analysis utilizes the output from model runs using two standardized experimental designs from the World Climate Research Programme's (WCRP) Coupled Model Intercomparison Project version 5 (CMIP5) (Taylor et al. 2012). The model data was downloaded from the Program for Climate Model Diagnosis and Intercomparison (PCMDI) web portal (http://cmip-pcmdi.llnl.gov/cmip5/data_portal.

html). The two simulations were based on the Representative Concentration Pathways (RCPs) forcing scenarios, created by the IPCC for AR5 (Moss et al. 2010). Four RCPs, each representing a range of possible radiative forcing values in the year 2100 relative to preindustrial levels, were used for simulations. These are based on a variety of factors including global emissions, forms of energy consumption, economic and social scenarios, and technological advancements (Moss et al. 2010). RCP 4.5 and 8.5 were chosen for this study to represent a range of possible scenarios looking towards the end of the 21st century.

This study uses seven fully coupled climate models (Table 2.1) and while many models had multiple ensemble members within each scenario, only one was used (r1i1p1). Specific models were chosen based on their treatment of physical lake surfaces, horizontal resolution, determination of precipitation type, and how well they simulate snowfall. As of the fall of 2012, there was no overarching study that had examined the ability of CMIP5 models to portray snowfall accurately. The models' capacity to represent snowfall in the study region is estimated based on previous versions outlined in the literature (Anandhi et al. 2011) in addition to the later work by Krasting et al. (2013).

There is some variety in the manner in which the models determine precipitation type, along with how lake surfaces are treated. Some of the models use a temperature based diagnostic scheme where below freezing temperatures in layers closest to the surface yielded precipitation falling as snow. Other models however are capable of representing ice, graupel, and clouds of mixed-phase into their microphysical schemes. This improvement to the schemes allow for precipitation type to be determined at time of condensation in the cloud; then as the hydrometeor falls, its mass can be converted from phase to phase depending on the temperature of the surrounding layer (Krasting et al. 2013).

The determination of the models' lake surface conditions is where the models differ the most in terms of processes important to lake-induced snow. Model treatments range from a coupled lake model, to a land model that has no representation of lake surfaces within it. Table 2.2 briefly summarizes the different models' treatment of the lakes with regards to their ice treatment, lake dynamics, dynamic lake extent and the presence of specific grid points defined for the Great Lakes. The IPSL and the HAD models have the least realistic representation of the lake surfaces. IPSL does not have a representation of a lake within its ORCHIDEE land surface model, and for its soil moisture calculations embedded within the SECHIBA hydrologic model, only 2 layers of soil are present (Lafont et al. 2012; Dufresne et al. manuscript; Krinner et al. 2005). The calculation of soil evaporation is via a bulk aerodynamic method using humidity and soil resistance however, once the top layer of soil is saturated, runoff occurs (Ducoudre et al. 1993). With an optional pond or floodplain module, first order simulations for small ponds that re-evaporate surface runoff and are re-infiltrated back into the soil as a different rate, but does not allow for a large pond or lake to be a land surface type (d'Orgeval et al. 2008). The HAD model has lakes represented as a fixed, specific fraction of a particular grid box that only provide a water source for evaporation and do not attempt to prognostically simulate water depth, storage or areal extent (Essery et al. 2003; Cox et al. 1999). The removal of evaporated water from the lakes occurs from the four-layer soil, when moisture is greater than the wilting point (Collins et al. 2008).

The MPI, CSIRO, GFDL and CESM models all have similar approaches, allowing the lake surfaces to freeze and thaw. The differences lie in how the models handle lake dynamics. MPI does not contain any lake dynamics and treats the ice formation with an "all or nothing" scheme where an ice to water fraction above 50%, receives a value of 100% and a value below 50% is given a value of zero ice cover (Roeckner et al. 2003). Ice formation is restricted until a layer of at least 0.1 m in thickness forms. Embedded within the CSIRO model are specific grid points for the Great Lakes (Figure 2.2) that allow those grids to behave more realistically, along with subroutines "surfa" and "surfa_riv" that allow ice fraction and temperature to be calculated (Gordon et al. 2002; Gordon et al. 2010). GFDL's model does have an ice formation scheme that allows the lakes to exchange mass and energy to the atmosphere and rivers, accounting for sensible heat fluxes across all phases (Donner et al. 2011). The CESM model has a more detailed yet simplistic lake model embedded within the land model where with constant lake water and extent, temperature is solved via surface fluxes in a 10-layer lake with an initialized temperature of 277K (Olsen et al. 2010; Neale et al. 2010). Based on the surface and lake temperatures, ice formation can occur.

GISS-E2-H seems to have the most realistic model representation of the lake surfaces that includes seasonal cycling of the lake waters, variable lake extent depending on specific conditions of the hydrologic cycle, and temperature determinants that allow for ice formation (Schmidt et al. 2014). Despite improvements and a reduction of ice cover by 20 to 50 days, ice conditions on mid-latitude lakes are still not tuned to the annual cycle, with an approximate phasing bias of a month (Schmidt et al. 2014).

2.3 Model Data and Grid Cell Declaration

Five different variables were examined from the model output for this study; snowfall flux (PRSN), total precipitation flux (PR), surface (skin) temperature (TS), 850 hPa temperature (TA), and two-meter temperature (TAS). PRSN is representative of all frozen types of precipitation while PR accounts for all types of precipitation whether that is frozen, convective or stratiform. Both PRSN and PR data originate in units of kilograms per square meter per second. To make these values more useful, they were converted from the flux to a depth of liquid water or snow water equivalent (SWE) in centimeters per month.

A critical component for this study is in the determination of each grid cell's classification. For the temperature portion of the study, the determination of a lake or non-lake cell is important. Cells considered a lake cell are used in the calculation of the surface to 850 hPa lapse rates, which serves as an indicator for lake effect snowfall potential. This was determined using a combination of two methods. First, if the models themselves declare specific grid cells to be Great Lakes cells, those cells were used, as in the case of the CSIRO model. If not declared specifically, grid cells containing a large percentage of Lakes Erie or Ontario within them were used as a "lake grid cell" in calculation of the lake lapse rate. Even if the grid cell is not composed entirely of lake surface in the model, with a large proportion being lake, an estimate of a lake lapse rate can still be determined from the model. Grid cells of each model were deemed “lake cells” or not, with teal and green used to represent the determination of Lake Erie and Lake Ontario respectively (Figure 2.3 a-g).

For the snowfall portion of the analysis, knowledge of whether a grid cell falls within the lake-induced snowfall belt or not is equally essential. With the assumption that an average synoptic snowfall system will have near equal snowfall amounts across neighboring grid cells, subtracting the snowfall of grid cells not in the lake-induced belt from the snowfall of cells in the lake-induced belt will eliminate the synoptic snowfall, leaving just a lake-induced snowfall total. Burnett et al. (2003) used a similar method of determining lake effect snowfall trend, looking at individual locations that fell within and outside of the lake snow belt.

The declaration of the lake-induced belt and non-lake-induced grid cells for the models is slightly more complicated than that of the lake surfaces. The primary determination of the lake-induced belt used here is based on Karmosky (2007). In this study, he classified the snowfall that fell in the Northeastern United States based on the synoptic situation, and broke situations down into three types: lake effect, synoptic, and ocean effect. His results also divided the study region into an approximate 1x1 degree gridded area showing the percentage of snowfall considered lake effect for each grid cell (Figure 2.4). This is the primary consideration for the lake-induced belt versus non-lake-induced grid cell differentiation used here. For a cell to be considered “lake-induced”, at least 25% of its seasonal snowfall had to be from lake processes (Karmosky 2007). The cutoff results in a lake-induced belt that is slightly larger than the lake effect belt defined in other literature. The traditional lake belt is approximately 80-100 km off the lakeshore (Figure 2.5) (Eichenlaub 1970; Dewey 1979; Norton and Bolsenga 1993; Scott and Huff 1996). A larger lake-induced snowfall belt is used to account for both lake-enhanced processes that can have a larger inland extent, along with traditional lake effect processes. Due to the horizontal resolution of the models used, they are unable to resolve traditional lake effect processes in a robust manner. To account for the models' relatively coarse resolution, this study combines "lake effect" snowfall and "lake-enhanced" snowfall into a single term, lake-induced snowfall.

Additionally, due to the focus on Lakes Erie and Ontario, any grid cells in which the other Great Lakes have a strong influence were classified as "Western Lake-Induced" and subsequently omitted from the analysis. This resulted in a majority of the grid cells to the north and west of Lakes Erie and Ontario falling under this classification for each model. Grid cells are determined for each model with blue shading represents the lake-induced belt cells, red shading represents non-lake-induced grid cells, and gray shading represents grid cells that were removed from the study due to the potential for lake-induced processes from the western Great Lakes (Michigan, Huron and Superior) (Figure 2.6 a-g).

2.4 Data Processing and Calculations

All of the variables in the original output had a single value representative of each grid cell for each month of the study period, from 2006 to 2100. To prevent unnecessary calculations and save on memory storage, a simple latitude and longitude test filtered the data to obtain values found within the study area. For precipitation specific variables (PRSN, PR) the monthly values were averaged by grid cell classification into lake-induced, non-lake-induced and western lake-induced types. This resulted in having only three values for each month for each model that were a representative average of the classification types. For temperature specific variables, the same process is conducted however here; the only classification of interest is lake or non-lake cell.

This study assumes a lake-induced season from October to March based on lake effect, lake-enhanced, and overall snow potential (Norton and Bolsenga 1993; Niziol et al. 1995; Notaro et al. 2013). The values for each respective variable are averaged across those months to yield a single seasonal value for each year across all models. This is done using the October, November and December values of year "x" and averaging them with January, February and March of year "x+1", with the year label of "x+1". A majority of the analysis takes place with this seasonal data. An ensemble mean, or mean of all of the models seasonal data is also calculated for all variables discussed above, and analyzed to provide an overall model projection that can easily be compared between diverse RCPs or with other studies.

2.5 Observational Data

2.5.1 Snowfall

Comparing model data to observations is a critical step in validation of the models. In this study, modeled snowfall, air and lake surface temperatures are compared to observations from a variety of sources. As outlined in Krasting et al. (2013), snowfall can be derived using temperature and precipitation climatologies. Using an empirical relationship between the ratio of snow and precipitation, determined by monthly two-meter temperature (Cehak-Trock 1958; Legates 1987; Rawlins et al. 2006), equation (1) is applied to the observational data set, where f represents the monthly mean ratio of total precipitation falling as snow and T is the monthly mean two-meter temperature.

$$f = \frac{1.0}{1.0+1.61 \times (1.35)^{T}} \tag{1}$$

The observational data used in the study is from the University of Delaware Global Surface Air Temperature and Precipitation Climatology, version 3.01 (Willmott and Matsuura 2014a,b). While full documentation is available (Willmott and Matsuura 2014a,b) version 3.01 of the Willmott-Matsuura climatology incorporates a number of station data sources including the Global Historical Climatology Network, the Global Surface Summary of Day, and station climatologies from Legates and Willmott (1990). The station values of monthly variables were interpolated to a 0.5 degree by 0.5 degree latitude and longitude grid via the spherical version of Shepard's algorithm, using an enhanced distance-weighting method (Shepard 1968; Willmott et al. 1985). Derived values were not converted to a snowfall measurement but left as SWE values.

The 30-year climatology of derived snowfall depicts a meridional gradient of seasonal (October-March) snowfall (SWE) across the study region (Figure 2.7), with higher values found to the east, and a maximum of 22.84 cm in southern Quebec. Each model's seasonal snowfall from 2006 – 2015 is spatially compared to the observed 30 year normal data from the derived Willmott-Matsuura data set (Figure 2.8). The meridional gradient in the derived snowfall data is supported by Krasting et al. (2013)'s work which shows a similar spatial pattern over the 55-year period relevant to this study. Their analyses show a slight negative snowfall bias over the region east of Lakes Erie and Ontario in their ensemble mean relative to the observed data set (Figure 2.9). They conclude that the patterns of relative maxima and minima are well represented by the models. One cautionary note is discussed regarding the lack of horizontal resolution in the models, making the models unable to resolve fine orographic features or robust lake-effect snow conditions (Krasting et al. 2013). This statement also holds true for this study.

Further comparisons of snowfall simulations to observations were made using a gridded snowfall dataset derived from an expansive set of Cooperative Observer Program (CO-OP) data from the National Weather Service (Kluver 2007). Kluver's (2007) data set is a 1 by 1 degree gridded result for the mean snowfall over the Northeast United States from 1949 to 1999 (Figure 2.10). Areas of higher snowfall are present downwind of Lake Erie and Lake Ontario. Downwind of Lake Erie, annual snowfall totals are in the range of 200-240 cm. Local maxima in snowfall are east of Lake Ontario along the Tug Hill Plateau and the Adirondack Mountains in

New York State, as a result of elevation and marginal ice formation on the lake. Snowfall values exceed 300 cm annually as a result of orographic uplift, in addition to lake effect snow impacting the area. High snowfall values are also prsent along the mountains in West Virginia due to lake-enhancement processes with the increase in elevation, and downwind of the other Great Lakes as a result of lake effect. Finally, areas in Maine and north into Quebec see broad spatial areas with high snowfall totals of 300 cm or more.

A similar distribution of SWE is seen in the models from 2006 to 2015, with areas of higher values downwind of both Lakes Erie and Ontario, in northern New England into Quebec, and in areas downwind of the other Great Lakes. For comparison purposes in this section only, for reasons explained in the following chapter, a 10:1snow to liquid precipitation ratio (Krasting et al. 2013) was used to convert the SWE model simulations to snowfall in cm. The magnitude of snowfall in the model simulations, in the areas downwind of Lake Ontario from 2006-2015, ranges approximately 160 – 280 cm of snow, depending on the model. Downwind of Lake Erie, snowfall values of 100 – 220 cm are seen within the models. These simulated values are lower than the observed snowfall values however this is not unexpected. Just as with the Willmott-Matsuura climatological comparisons, the models are unable to resolve traditional lake effect processes robustly. With traditional lake effect contributing between 10 and 50% of annual snowfall in these regions (Norton and Bolsenga 1993; Scott and Huff 1996) and a lack of traditional lake effect processes being resolved, one would expect modeled snowfall to be less than observed values. Additionally, with this observed data set encompassing a 52-

year period during which increases in snowfall were noted, annually averaged snowfall values should not be compared directly without some caution.

On the whole, the simulated snowfall data has a similar spatial pattern to both the derived and observed snowfall patterns in the study region. While the magnitude of snow is less in the models due to issues resolving small scale processes effectively, the models still are able to capture snowfall magnitude reasonably well.

2.5.2 Lapse rates

When validating the models lapse rates relative to observations, the National Centers for Environmental Prediction (NCEP) Reanalysis (Version 2) dataset is used (Compo et al. 2011). The dataset was provided by the NOAA/OAR/ESRL PSD, Boulder, Colorado, USA, from their website at http://www.esrl.noaa.gov/psd/. Atmospheric temperatures at 850 hPa are averaged over the individual lakes and because of the available horizontal resolution, were given a single value over the entire lake for the normal period of 1981-2010. The same process is completed for the surface skin temperature, the proxy for lake temperature, using the same dataset. Over the two lakes, the lapse rates were quite similar, with temperature differences of 4.55 K between the surface and 850 hPa for Lake Ontario, and 4.75 K between the two levels for Lake Erie. These values are within a degree of the models' simulated lapse rates for the period 2006 – 2015. For Lake Ontario and Lake Erie, the ensemble averaged temperature difference is 5.15 and 5.35 K, suggesting that the models are slightly more unstable during this period than observations by about 0.6 K. However it should be noted that examining the physical lake temperatures from the Great Lakes

Research Lab (GLRL), both the models and the NCEP Reanalysis data have considerable cold biases relative to the GLRL dataset. Averaged over the period 1992-2012 (the length of record), during the season of study, lake surface temperatures for Erie and Ontario were 279.2 and 278.9 K respectfully, compared to approximately 276.3 and 273.4 K for NCEP Reanalysis and 275.0 and 273.1K for the model ensemble. The colder surface temperature bias results in a less than observed lapse rate. This should result in the models being less successful in simulating lake-induced snow processes with a more stable model-simulated environment present.

Table 2.1. List of CMIP5 models used in this study, with full expansions.

Model Name	Expansion	Resolution (°Lat x °Lon)
CESM1-CAM5	National Center for Atmospheric Research Community Earth System Model version 1.0, Community Atmospheric Model version 5.0	0.9375 x 1.25
CSIRO-Mk3.6	Commonwealth Scientific and Industrial Research Organization Mark, version 3.6.0	1.875 x 1.875
GFDL-ESM2M	Geophysical Fluid Dynamics Laboratory Earth System Model with Modular Ocean Model 4 (MOM4) component (ESM2M)	2.0 x 2.5
GISS-E2-H	Goddard Institute for Space Studies Model E, coupled with the HYCOM ocean model	2.0 x 2.5
HAD-GEM2-ES	Hadley Centre Global Environment Model, version 2 – Earth System	1.24 x 1.875
IPSL-CM5A-MR	Institut Pierre Simon Laplace Climate Model, version 5A, Medium Resolution	1.25 x 2.5
MPI-ES-MR	Max Planck Institute Earth System Model, Medium resolution	1.875 x 1.875

Table 2.2. Model lake treatments.

Model	**Freeze/Thaw**	**Lake Dynamics**	**Dynamic Extent**	**Special Great Lakes Surface**
CESM	YES	YES	NO	NO
CSIRO	YES	YES	NO	YES
GFDL	YES	YES	NO	NO
GISS	YES	YES	YES	NO
HAD	NO	NO	NO	NO
IPSL	NO	NO	NO	NO
MPI	YES	NO	NO	NO

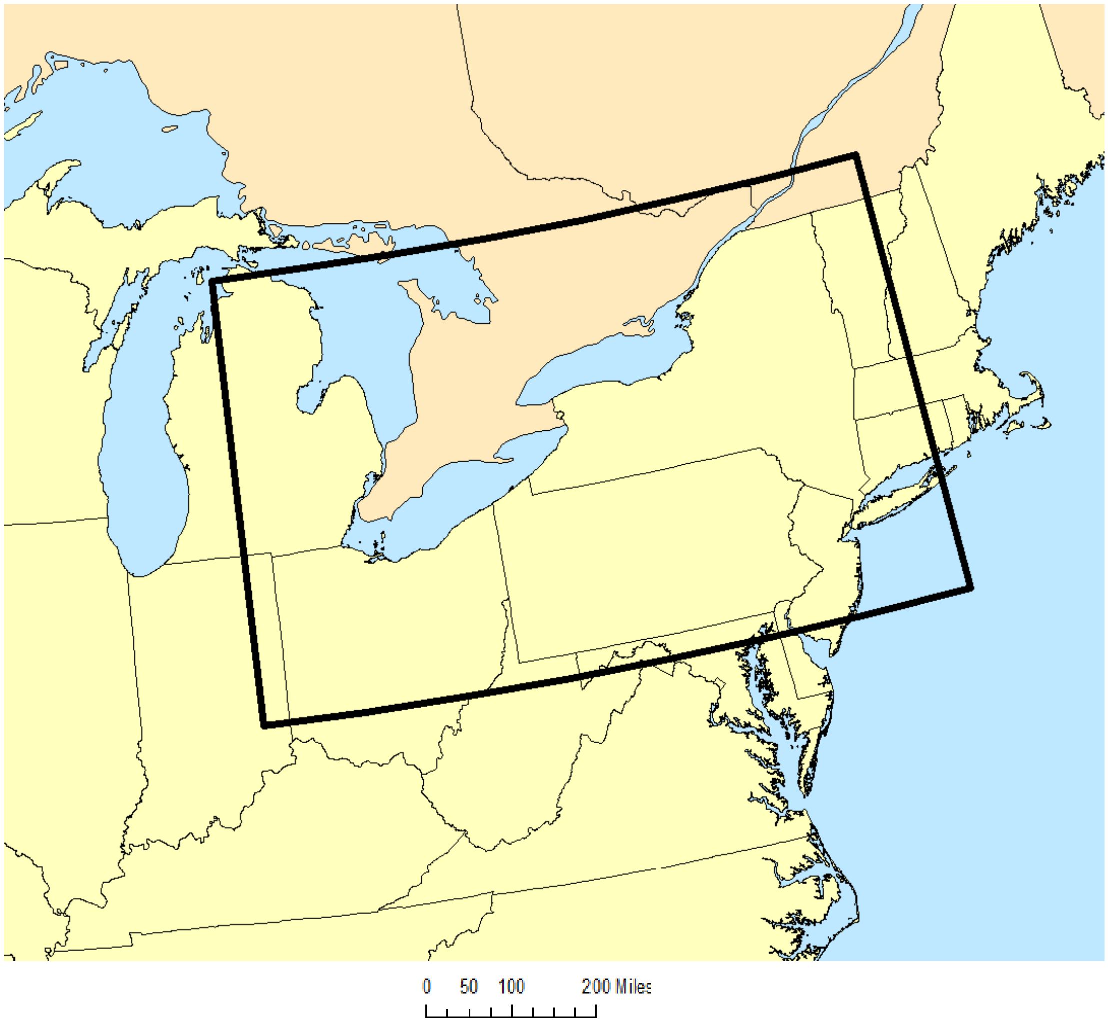

Figure 2.1. Study area encompassing approximately 40 to 45 °N and 72.5 to 85°W.

```
(i=) 144 145 146 147 148 149 150 151 152 153
   -+---+---+---+---+---+---+---+---+---+---+-
    |   |  Superior |   |   |   |   |   |   | (j=)
    | . | L | L | L | . | . | . | . | . | . |  74
    |   |194.   |195|   |   |   |   |   |   |
   -+---+---+---+---+---+---+---+---+---+---+-
    |   |   |   M   |   Huron   |   |   |   |
    | . | . | . i L | L | L | L | . | . | . |  73
    |   |   |   c   |   |   |185|   |   |   |
   -+---+---+---h---+---+---+---+---+---+---+-
    |   |   |   i   |   |   |   |  Ontario  |
    | . | . | . g L | . | L | . | . | L | . |  72
    |   |   |   a   |   |   |   |   |176|   |
   -+---+---|---n---+---+---+---+---+---+---+-
    |   |   |   |   |   | Erie  |   |   |   |
    | . | . | . | . | . | L | L | . | . | . |  71
    |   |   |   |   |   |166|   |   |   |   |
   -+---+---+---+---+---+---+---+---+---+---+-
```

Figure 2.2. Specific Great Lakes grid points in CSIRO (Gordon et al. 2010).

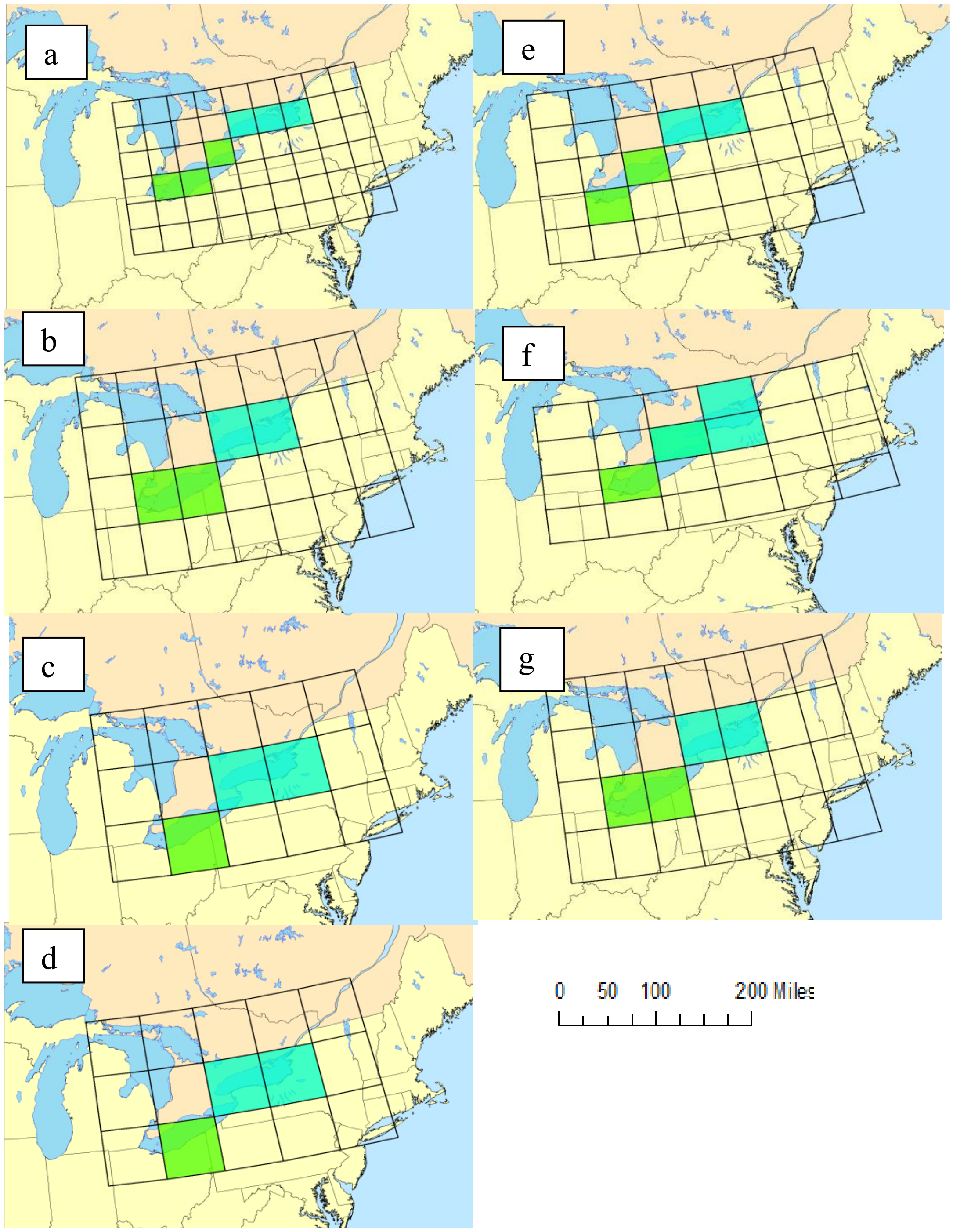

Figure 2.3. Determination of lake grid cells for models (a) CESM, (b) CSIRO, (c) GFDL, (d) GISS, (e) HADLEY, (f) IPSL, and (g) MPI.

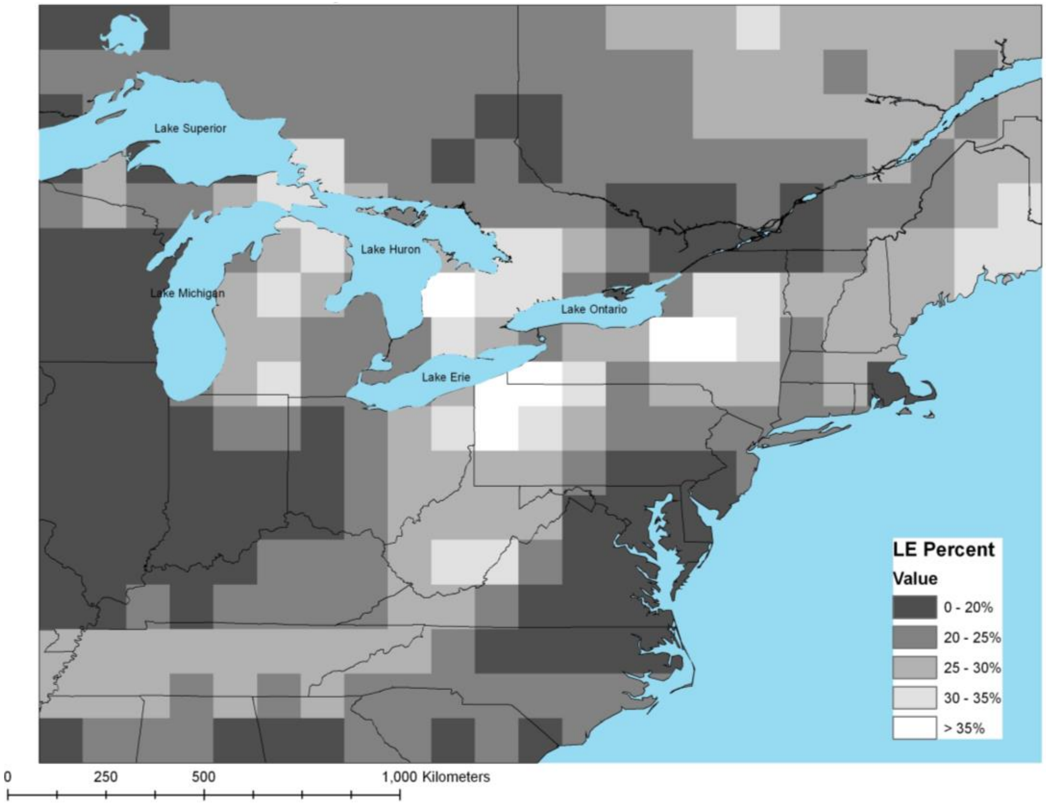

Figure 2.4. Percentage of snowfall from lake effect events (Karmosky 2007).

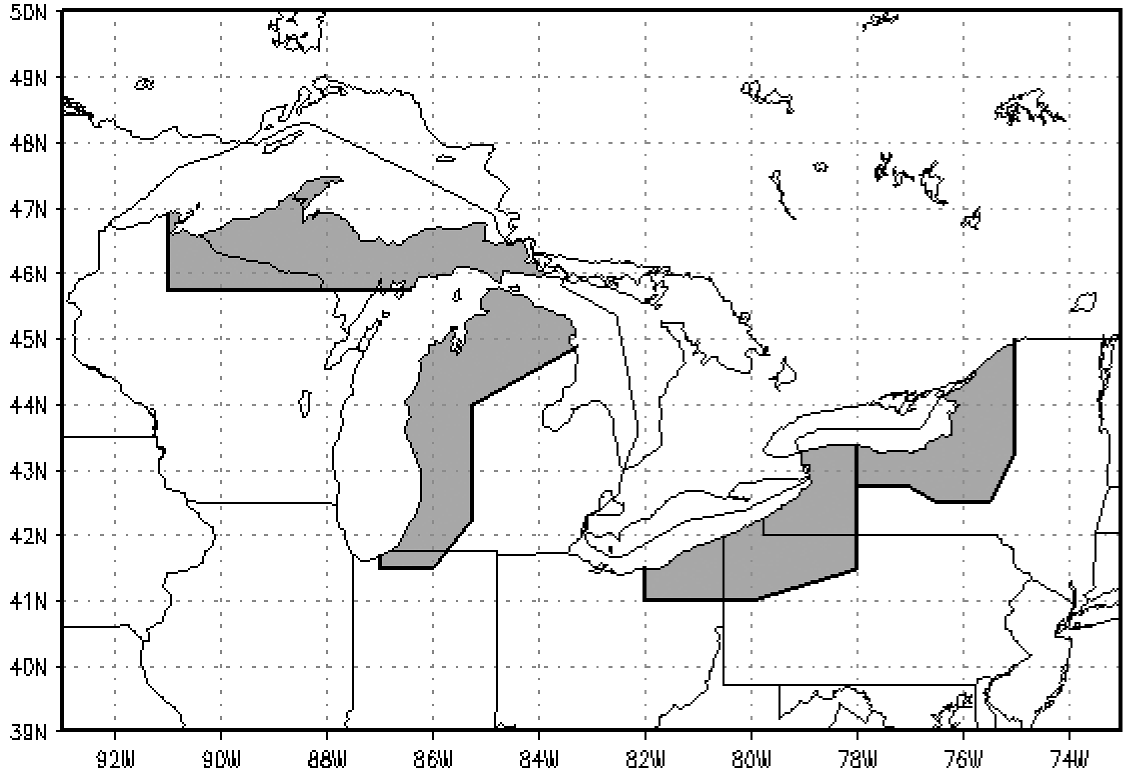

Figure 2.5. Typical lake effect Snowbelt extent (Norton and Bolsenga 1993).

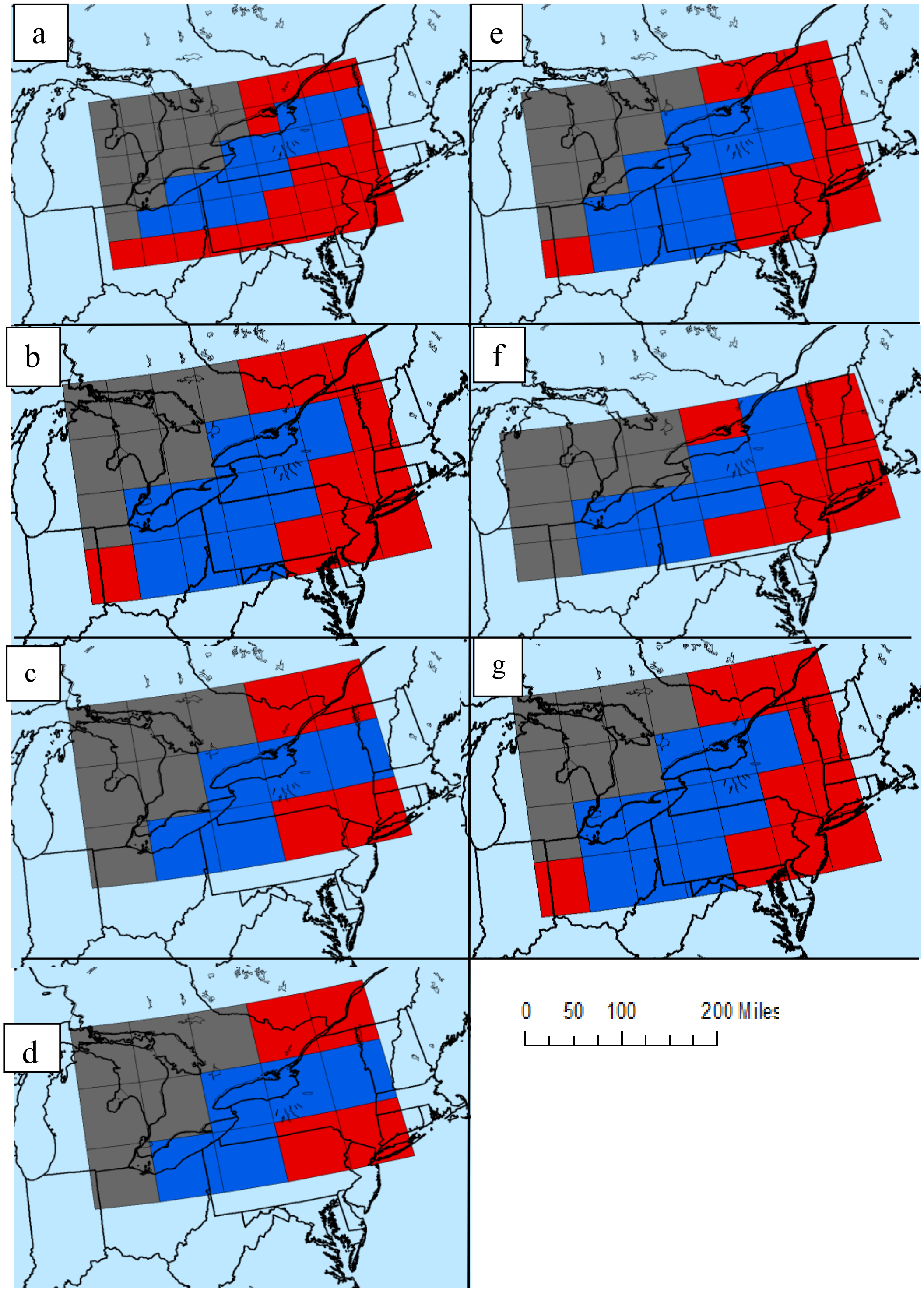

Figure 2.6. Determination of the lake-induced belt grid cells (a) CESM, (b) CSIRO, (c) GFDL, (d) GISS, (e) HADLEY, (f) IPSL, and (g) MPI.

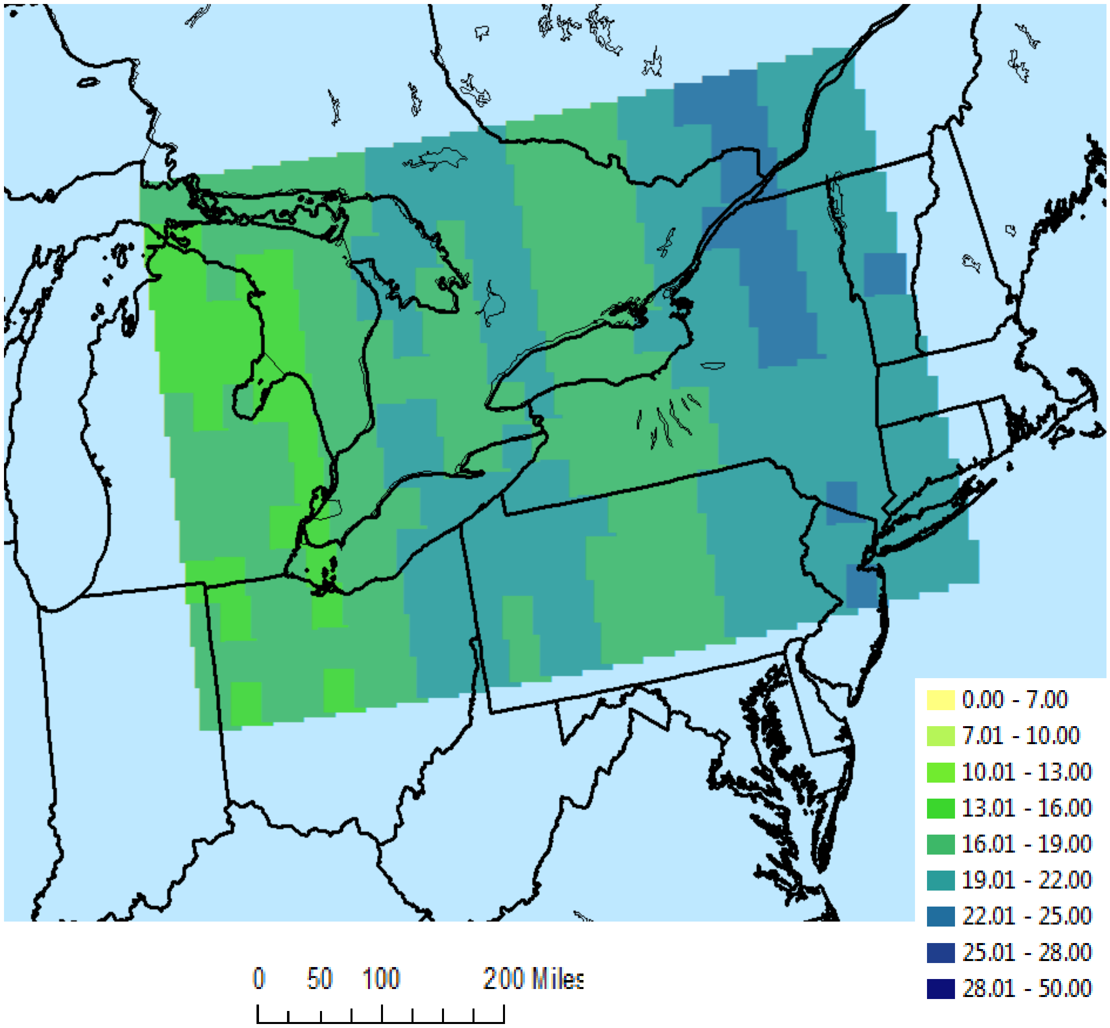

Figure 2.7. 1981 - 2010 average seasonal snowfall from Willmott-Matsuura-derived data (cm).

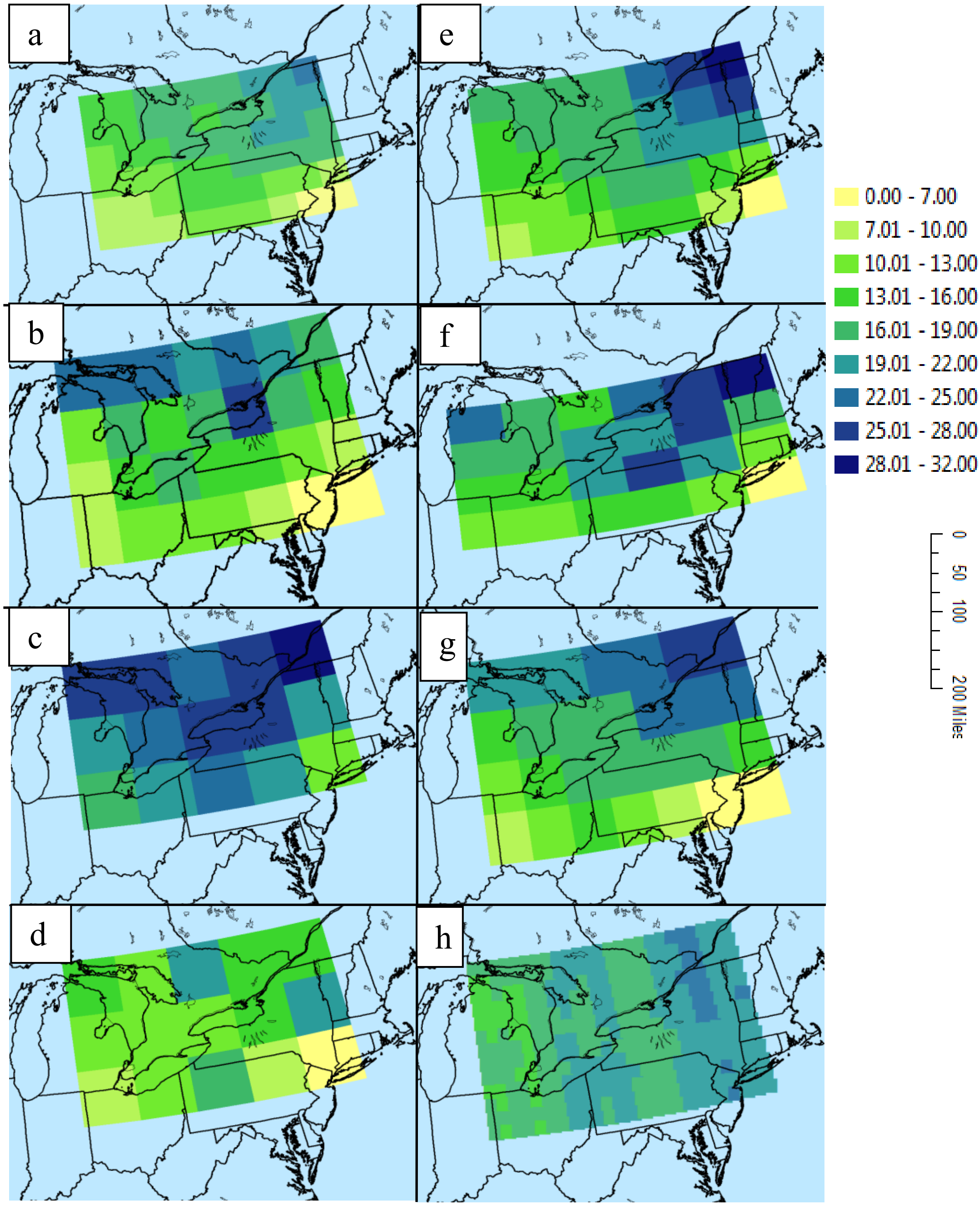

Figure 2.8. Spatial SWE 2006-2015 in cm for (a) CESM, (b) CSIRO, (c) GFDL, (d) GISS, (e) HADLEY, (f) IPSL, (g) MPI and (h) Willmott-Matsuura-derived.

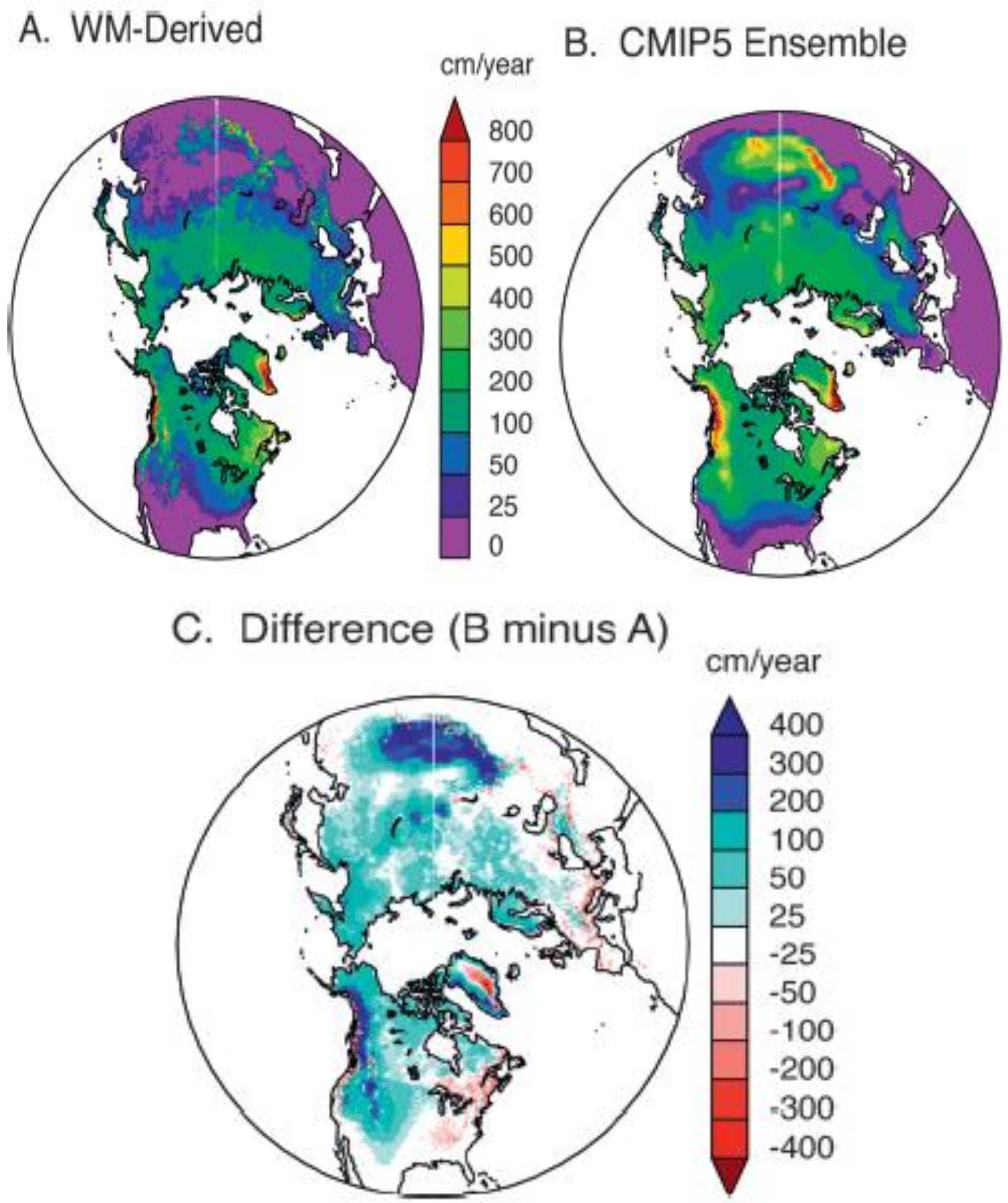

Figure 2.9. Evaluation of simulated snowfall climatology (Krasting et al. 2013).

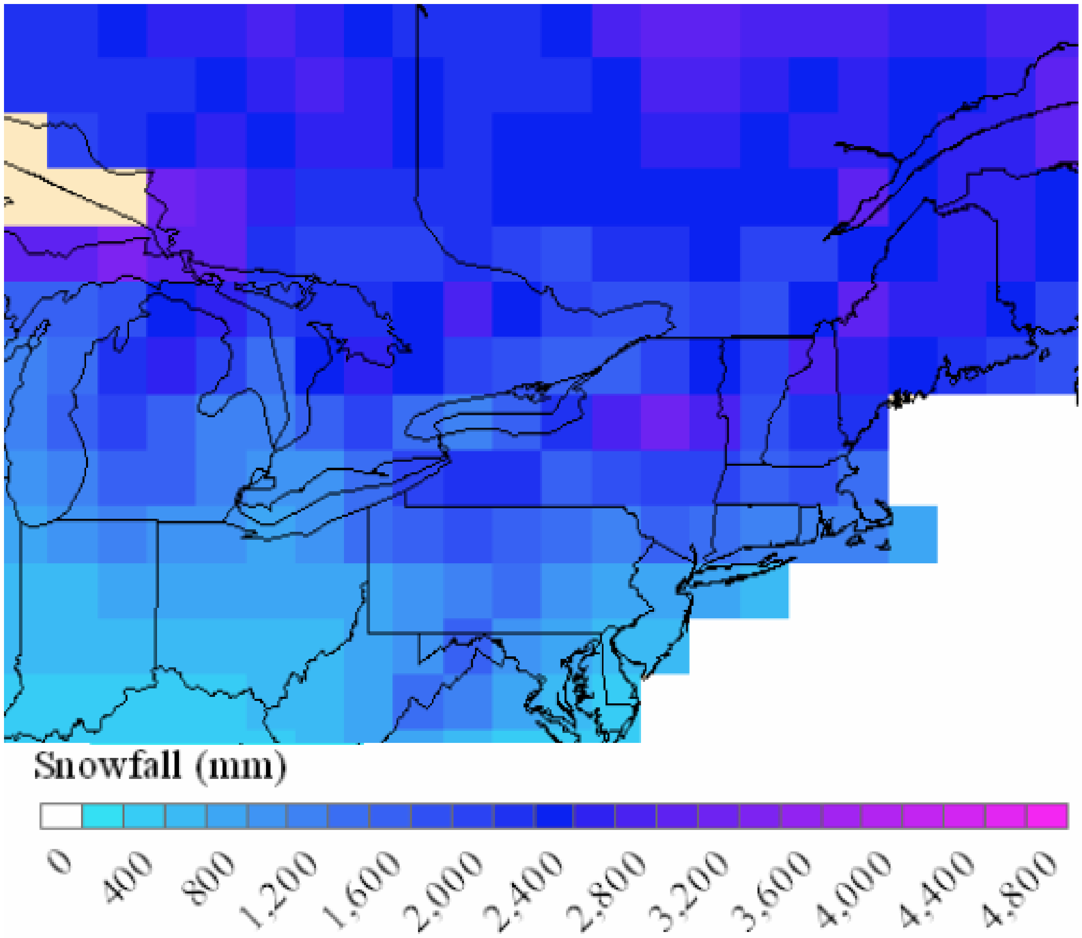

Figure 2.10. Observed snowfall in the Northeast from 1949-1999 from NWS Cooperative weather stations (Kluver 2007).

Chapter 3

SNOWFALL TRENDS AND DETECTION OF A LAKE-INDUCED SIGNAL

When examining the snowfall flux, values were converted to SWE in cm. This is done to avoid the conversion back to snow depth, as the snow-liquid water ratio can vary significantly from event to event. Typically, lake effect events have a SWE ratio of 18-1 to 25-1, with some events being as low as 6-1 (Ellis and Johnson 2004).

3.1 Overall Snowfall Trends

Before looking specifically at trends in individual grid cells, a cursory examination of the seasonal snowfall across the entire study area is conducted. In both RCPs, snowfall declines in all simulations during the entire period (Figure 3.1, a-b). In RCP 4.5, the ensemble mean reveals a decline of nearly 21% in snowfall by the end of the century with a regression correlation coefficient of 0.37 ($p<0.0001$). RCP 8.5 has a much stronger decline across the time period. Here the ensemble average reveals a decrease in snowfall of approximately 46% by the end of the century. A linear regression fit to the ensemble mean yields a correlation coefficient of 0.75 ($p<0.0001$). Strong variability is present within the individual models, giving a large range in potential outcomes. The two ensemble means stay close in projected snowfall until about mid-century when they begin to diverge, and by the end of the century there is an approximate 27% difference in snowfall totals between RCP 8.5 and 4.5 (Figure 3.2).

3.2 Lake-Induced Belt Results

Beginning with RCP 4.5, in the lake-induced belt, a notable decrease in seasonal snowfall are present in all seven models (Figure 3.3). At the start of the period, a range in values of 10 cm SWE is seen between the models. By the end of the period, this range has increased to 13 cm indicating divergence of the models with time, creating more uncertainty later in the portion of the 21st century. There is inter-annual variability within an individual model, along with in the difference between models in a given year. These differences between models in a given year are expected, as the simulations are fully coupled, and therefore each model generates its own sequence of climate variability. The ensemble mean is used to aid in the interpretation of the overall trend in model projections. When examining the ensemble mean, snowfall declines by just over 20% by the end of the century. The correlation coefficient of this trend is 0.34 ($p<0.0001$). To further examine the data, a five-year winter-seasonal (October – March) mean is also created. This reveals a change in the snowfall trend that is not as easily detected using annual data. Over the first 50 years of the period, there is a strongly correlated ($R^2=0.63$, $p<0.0001$) decrease in snowfall of 16% (Figure 3.4). However, over the second half of the century this trend ceases and no trend is present.

In RCP 8.5 there is more a pronounced decline of snowfall over the time period for the lake-induced belt, as expected based on the stronger radiative forcing. The variability of the individual models is similar to the previous RCP discussed, however the models tend to be more diverse during the first half of the century, and then converge during the second half (Figure 3.5). This is indicative of the models projecting more similar outcomes over time. In the ensemble mean, snowfall decreases (R^2=0.72, p<0.0001) by nearly 45% by the end of the century. Looking at the data with five-year averages, an initial increase in snowfall over the first quarter century occurs, followed by a sharp decline (Figure 3.6). During the first 25-year period, snowfall increases by approximately 12% (R^2=0.50, p<0.0001) with an increase of 0.7 cm SWE per decade. This is followed by a decrease for the remaining part of the century of 47% (R^2=0.93, p<0.0001) with a decline of 1.1 cm per decade.

When comparing the two ensemble means (Figure 3.7), one for each RCP, they are in close agreement during the first half of the century before they begin to diverge with RCP 4.5 leveling out as RCP 8.5 declines rapidly. By 2070 the RCPs have completely separated and are on two different trajectories with RCP 8.5's snowfall being approximately half that see in RCP 4.5 by the end of the century.

3.3 Non-Lake-Induced Grid Cell Results

For the non-lake-induced grid cells, similar trends to the lake-induced belt are seen. In RCP 4.5 there is a decrease of 21% in seasonal snowfall at the end of the century compared to the beginning of the century (R^2=0.37, p<0.0001) (Figure 3.8). When the five-year ensemble mean data is examined, the same mid-century trend is apparent (Figure 3.9). The first half-century shows the same decline of 16% (R^2=0.82, p<0.0001) in snowfall as the lake-induced belt, and during the second half of the century, there is effectively no trend in snowfall values.

For RCP 8.5, there is convergence of the individual model by the end of the century in the non-lake-induced grid cells as in previous results, likely due to increasing temperatures resulting in less and less snow (Figure 3.10). Here the ensemble average decline in snowfall is present as well, with a decrease of 46% (R^2=0.75, p<0.0001). The five year averaged data (Figure 3.11) yields a similar increase for the first 25 years followed by a sharp decline, however here the increase and subsequent decrease are not as pronounced as in the lake-induced belt. The first quarter century increase is on the magnitude of only 4%, while the latter decline was 43% (R^2=0.95, p<0.0001) at about 0.9 cm per decade.

When comparing the two ensemble means for the non-lake-induced belt (Figure 3.12), the two RCPs are in close agreement for the first half of the century before diverging. RCP 4.5 levels out by 2050 as RCP 8.5 starts to decline. The RCPs have completely separated themselves by 2070 and are on two different trajectories with RCP 8.5's snowfall being approximately half that seen in RCP 4.5 by the end of the century. The only major difference between the projections for the lake-induced belt and non-lake-induced grid cells is the magnitude of the SWE values.

3.4 Lake-Induced Signal

As discussed previously, with the assumption that synoptic scale systems will produce nearly the same amount of precipitation in neighboring grid cells, taking the difference between the lake-induced belt and non-lake-induced grids will result in only a lake-induced signal remaining.

Figure 3.13 shows this process for RCP 4.5 where the difference between the SWE ensemble mean of the lake-induced belt and the non-lake-induced grid cells is plotted with the range of the individual model values. The ensemble mean is centered on 1.8 cm with a range between 0.1 and 3.7 cm (t-ratio: 23.02, $p < 0.0001$) supporting the idea that the lake-induced belt and non-lake-induced grid cell snowfall ensemble means are statistically different. By averaging out the seasonal yearly data into decadal periods, there is a decline of 25% of SWE (R^2 =0.33, $p<0.001$) (Figure 3.14). This implies that over time, the difference between lake-induced and non-lake-induced snowfall is diminishing, with lake-induced snowfall becoming less prominent. Put another way, lake-induced snowfall declining at a faster rate than non-lake-induced snowfall in the region. However, it should be noted that there is minimal practical significance of a half centimeter decline in over the 94-year study period with regards to the hydrologic cycle.

RCP 8.5 also has a large amount of individual model variability present in the difference between lake-induced belt and non-lake-induced grid cells. Extremes ranged from 9 cm to -5 cm of SWE (Figure 3.15). The ensemble mean is slightly lower than that of RCP 4.5, but still statistically significant with an average 1.64 cm difference (t-ratio: 19.61, $p < 0.0001$) between the two snowfall classification types and a range between -0.5 and 3.9 cm. There is a more prominent decline seen in the relationship in this scenario. An examination of the decadal averaged values yields a (R^2=0.42, p=0.004) decline of 37% (Figure 3.16). This implies that in RCP 8.5, lake-induced snowfall is becoming less measureable with time, but again, the practical significance of approximately 0.5 cm of SWE over a 94-year period is minimal.

These results suggests that seasonally, there is indeed a statistically significant ($p < 0.0001$) signal of lake-induced snowfall present within the models and that the GCMs used in this study are capable of resolving some lake/atmosphere snow processes for both RCP scenarios.

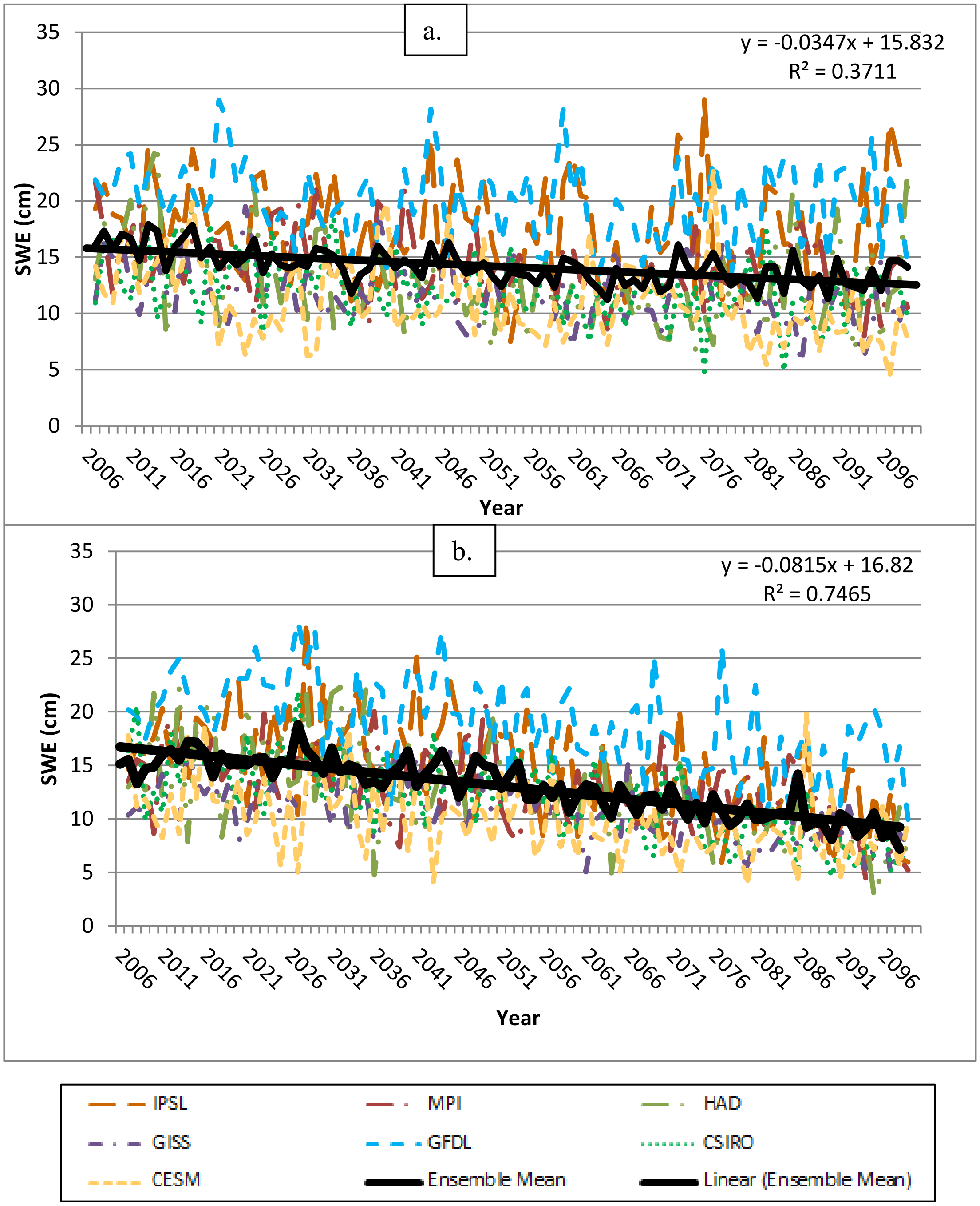

Figure 3.1. Regional SWE for (a) RCP 4.5, and (b) RCP 8.5.

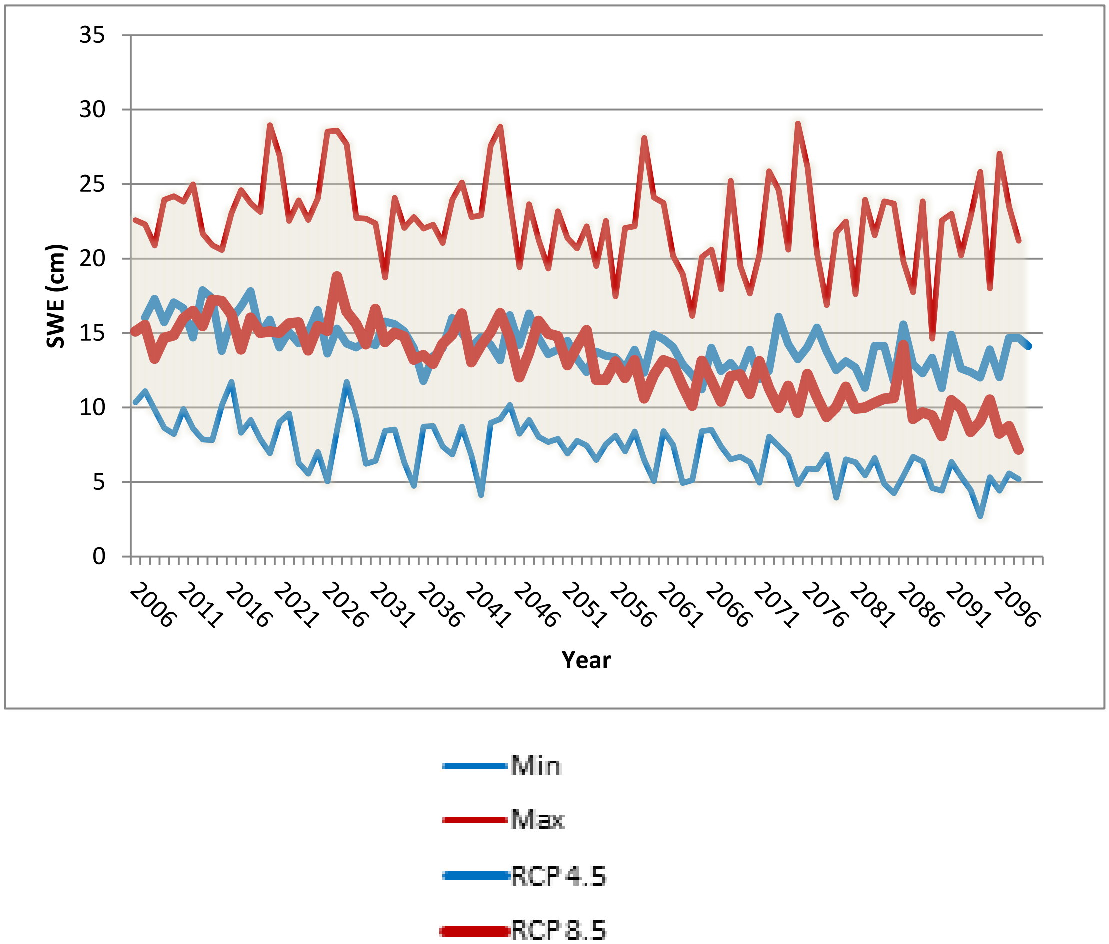

Figure 3.2. Regional SWE RCP comparison.

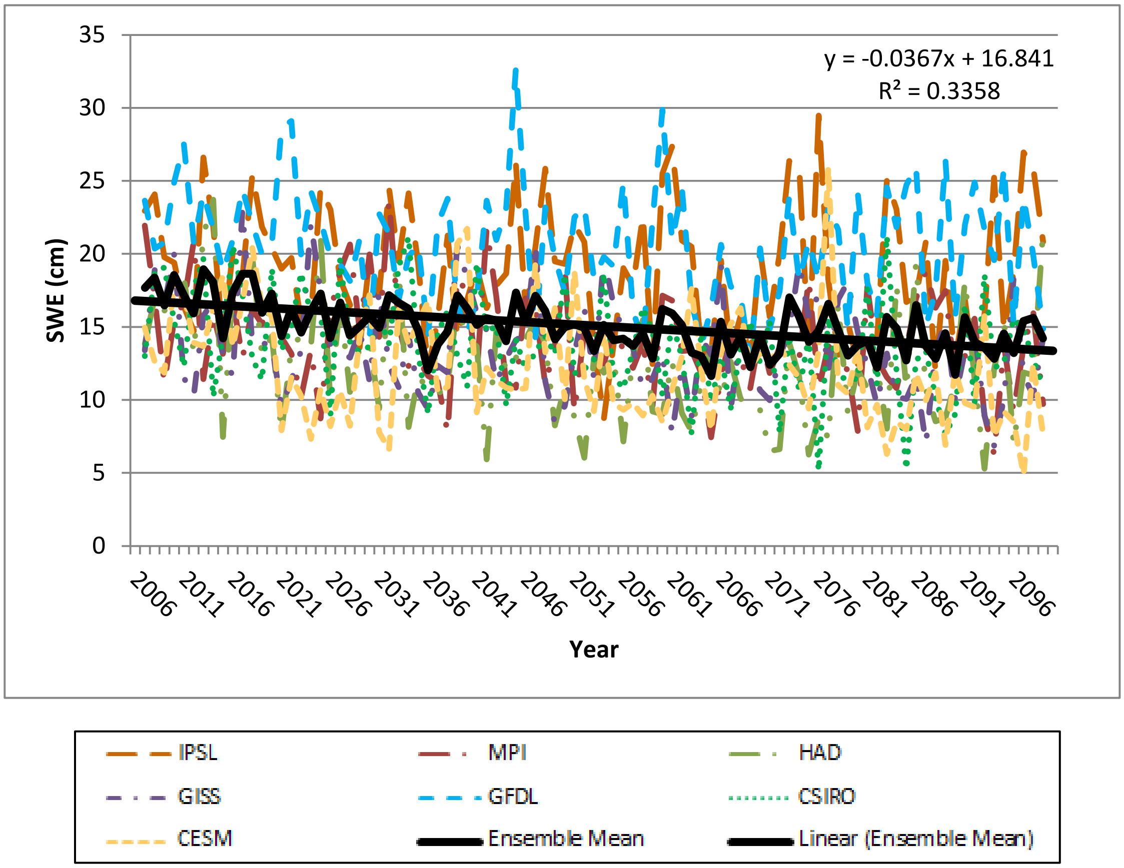

Figure 3.3 Lake-induced belt SWE, RCP 4.5.

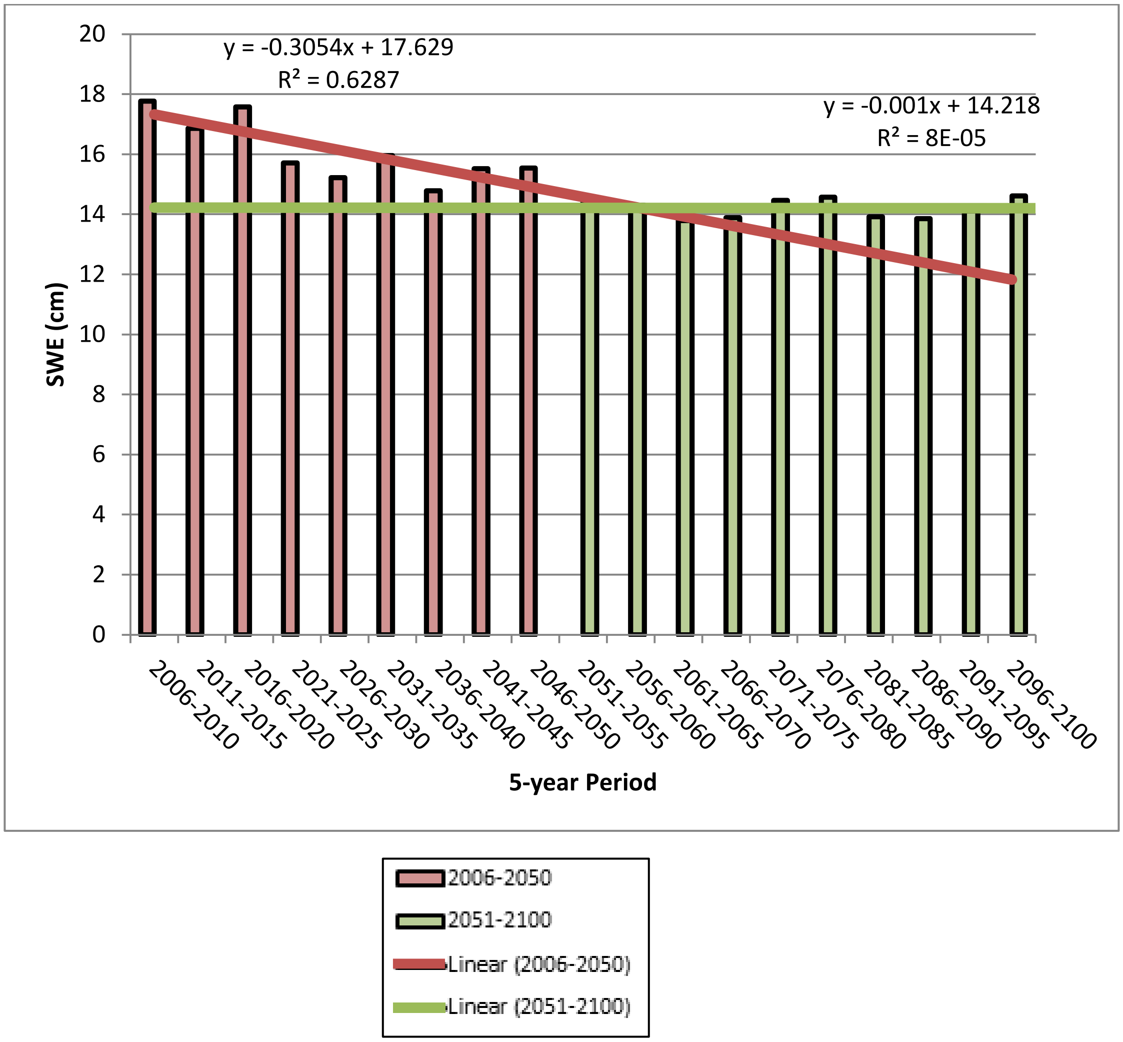

Figure 3.4. Five year average lake-induced belt SWE, RCP 4.5.

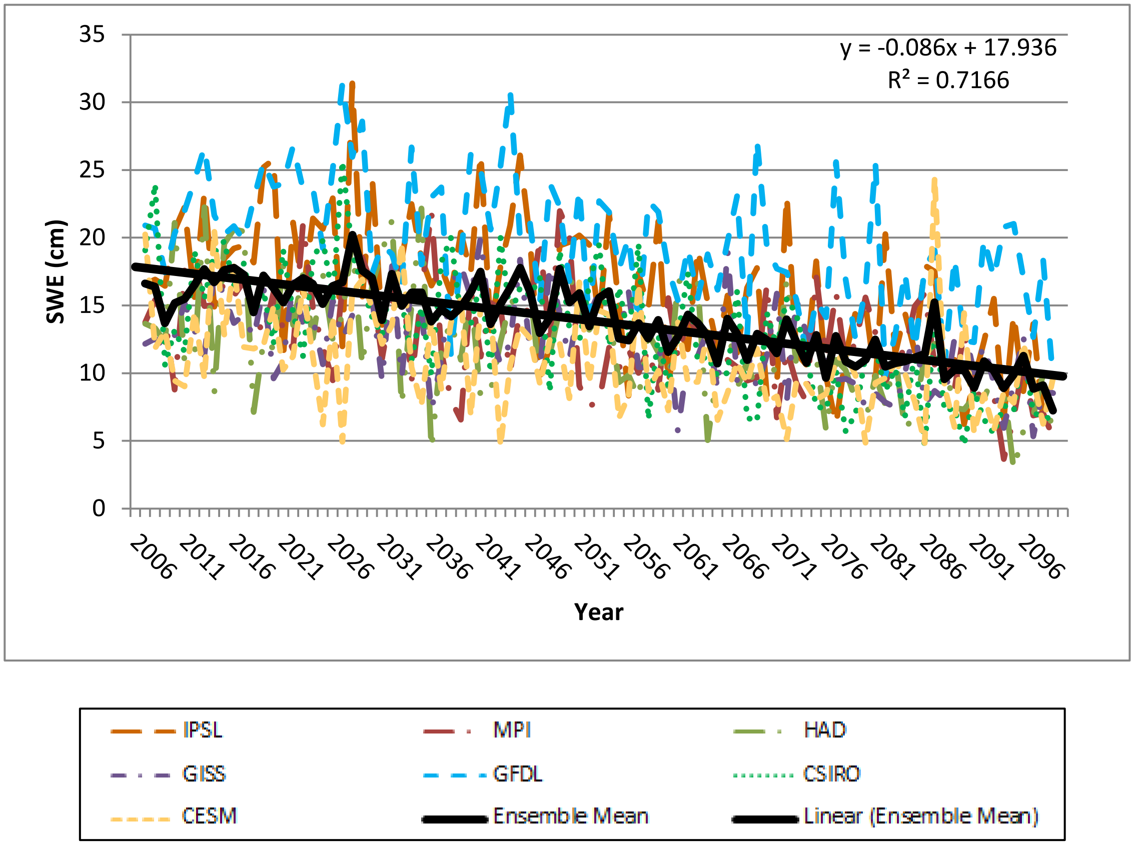

Figure 3.5. Lake-induced belt SWE, RCP 8.5.

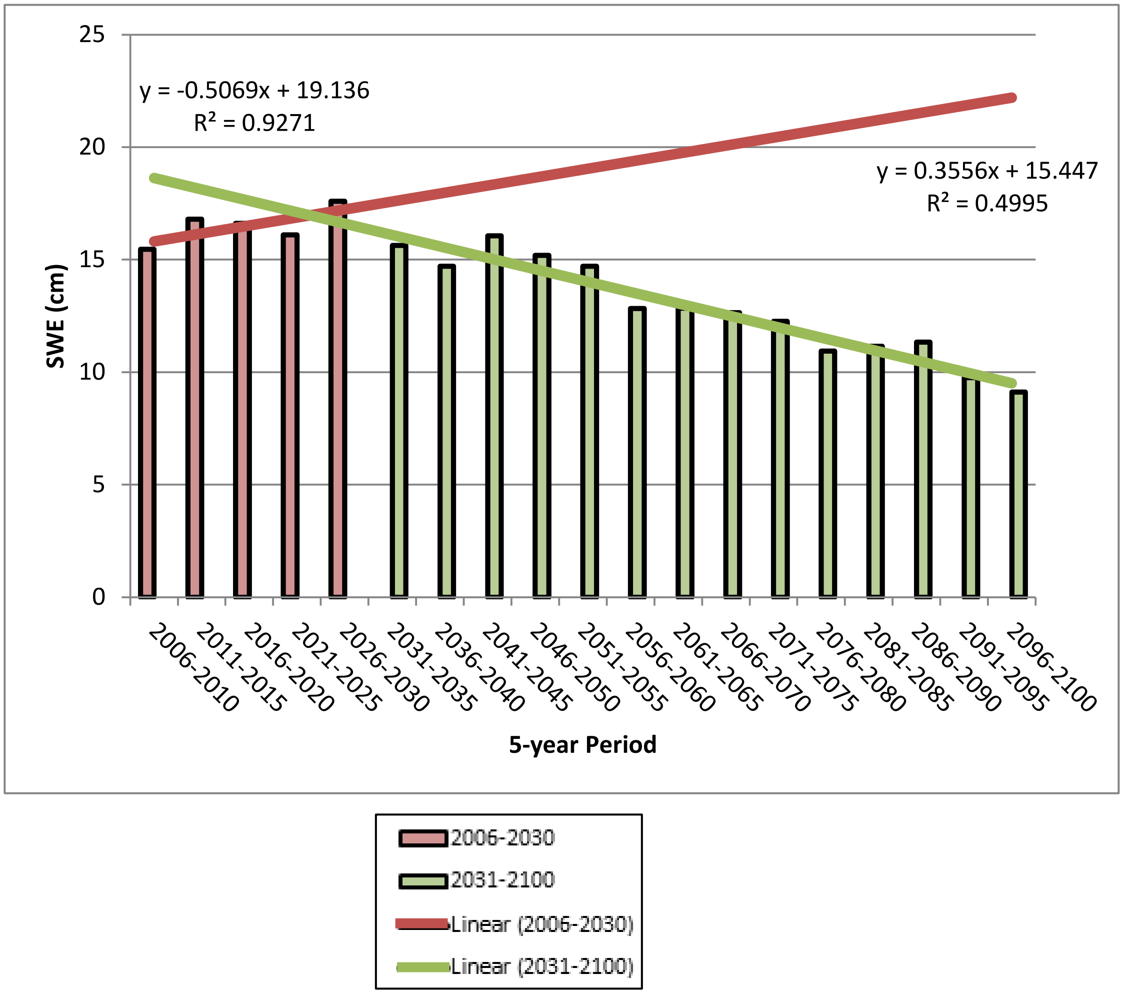

Figure 3.6. Five year average lake-induced belt SWE, RCP 8.5.

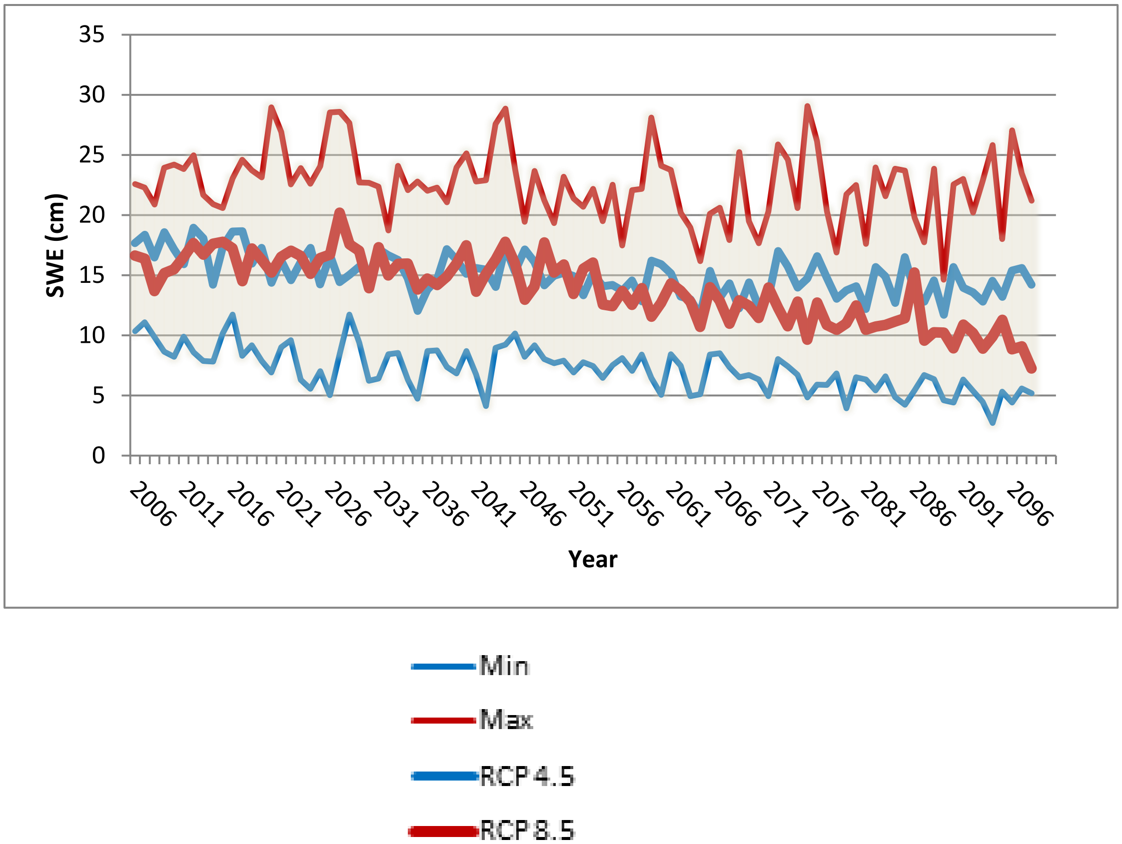

Figure 3.7. Lake-induced belt SWE, RCP comparison.

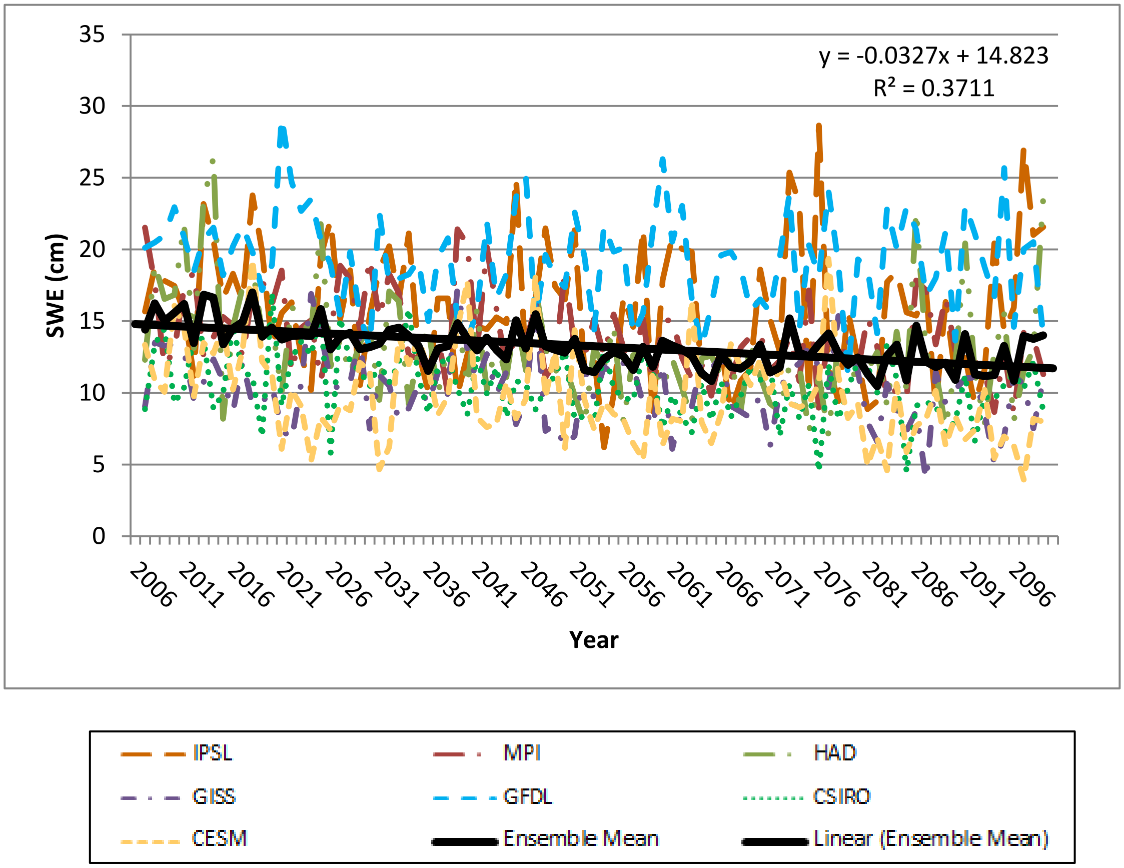

Figure 3.8. Non-lake-induced grid cell SWE, RCP 4.5.

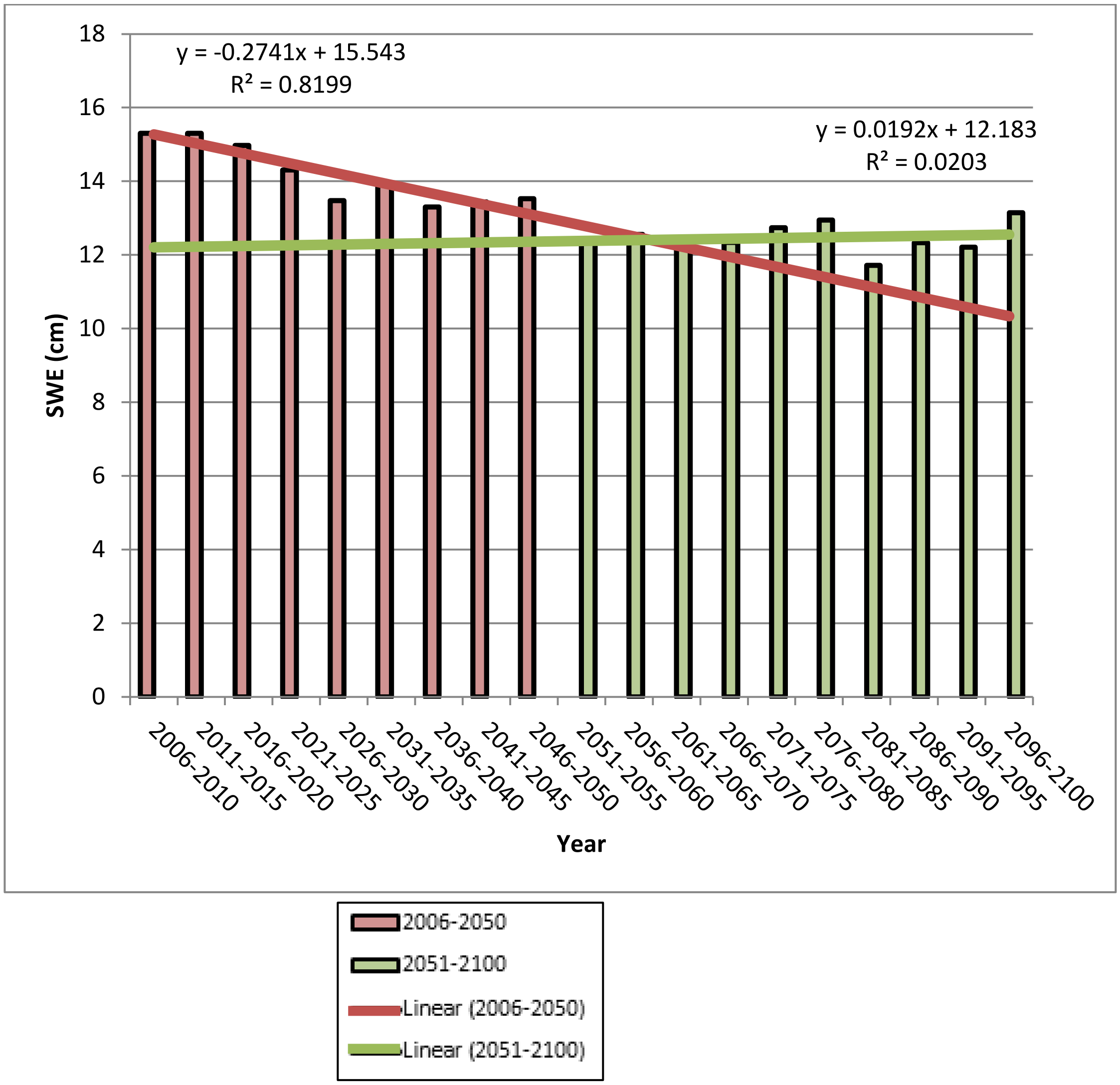

Figure 3.9. Five year non-lake-induced grid cell SWE, RCP 4.5.

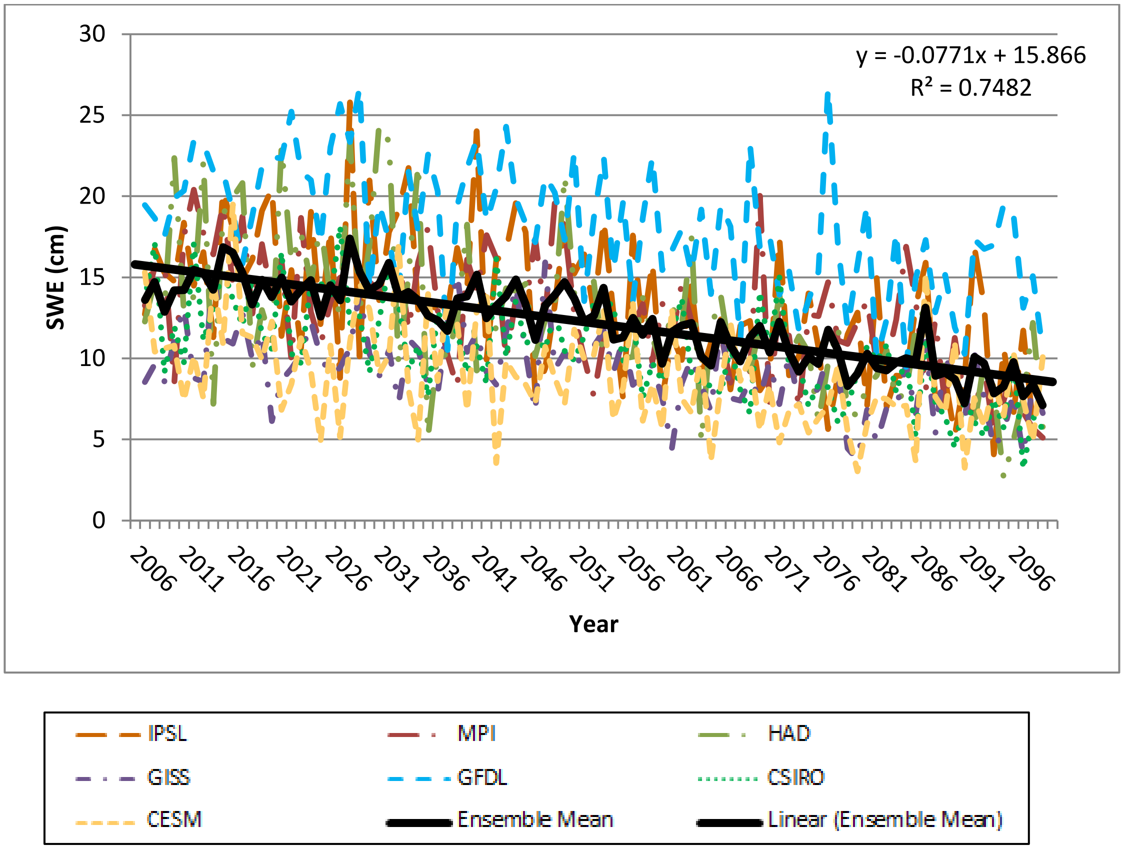

Figure 3.10. Non-lake-induced grid cell SWE, RCP8.5.

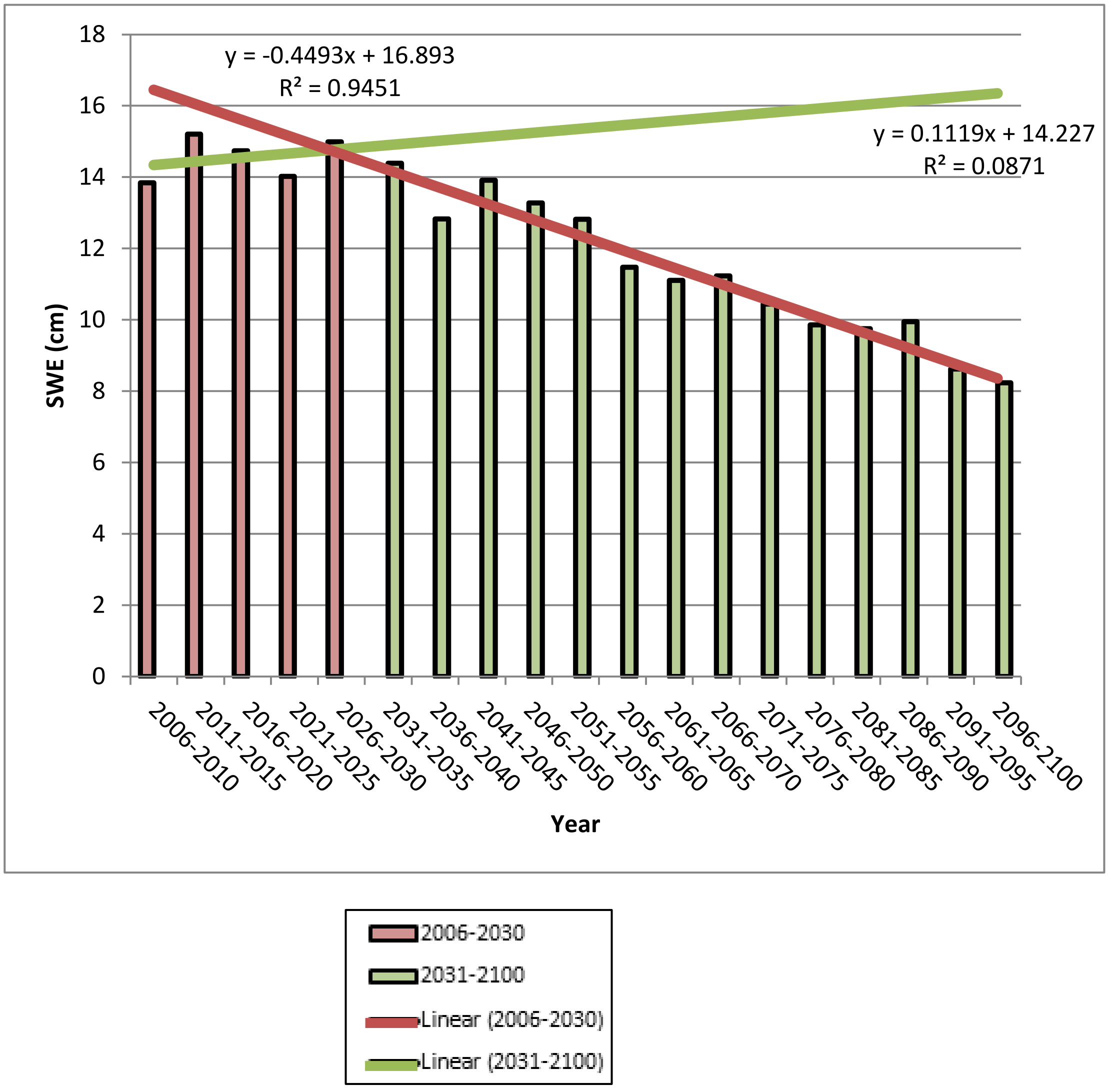

Figure 3.11. Five year non-lake-induced grid cell SWE, RCP 8.5.

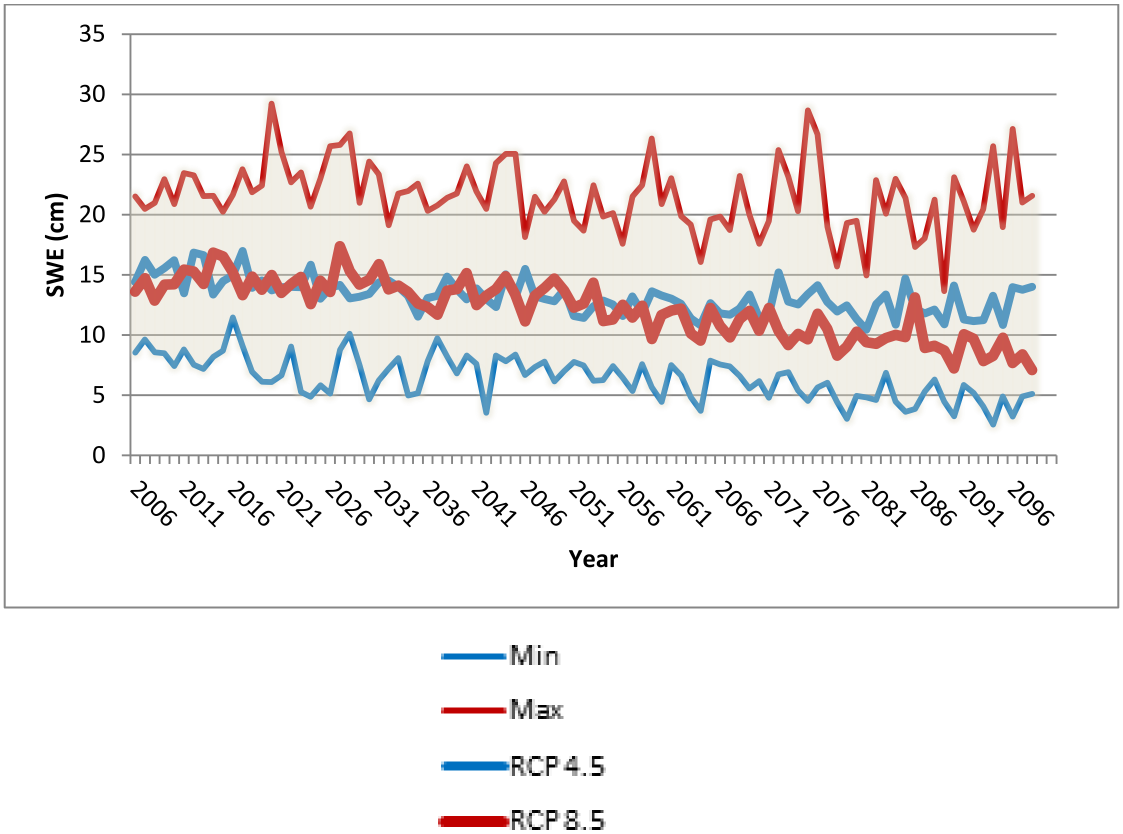

Figure 3.12. Non-lake-induced grid cell SWE, RCP comparison.

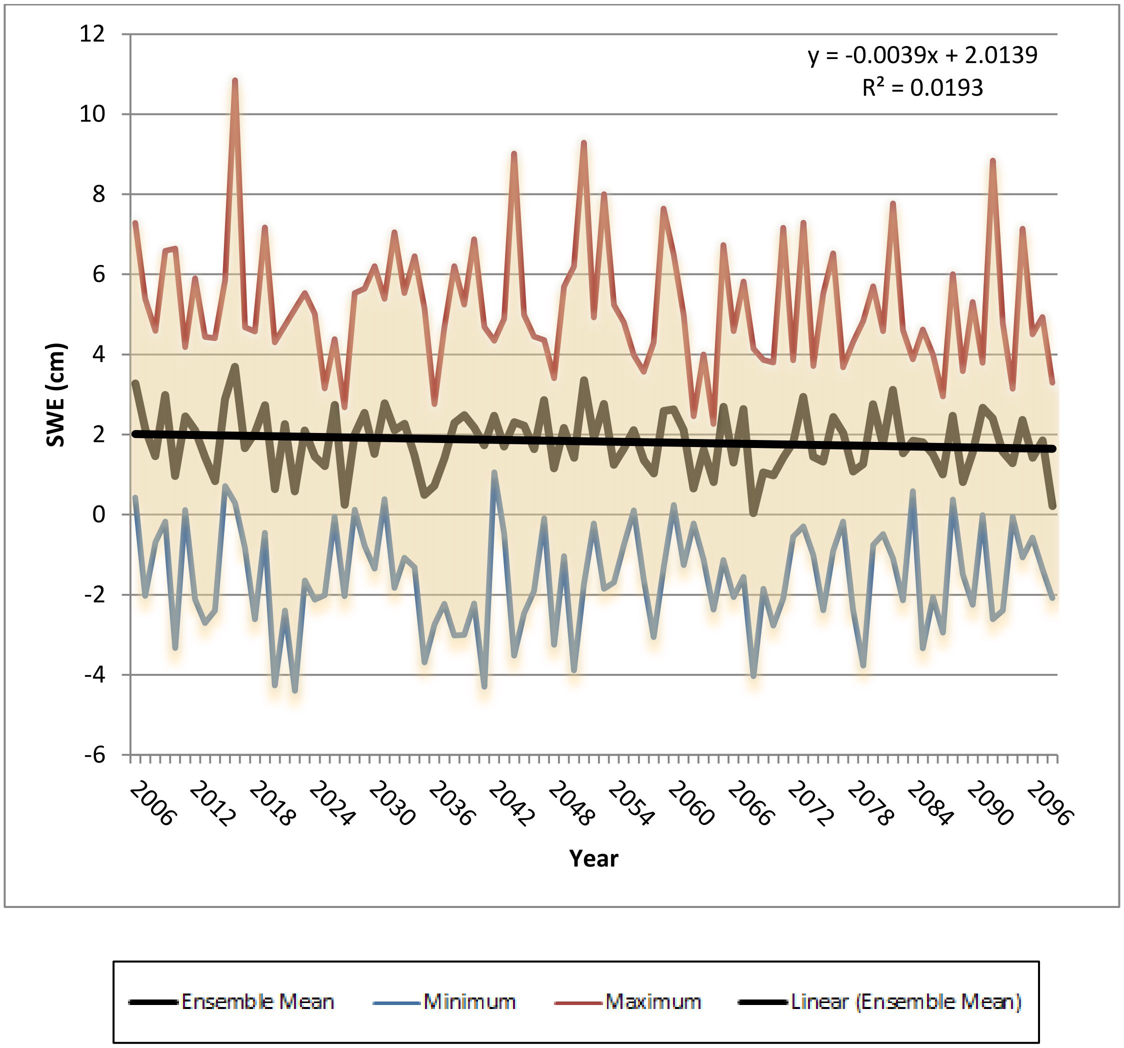

Figure 3.13. Lake-induced belt and non-lake-induced grid cell SWE difference, RCP 4.5.

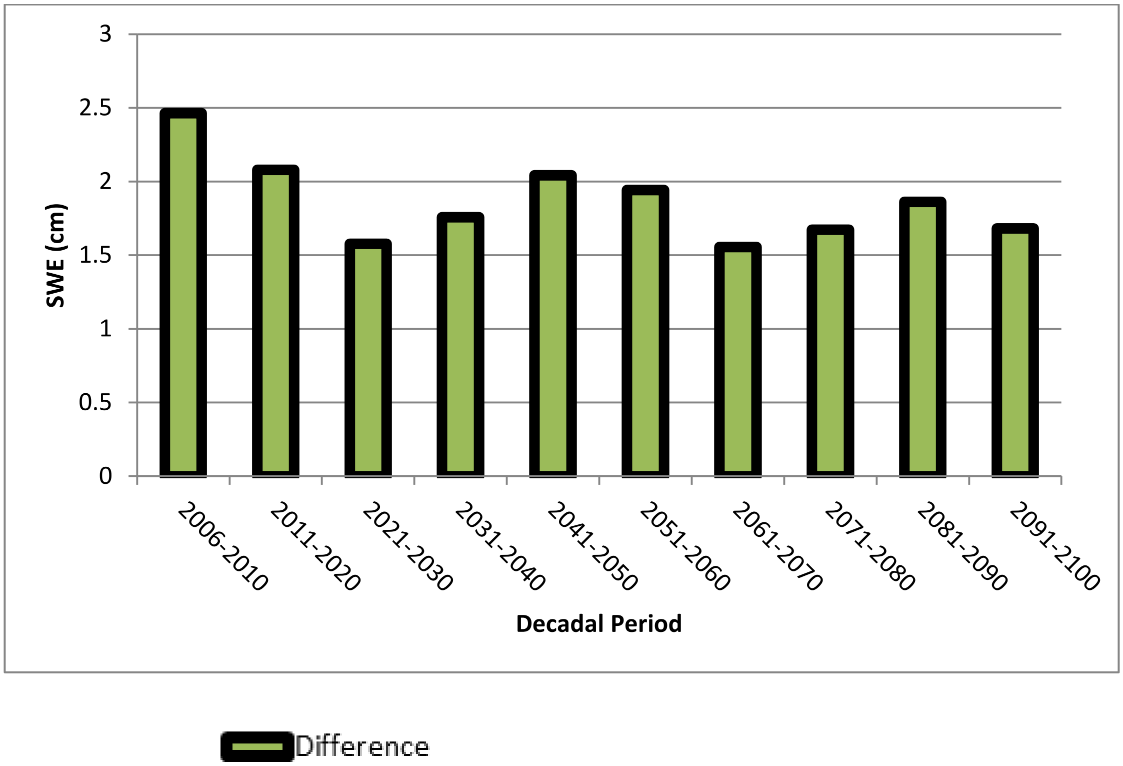

Figure 3.14. Lake-induced belt and non-lake-induced grid cell decadal SWE difference, RCP 4.5.

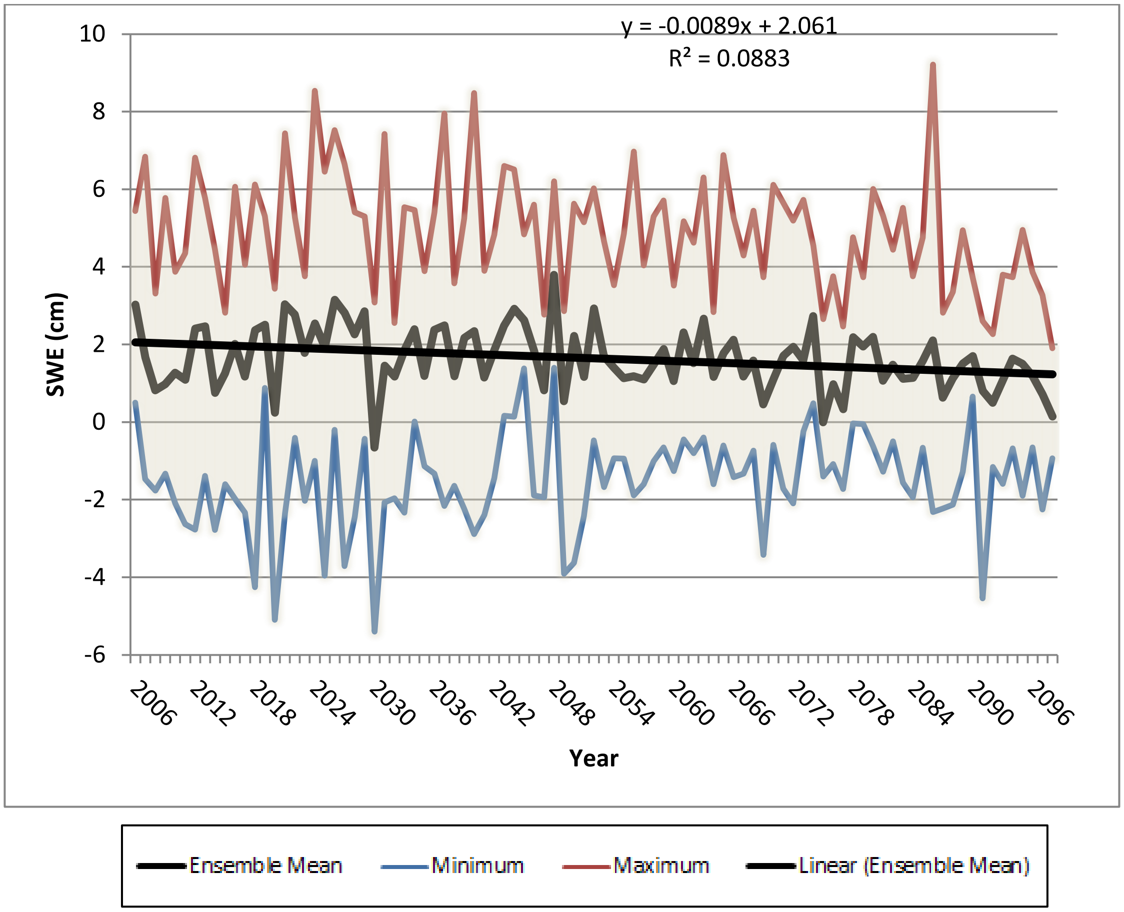

Figure 3.15. Lake-induced belt and non-lake-induced grid cell SWE difference, RCP 8.5.

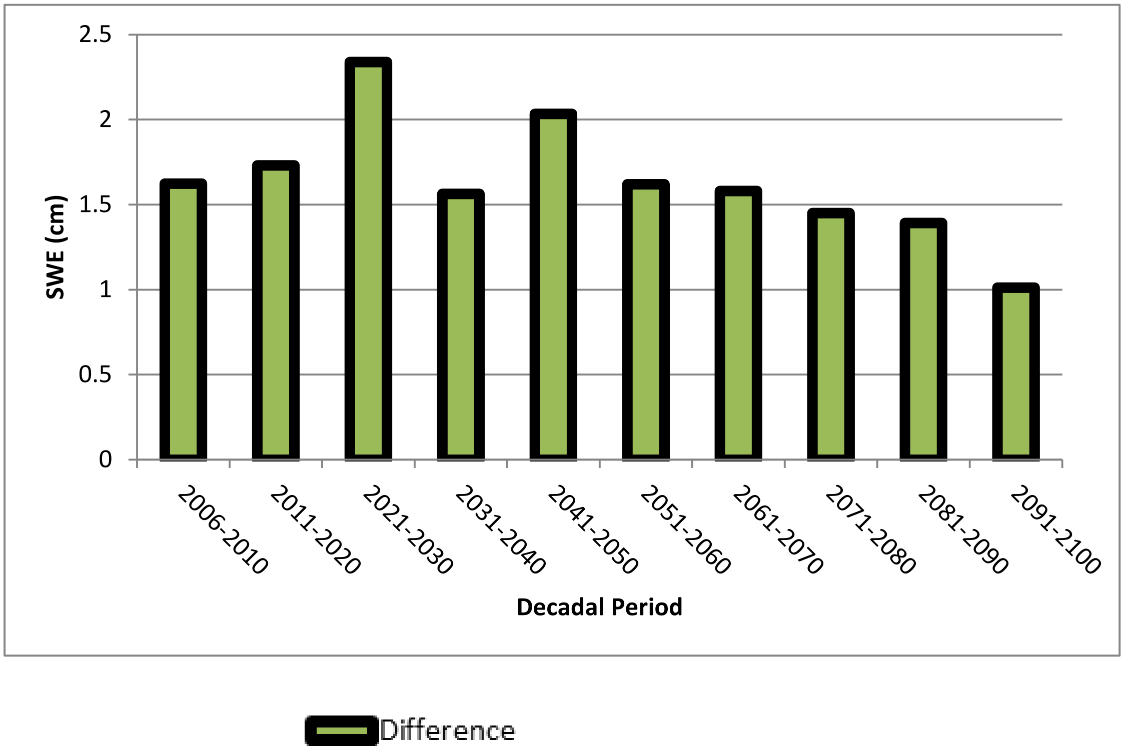

Figure 3.16. Lake-induced belt and non-lake-induced grid cell decadal SWE difference, RCP 8.5.

Chapter 4

EXPLANATION OF SNOWFALL TRENDS

The cause(s) of the apparent trends in lake-induced snowfall are examined using a calculated lapse rate over the lakes, the two-meter air temperature for the region and by examining the proportion of precipitation that falls as snow.

4.1 Lake Lapse Rates

As discussed in the methodology, the difference between the lake surface temperature and the overlying 850 hPa temperature is an indication of the boundary layer instability, and thus the potential for lake effect processes. With a larger lapse rate, one can expect a more unstable environment and thus there exists a higher potential for lake-induced snowfall. Note that given the seasonal averaging employed here, the lapse rates are likely to be considerably lower than the typical lapse rate expected of a lake-induced event.

Geographically, Lake Erie is located further south than Lake Ontario implying that both lake surface and corresponding upper air temperatures would be warmer than Lake Ontario. However, as it is shallower and more prone to freezing during the winter months, the surface of Lake Erie may often be colder than ice-free Lake Ontario. The balancing of these two processes has a direct impact on the lapse rate over the lakes and is seen in the observations.

4.1.1 Lake Erie

In the RCP 4.5 scenario, surface temperature in the lake grid cells increases from an average of 275 K over the first decade to approximately 277.4 K during the final decade of the time period (Figure 4.1) yielding a total increase of 2.7 K (R^2=0.78, p<0.0001). The 850 hPa temperature similarly increases by 2.3 K (R^2=0.70, p<0.0001) over the time period with values averaging 269.7 K in the first decade compared to 271.86 over the final decade (Figure 4.2). These values lead to an averaged lapse rate of 5.4 K from the surface to 850 hPa (Figure 4.3). Examining the trend, there is a moderately correlated (R^2=0.25, p<0.0001) ensemble mean increase of 7%, however there is significant variation between the models in this calculation depending on the model's treatment of the lake surface and the overall lake dynamics. The IPSL, GFDL, and CSIRO models had higher lapse rates than the remaining four by approximately 1.5 to 2.0 K. It is unclear how models with such differing lake treatments arrived at relatively similar lapse rates. This result would imply that over time, there is a slightly more unstable environment over the lakes.

This same trend is seen in the RCP 8.5 scenario but with a more drastic increase. The lake surface temperature had an increase of 5.1 K (R^2=0.93, p<0.0001) over the period with the first to last decadal values being 275 K and 279.7 K respectively (Figure 4.4). The 850 hPa temperature over the grid cells also increased, but by 4.3 K (R^2=0.89, p<0.0001), with a decadal range of 269.8 to 273.8 K (Figure 4.5). The calculated lapse rate has an average of approximately 5.2 K (Figure 4.6). The trend in the lapse rate is more pronounced in RCP 8.5 with an increase of 16%

(R^2=0.51, $p<0.0001$), but the rate itself is actually lower than in the previous scenario. Just as in RCP 4.5, there is a clear division between the models with varying lake surface representation.

4.1.2 Lake Ontario

For Lake Ontario, the models show generally cooler temperatures than for Lake Erie of the magnitude of approximately 1.7 K for RCP 4.5 and 1.85 K for RCP 8.5, but very little difference with regards to the lapse rates. This would support that latitude is a more important factor in the determination of temperature than the lake surface. In RCP 4.5, there is strong convergence of the model data for the lake surface temperatures with the exception of the IPSL model, which project temperatures that are on average 4.0 K warmer than the ensemble mean. The ensemble mean shows an increase just shy of 3.0 K (R^2=0.79, $p<0.0001$) with values ranging 1.0 K in both directions about the mean (Figure 4.7). When examining the 850 hPa temperatures, there is an increase present of 2.4 K over the period (R^2=0.72, $p<0.0001$) with a similar range around the ensemble mean of about 1.0 K above and below (Figure 4.8). The calculation from these values yields an average seasonal lapse rate of 5.1 K between the surface and 850 hPa level, with an increase of 11% (R^2=0.37, $p<0.001$) by the end of the century (Figure 4.9). As with Lake Erie, Lake Ontario also has two groups of model lapse rates, the lower one consisting of CESM, GISS, HAD, and MPI and the higher valued group including the GFDL, IPSL and CSIRO models. Because of the projected warm surface temperatures in the IPSL model, the lapse rate is higher than the ensemble mean by 65%.

The RCP 8.5 scenario was similar to RCP 4.5 with strong increases in surface and 850 hPa temperature fields. The surface temperature ensemble mean had a strong (R^2=0.94, p<0.0001) increasing trend of 5.6 K over the 94-year period with the decadal average values being 273.1 and 278.2 K respectively (Figure 4.10). Figure 4.11 shows the individual model projections of seasonal 850 hPa temperatures with the ensemble mean. From the first to last decade, there is an average increase from 268.0 to 272.2 K with a total increase of 4.5 K during the period (R^2=0.9, p<0.0001). This leads to a lapse rate ensemble mean over Lake Ontario of 5.7 K from the surface to 850 hPa (Figure 4.12). Over the period, there is an increase of 23% (R^2=0.61, p<0.0001) in the lapse rate values.

There are statistical correlations (R^2=0.31-0.46, p < 0.001) present between the lapse rate and lake-induced belt snowfall changes for both Lakes Ontario and Erie for RCP 4.5 and (R^2=0.35-0.46, p <0.0001) for RCP 8.5. However, these are not tied to causation. Physically, an increase in atmospheric instability should result in increased convection and increased lake-induced snowfall but that is not seen in the data. Under both scenarios for each lake, the simulated lapse rates are simply too low to conclude that they played a substantial role in the development of lake-effect snowfall processes. One would expect lapse rates to be almost double the modeled values to be indicative of enough instability for noteworthy lake effect snowfall. Relative to observations discussed in the methodology however, simulated lapse rates are in line with NCEP Reanalysis data. This would suggest there is a possibility that lapse rates can explain some lake-induced snowfall trends. It is more likely however, that increases in lapse rates could have an impact on lake effect precipitation falling as rain. Nevertheless, by looking seasonally, brief windows of atmospheric instability that may have produced lake-induced snowfall are balanced out with stable conditions. Trends in lapse rates over the lakes are not conclusive enough to result in a direct cause and effect relationship with lake-induced belt snowfall.

4.2 Two-meter Temperatures

Because of the lack of a strong relationship between the averaged seasonal lapse rate and declining snowfall, both overall and lake-induced, examination of the two-meter temperatures should serve as an indication of whether projected temperatures are too warm to produce consistent snowfall. It should be noted that these values are seasonal averages and that average temperatures above freezing, do not imply that individual days or even months are not cold enough to support snowfall. Two-meter temperatures are averaged over both the lake-induced belt and non-lake-induced grid cells. For RCP 4.5, no discernable difference is present between the lake-induced belt and the non-lake-induced grid cells over time (Figure 4.13). However, in RCP 8.5, there is a slight change in the ratio over time, with the non-lake-induced grid cells becoming somewhat warmer than lake-induced belt cells by the end of the period (Figure 4.14). Because there is no substantial difference in two meter temperature between the lake-induced belt and non-lake-induced grid cells, trends over the entire study area are used for analysis.

In RCP 4.5, there is an increase of 2.8 K ($R^2 = 0.78$, $p<0.0001$) from 273.7 K in 2006-2015 to 276.2 K in 2091-2100 (Figure 4.15). This rate of temperature increase (0.030K/year) is on the same order as the lake-induced belt snowfall decrease seen in

RCP 4.5 (-0.036cm/year). When comparing the two trends (Figure 4.16), seasons with anomalously warmer temperatures correspond to seasons with anomalously lower snowfall totals. Examining further, Figure 4.17 shows the relationship between the two variables (R^2=0.55, $p < 0.0001$). In 75% of seasons, a decrease (increase) in temperature corresponds to an increase (decrease) in snowfall (Figure 4.18).

For the RCP 8.5 scenario, an increase in two-meter temperatures of 5.5 K (R^2=0.94, $p<0.0001$) is seen (Figure 4.19) changing from 273.8 K in 2006-2015 to 278.6 K in 2091-2100. The rate of temperature increase is 0.058/year, which is less steep than the rate of decrease in lake-induced belt snowfall of -0.086/year for RCP 8.5. Figure 4.20 compares the two trends where just as in RCP 4.5; seasons with warmer (cooler) temperatures correspond with seasons of less (more) lake-induced belt snowfall. Here, the relationship (R^2=0.82, $p < 0.0001$) between temperature and snowfall is stronger (Figure 4.21).

For both scenarios, with correlations above 0.55 R^2, it is reasonable to conclude that two-meter temperature of the region has a significant impact on the lake-induced grid cell's snowfall. The relationship between two-meter temperature and the snow defined as lake-induced is examined, and as expected, because of the minimal significance of the change in lake-induced snow over time, there is no correlation to two-meter temperature changes.

4.3 Percentage of Precipitation Falling as Snow

The previous analysis suggests a strong association between simulated increases in two-meter temperatures and decreases in snowfall. However, it is unclear whether total precipitation is decreasing in response to warming, or whether the ratio of snowfall to precipitation is decreasing. Examination of the total precipitation (snowfall and liquid) during the snowfall season (October – March), indicates that both RCP scenarios show increases through the study period. The ensemble mean in RCP 4.5 has an increase of 6.28 cm of precipitation (R^2=0.24, $p<0.0001$) over the 94-season period, or a 12% increase from the average of the first decade (Figure 4.22). The ensemble mean of RCP 8.5 shows a similar increase of 6.30 cm of precipitation (R^2=0.26, $p<0.0001$), an 11% increase from the initial decade of the study period (Figure 4.23).

When comparing the difference in precipitation between the lake-induced belt and non-lake-induced grid cells, there is almost a 40% strengthening in the magnitude of the negative trend between the two types. This means non-lake-induced cells show a faster increasing trend in precipitation over time for both RCPs. It should be noted however, that this 40% negative increase has a value of only 1.1 cm of precipitation. The relationships between precipitation and temperature are present (R^2=0.24-0.26, $p < 0.0001$). However, because both classifications show increasing trends in precipitation for both RCP scenarios, this implies that changes in precipitation magnitude are not responsible for the decline in snowfall. On an interesting note, there is a difference in the magnitude of precipitation values between the lake-induced belt and the non-lake-induced cells. For RCP 4.5 precipitation values of the ensemble mean are 2.9 cm greater on average in the non-lake-induced grid cells than in the lake-induced belt (Figure 4.24). RCP 8.5 also shows greater precipitation in the non-lake-induced cells on the order of 3.35 cm (Figure 4.25). This indicates that while there is more snowfall in the lake-induced belt, there is actually less overall precipitation for both RCPs in comparison to non-lake-induced cells.

An examination of the ratio of snowfall to total precipitation suggests that warmer temperatures are associated with decreasing snowfall over time, at different rates depending on the grid cell classification. The non-lake-induced grid cells have an ensemble mean decrease in the percentage of precipitation falling as snow of 31% (R^2=0.56, $p<0.0001$), declining from roughly 27% during the first decade to roughly 18.5% by the last decade in RCP 4.5 (Figure 4.26). In RCP 8.5 there is a more pronounced decrease of 50% (R^2=0.80) in the percentage of precipitation falling as snow, declining from approximately 28% to 14% (Figure 4.27). The respective RCP correlations of the percent of snow to two-meter temperature are 0.76 R^2 and 0.86 R^2 with $p < 0.0001$. In the lake-induced belt, the decrease in the snow to total precipitation ratio is just over 29% (R^2=0.50, $p<0.0001$), declining from approximately 33% to 23% in RCP 4.5 over the study period (Figure 4.28). The decrease seen in RCP 8.5 is more pronounced just as in the non-lake-induced grid cells, with a decline in the percentage of precipitation falling as snow of 51% (R^2=0.77, $p<0.0001$) over the study period (Figure 4.29). The relative correlations to two-meter temperatures are also promising, with respective values of 0.75 and 0.85 R^2 ($p < 0.0001$).

The decrease in snowfall to total precipitation is very similar between the lake-induced belt and non-lake-induced grid cells for each RCP scenario. However, when comparing the lake-induced belt to the non-lake-induced grid cells, the magnitude of the differences was apparent. In RCP 4.5, an average difference of 15.7% (t-ratio: 29.44, $p < 0.0001$) occurs between the lake-induced belt and non-lake-induced grid cells' percentage of precipitation falling as snow. RCP 8.5 had a slightly lower average difference of 16.4% (t-ratio: 25.4, $p < 0.0001$), in favor of lake-induced grid cells. This means that across both scenarios, the lake-induced belt has a snow to precipitation ratio that is 15-16% higher, and that snowfall is more predominant here than in the non-lake-induced cells. This conclusion is reflected in the snowfall results discussed above. There is a decreasing trend in the difference between the 2 ratios over time for both RCP 4.5 and 8.5. RCP 4.5 declined by 18% (Figure 4.30) and RCP 8.5 declined by 53% (Figure 4.31). This implies that similar to the simulated snowfall data, the snowfall difference between the two grid types becomes less prominent over time and lake-induced snowfall is declining more rapidly than the overall snowfall that is not enhanced or induced by the lakes.

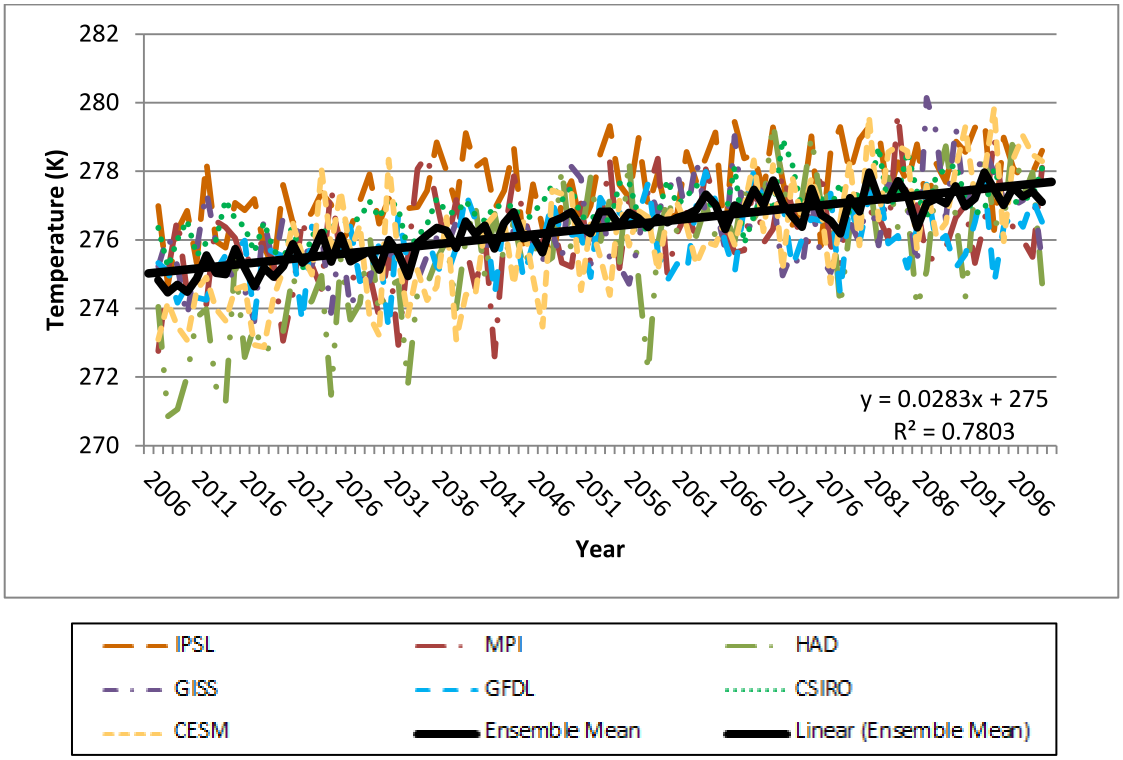

Figure 4.1. Lake Erie surface temperatures, RCP 4.5.

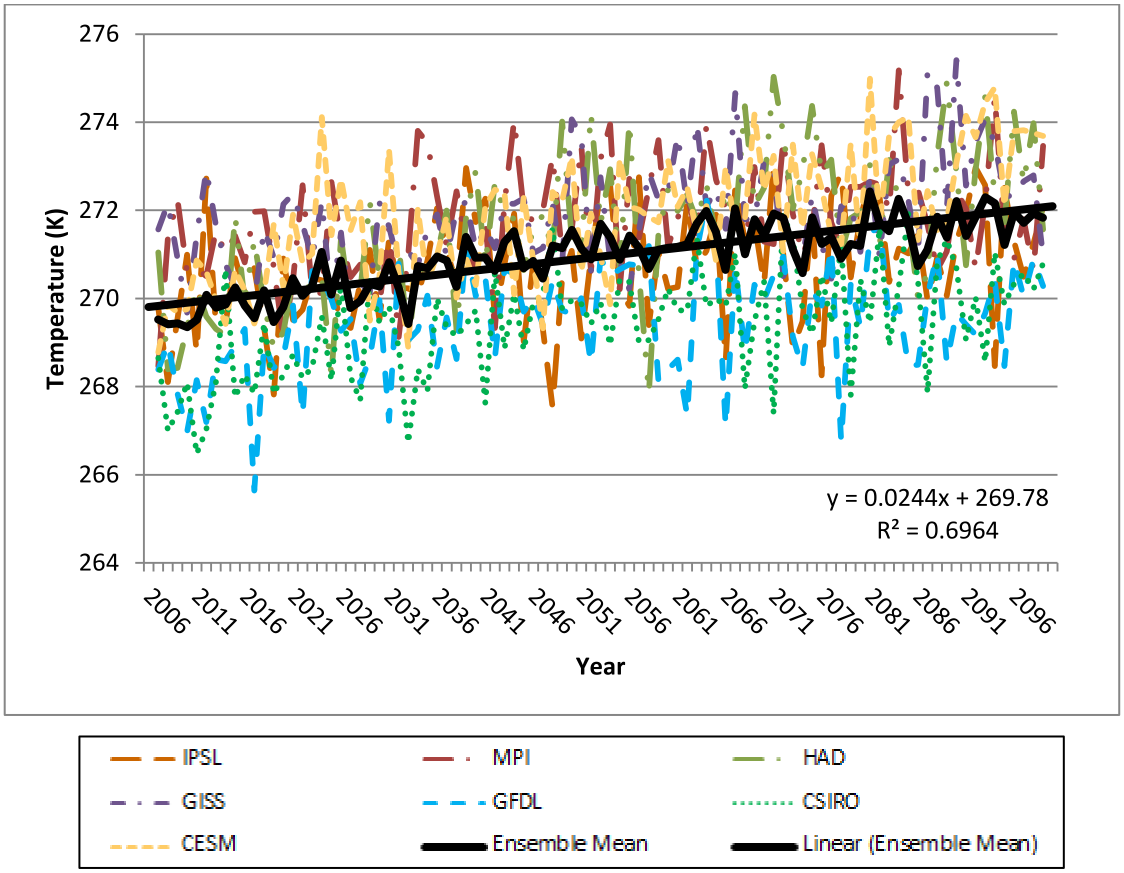

Figure 4.2. Lake Erie 850-hPa temperatures, RCP 4.5.

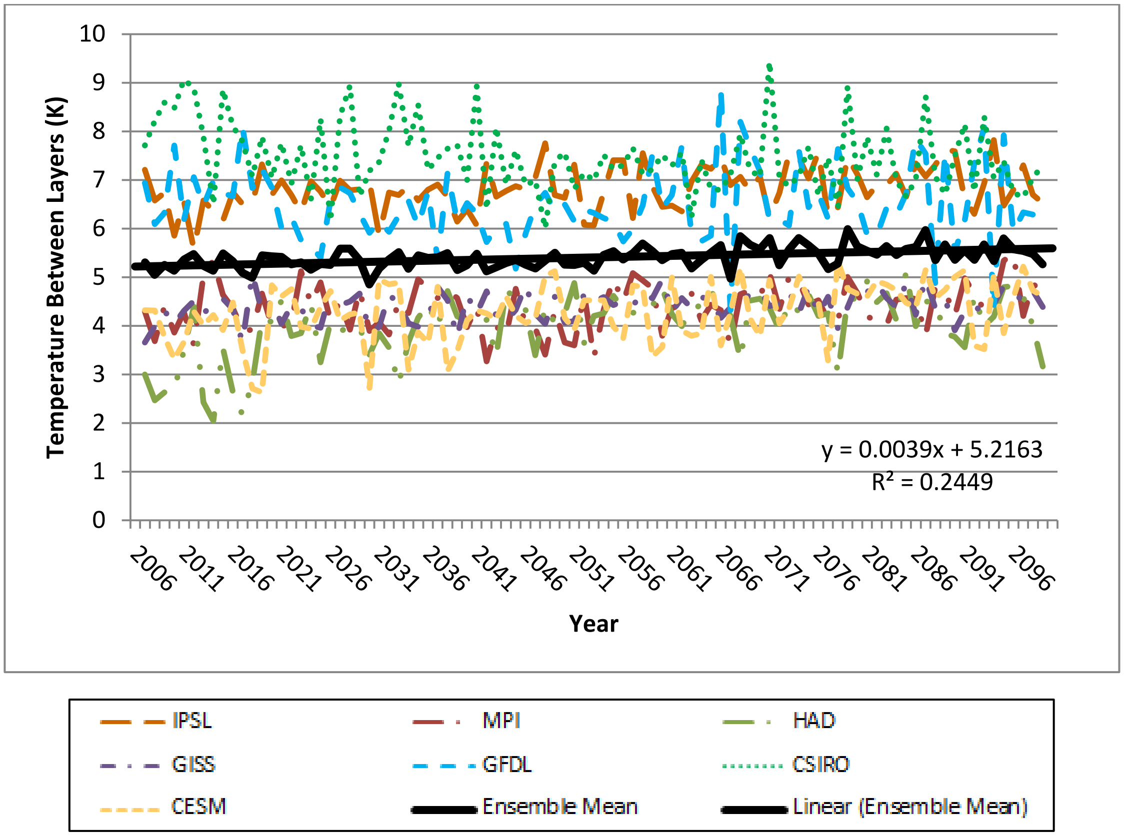

Figure 4.3. Lake Erie lapse rates, RCP 4.5.

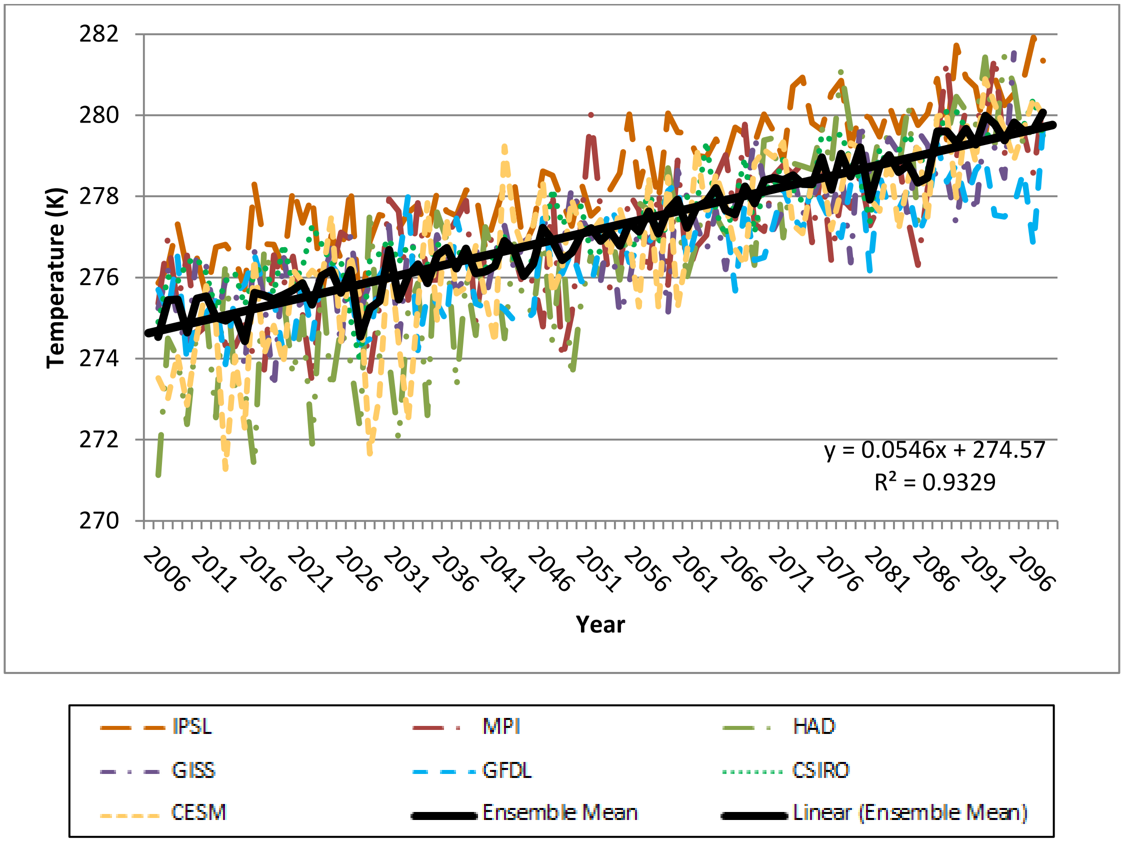

Figure 4.4. Lake Erie surface temperatures, RCP 8.5.

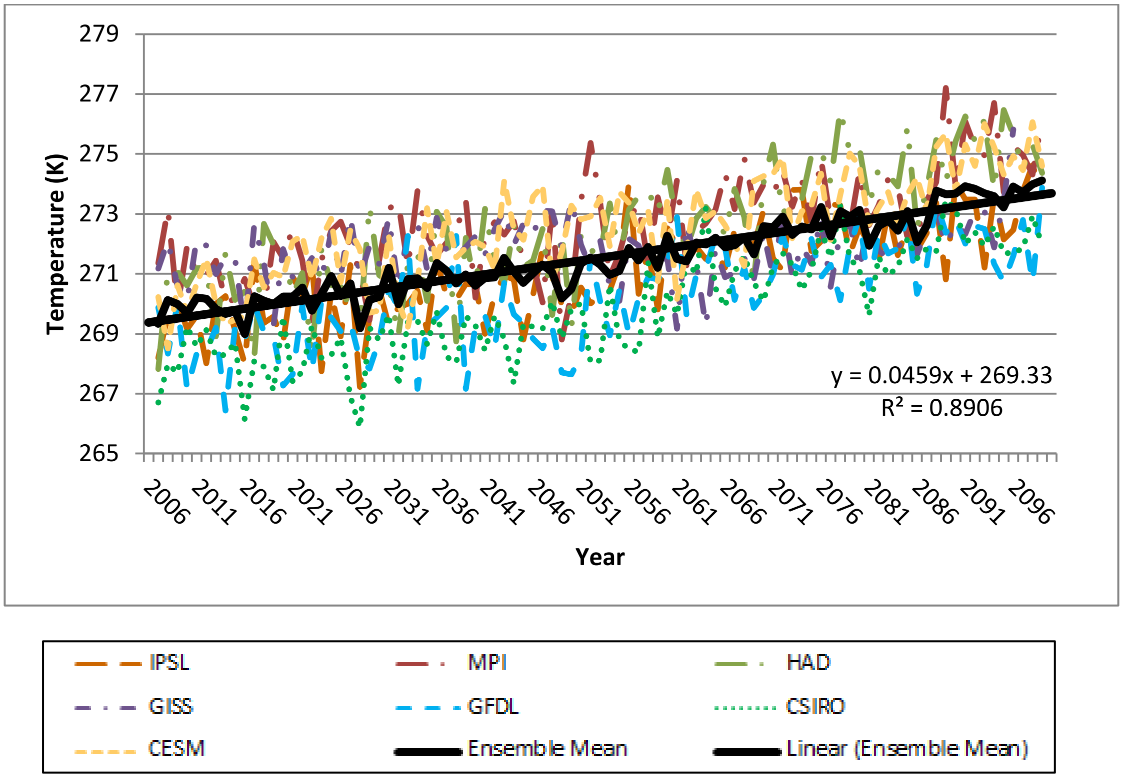

Figure 4.5. Lake Erie 850-hPa temperatures, RCP 8.5.

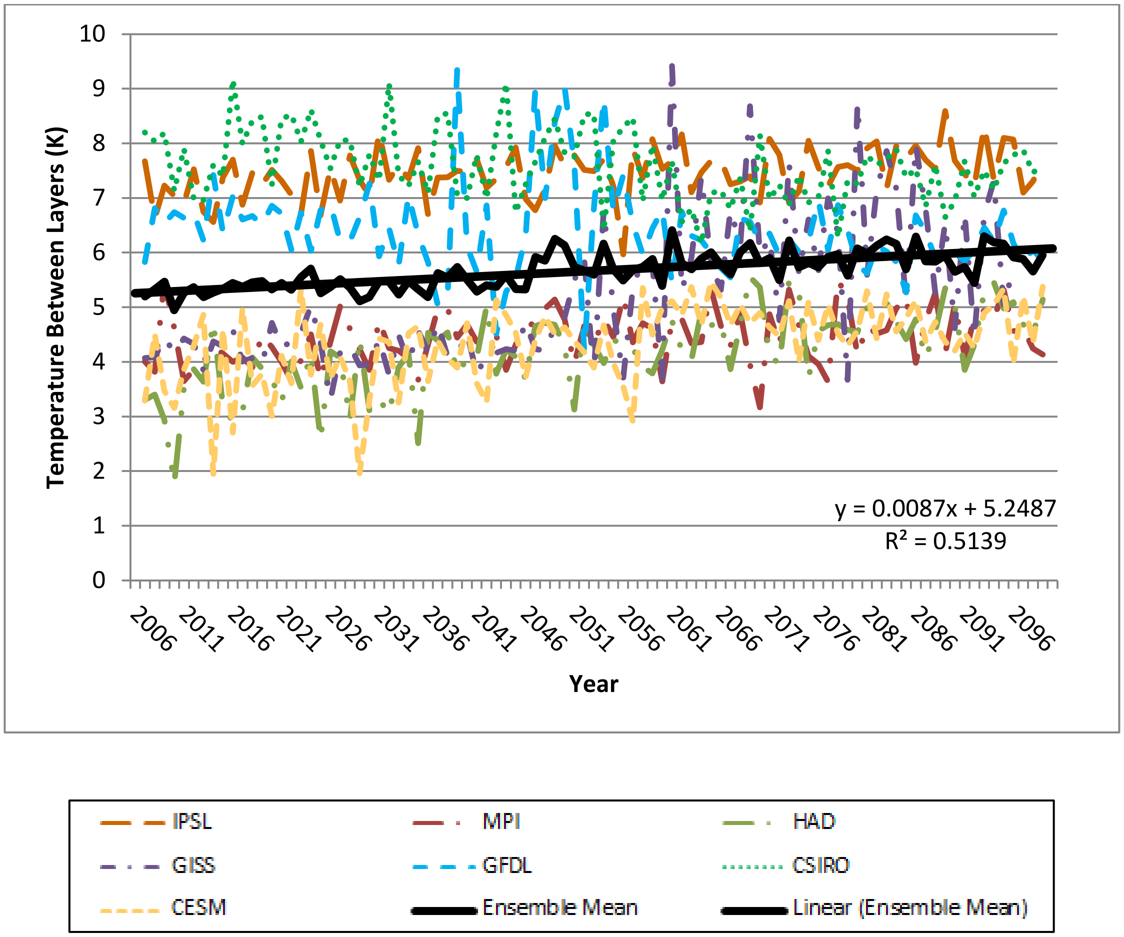

Figure 4.6. Lake Erie lapse rates, RCP 8.5.

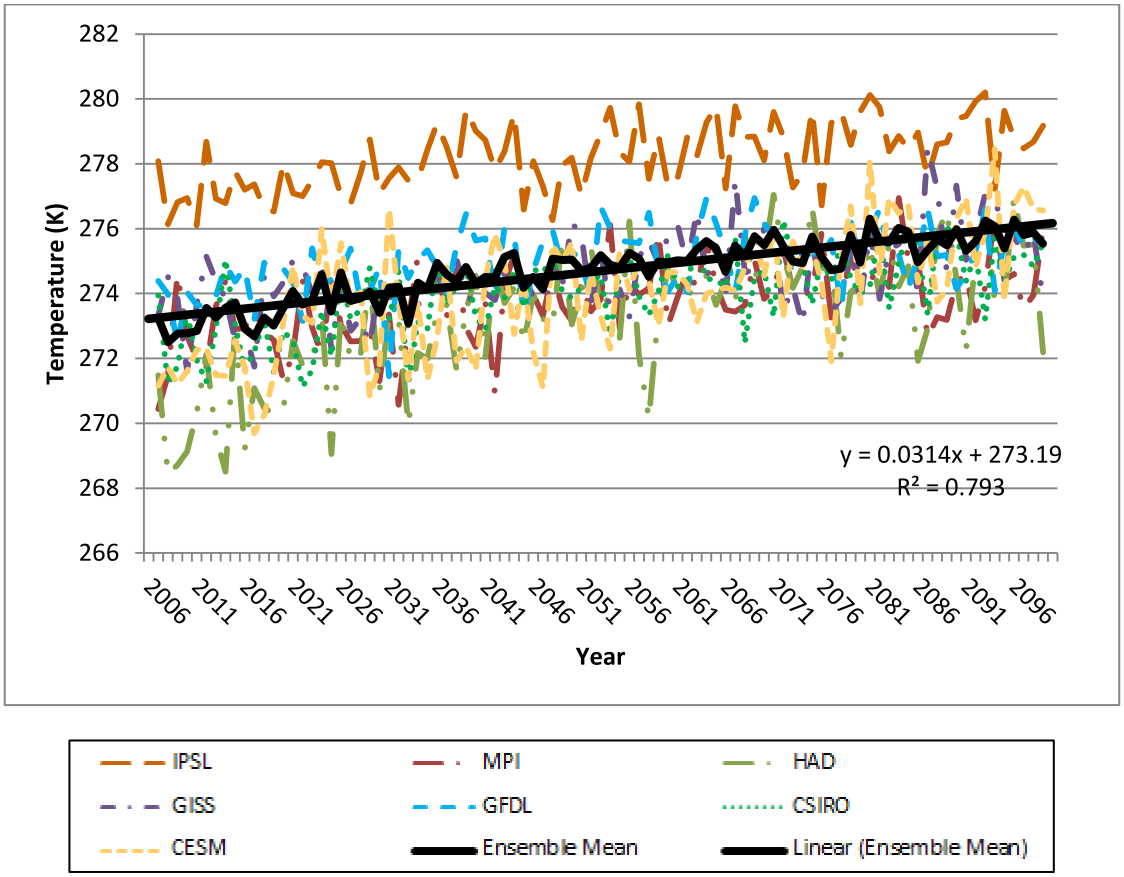

Figure 4.7. Lake Ontario surface temperatures, RCP 4.5.

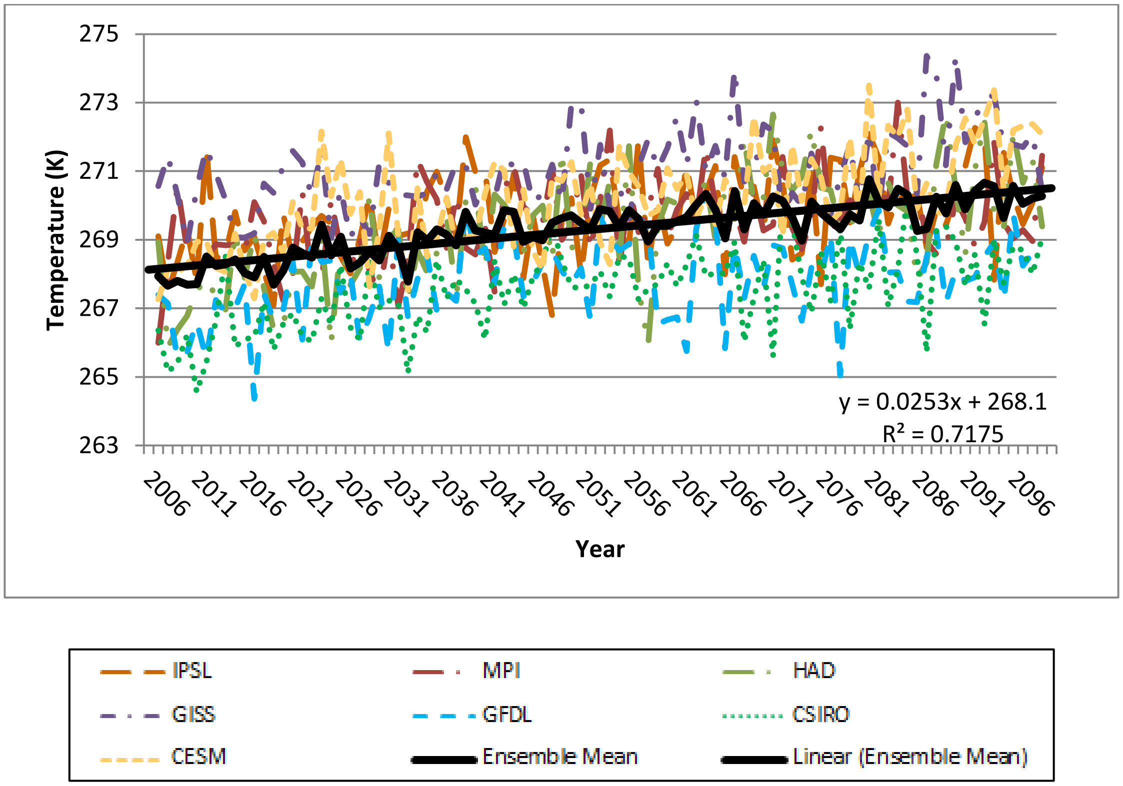

Figure 4.8. Lake Ontario 850-hPa temperatures, RCP 4.5.

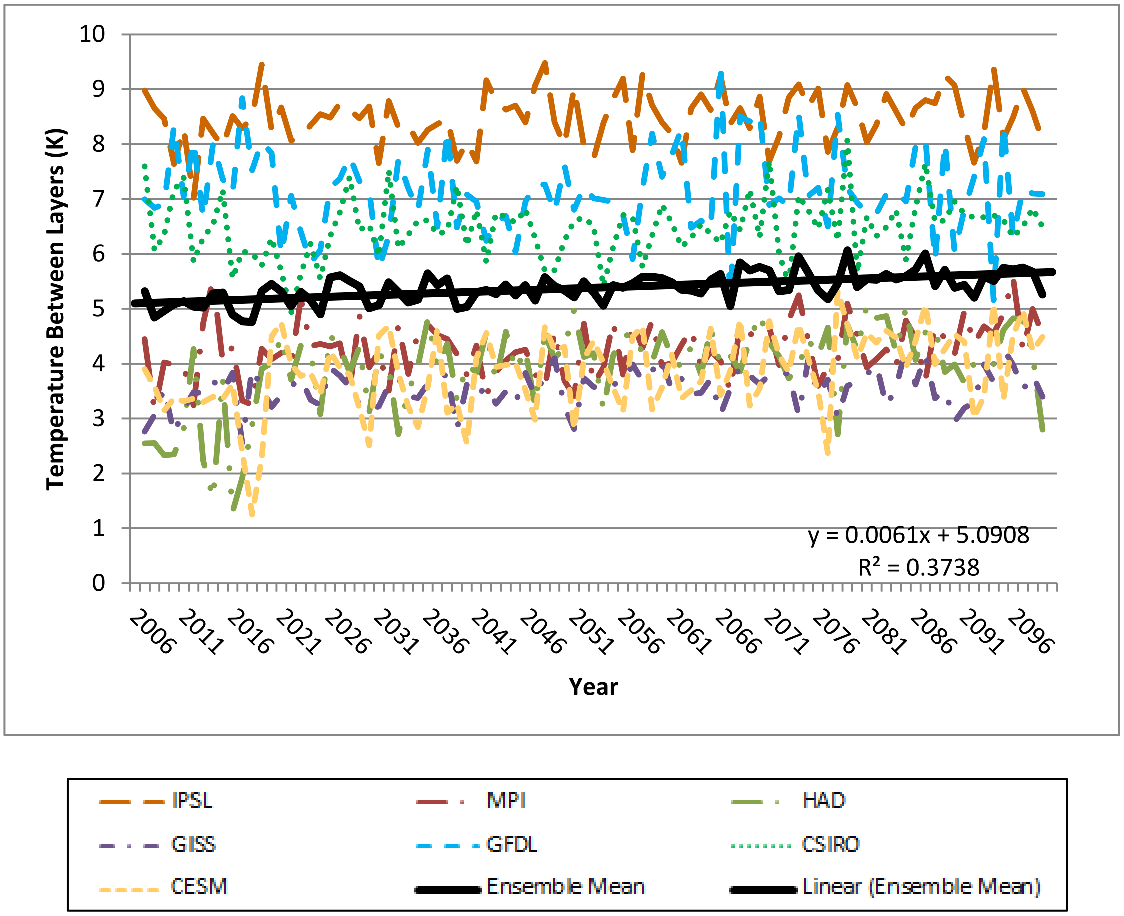

Figure 4.9. Lake Ontario lapse rates, RCP 4.5.

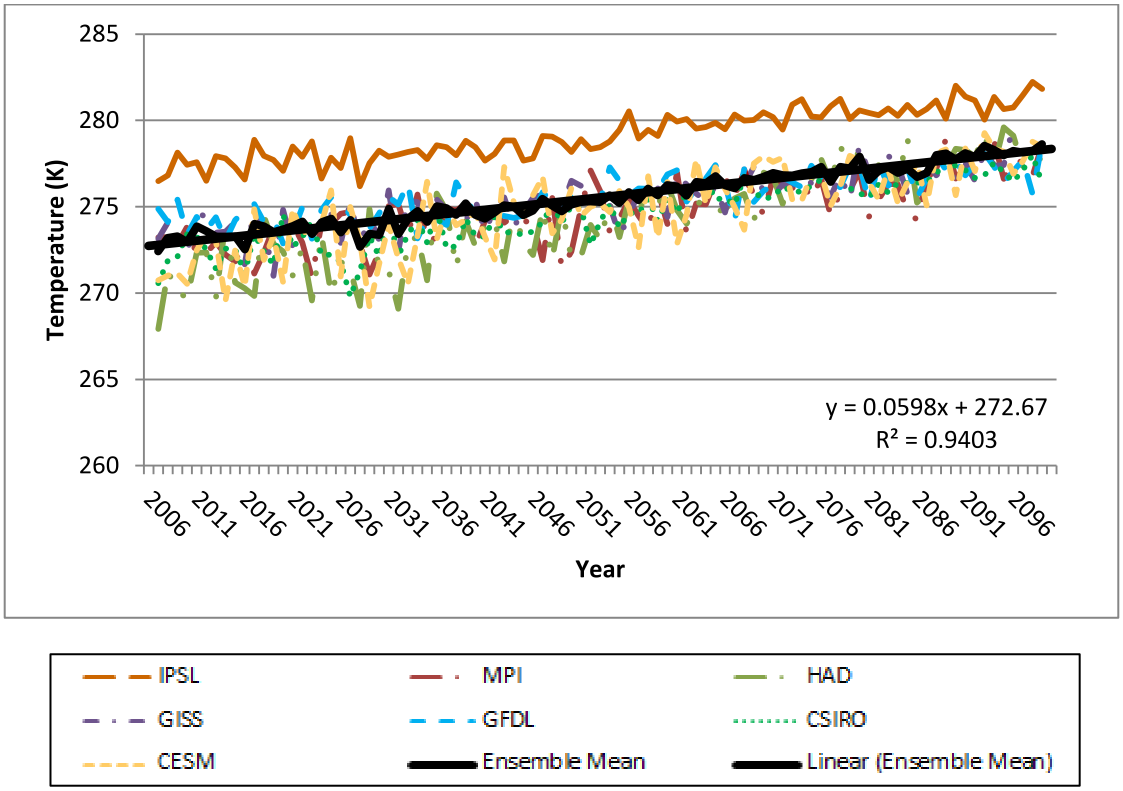

Figure 4.10. Lake Ontario surface temperatures, RCP 8.5.

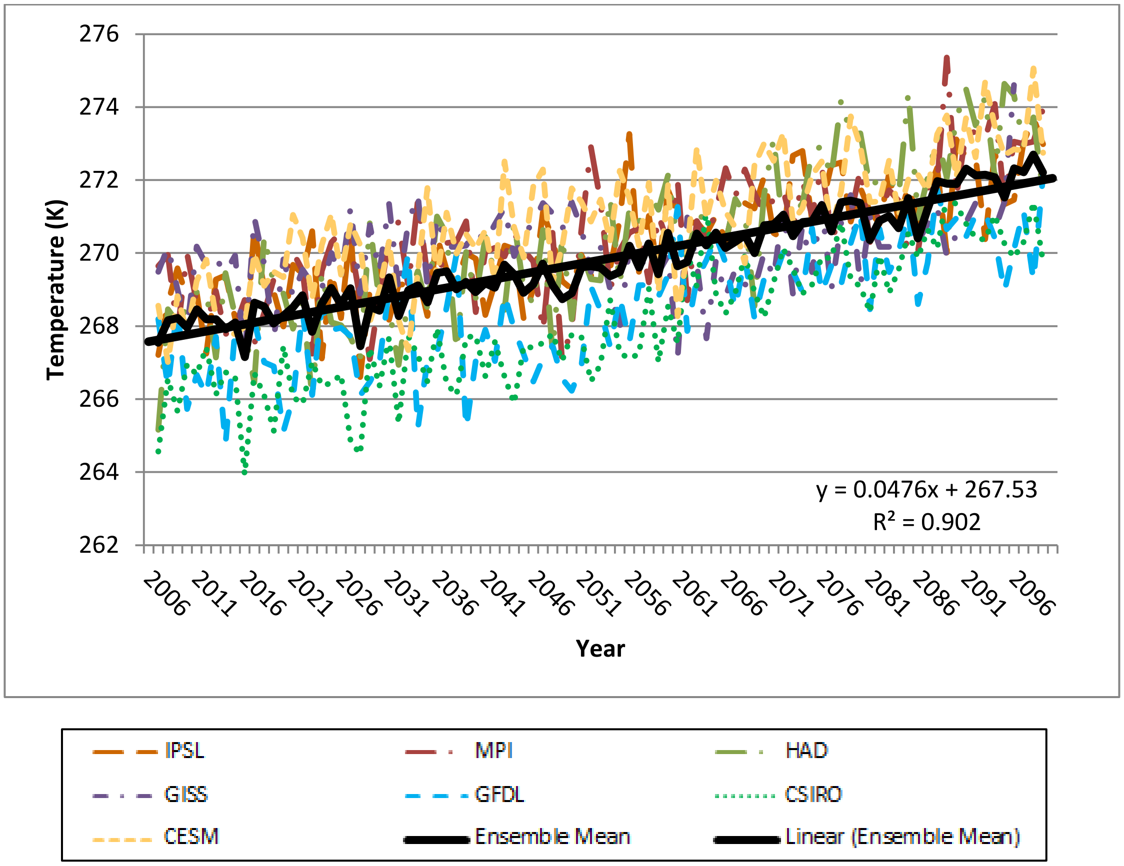

Figure 4.11. Lake Ontario 850-hPa temperatures, RCP 8.5.

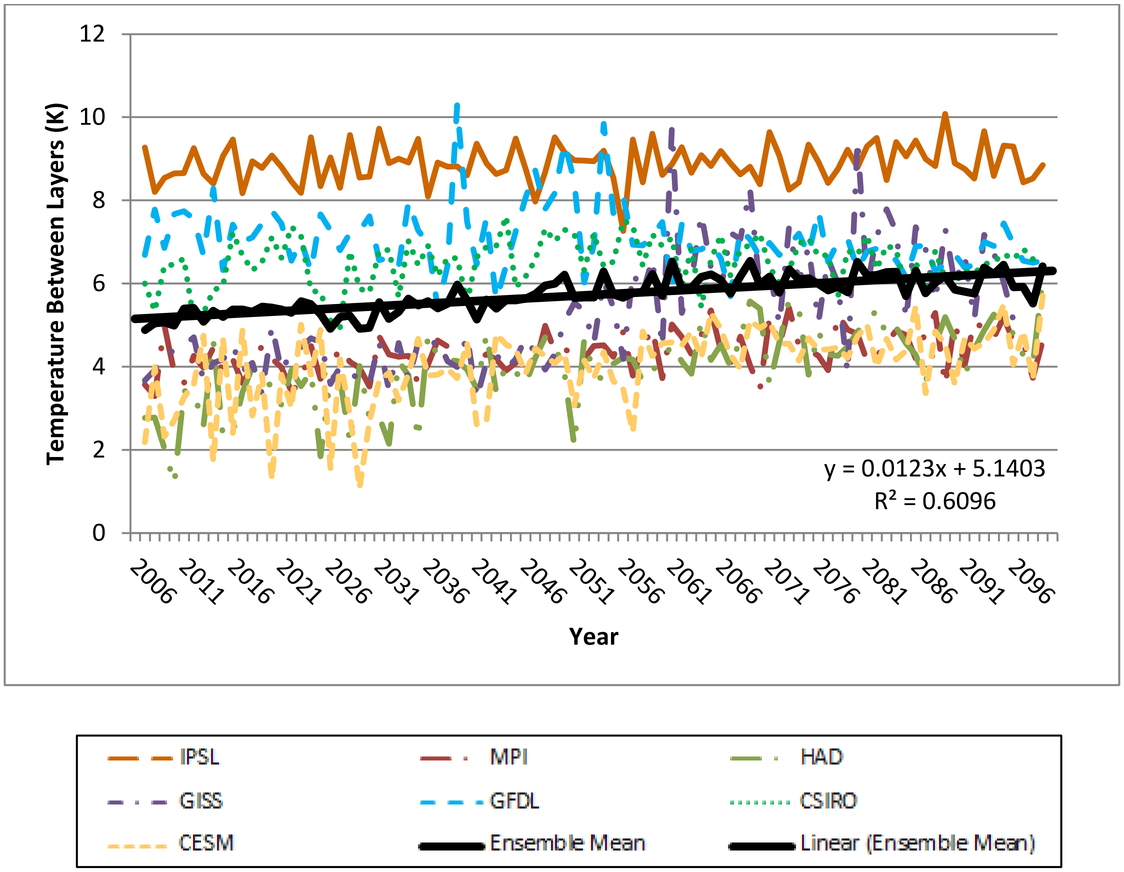

Figure 4.12. Lake Ontario lapse rates, RCP 8.5.

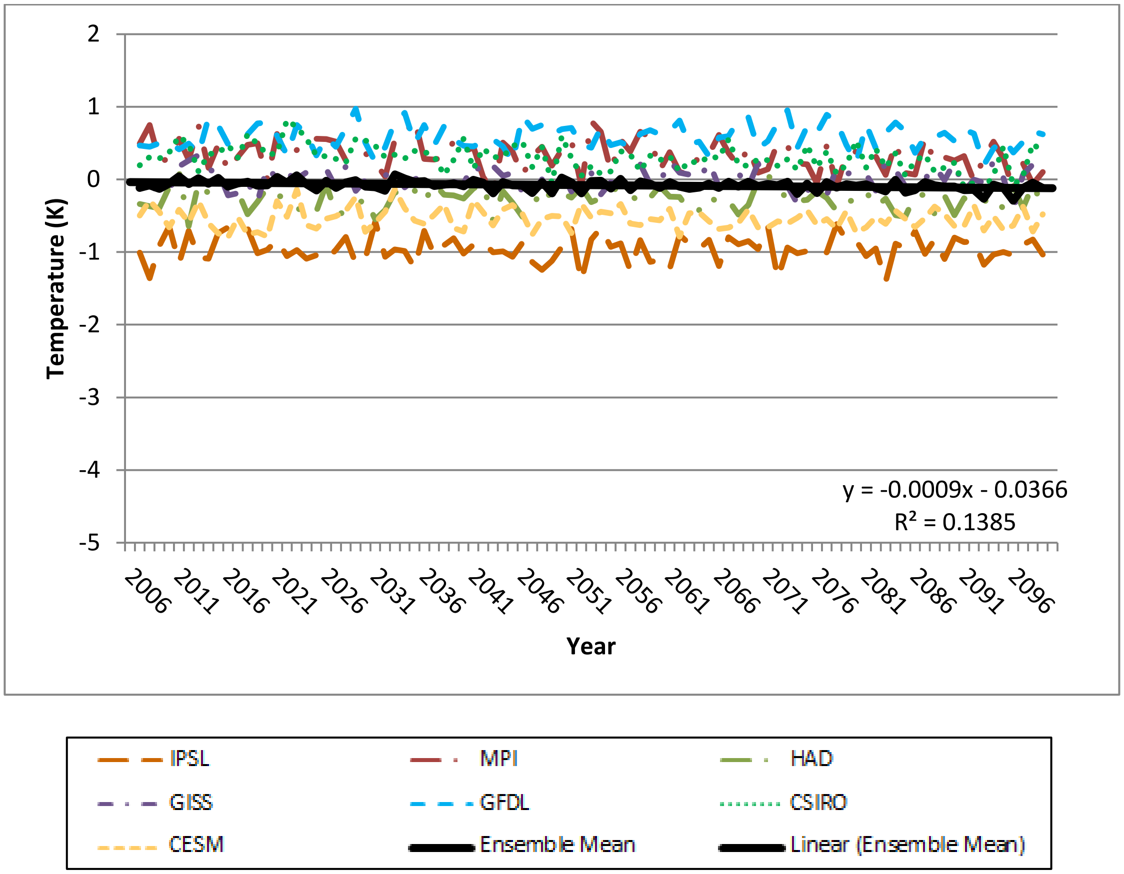

Figure 4.13. Two-meter temperature differences between the lake-induced belt and non-lake-induced grid cells, RCP 4.5.

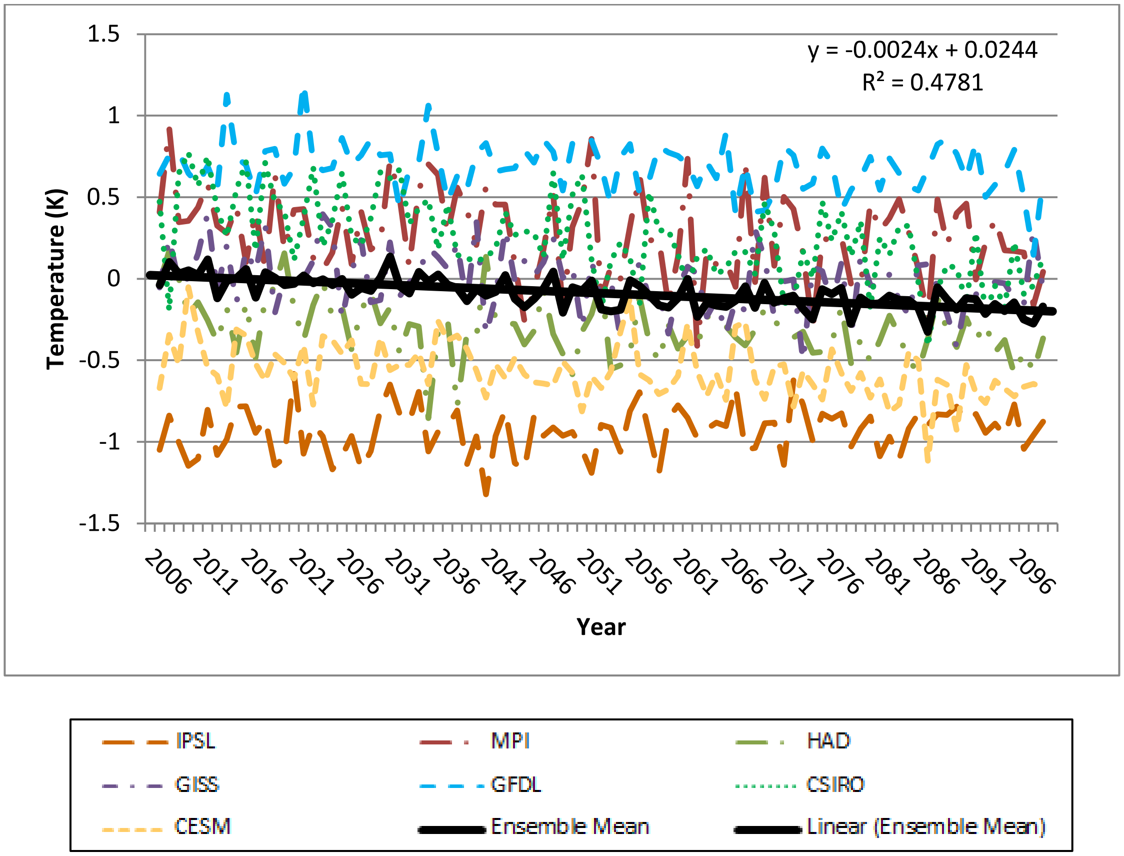

Figure 4.14. Two-meter temperature differences between the lake-induced belt and non-lake-induced grid cells, RCP 8.5.

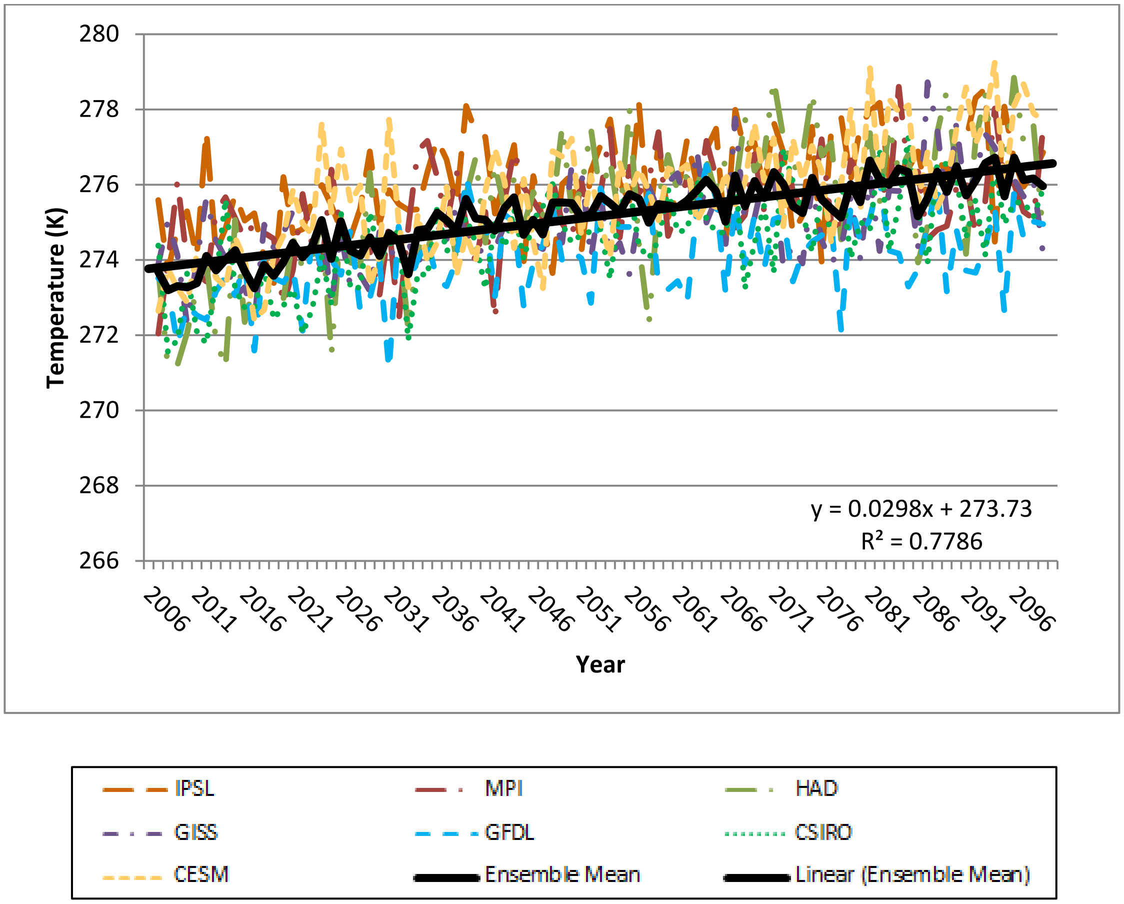

Figure 4.15. Two-meter temperatures, RCP 4.5.

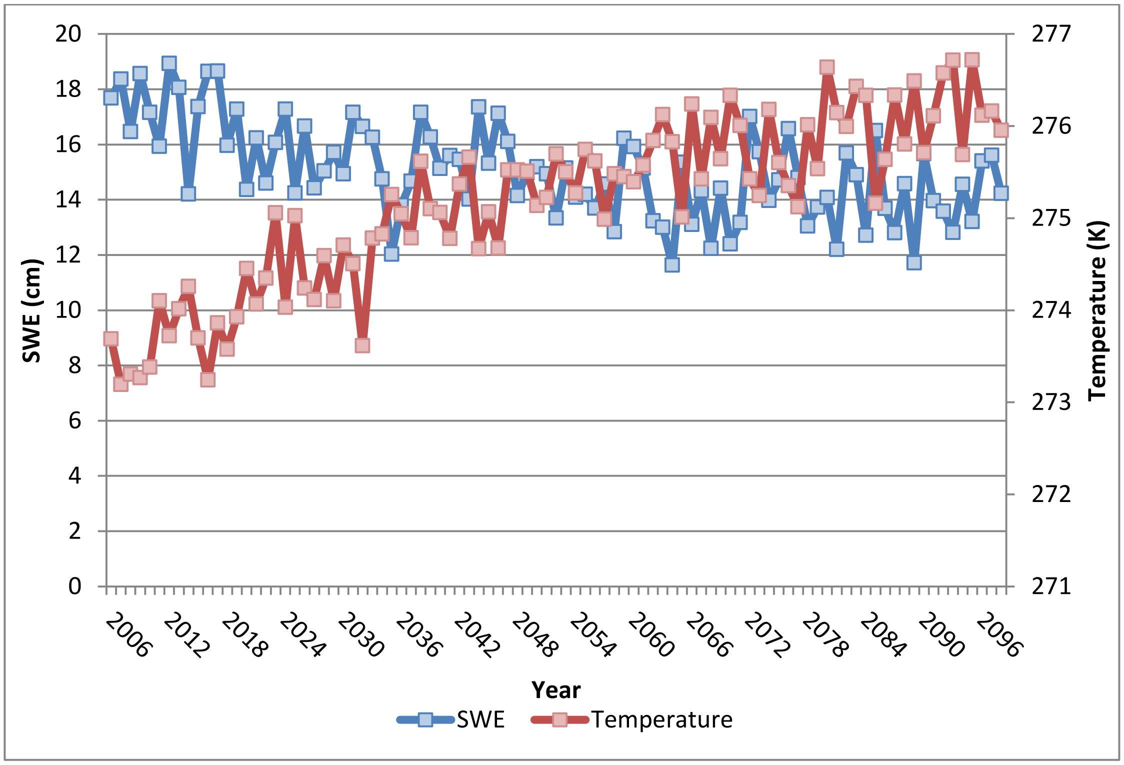

Figure 4.16. Two-meter temperature and lake-induced belt snowfall ensemble means, RCP 4.5.

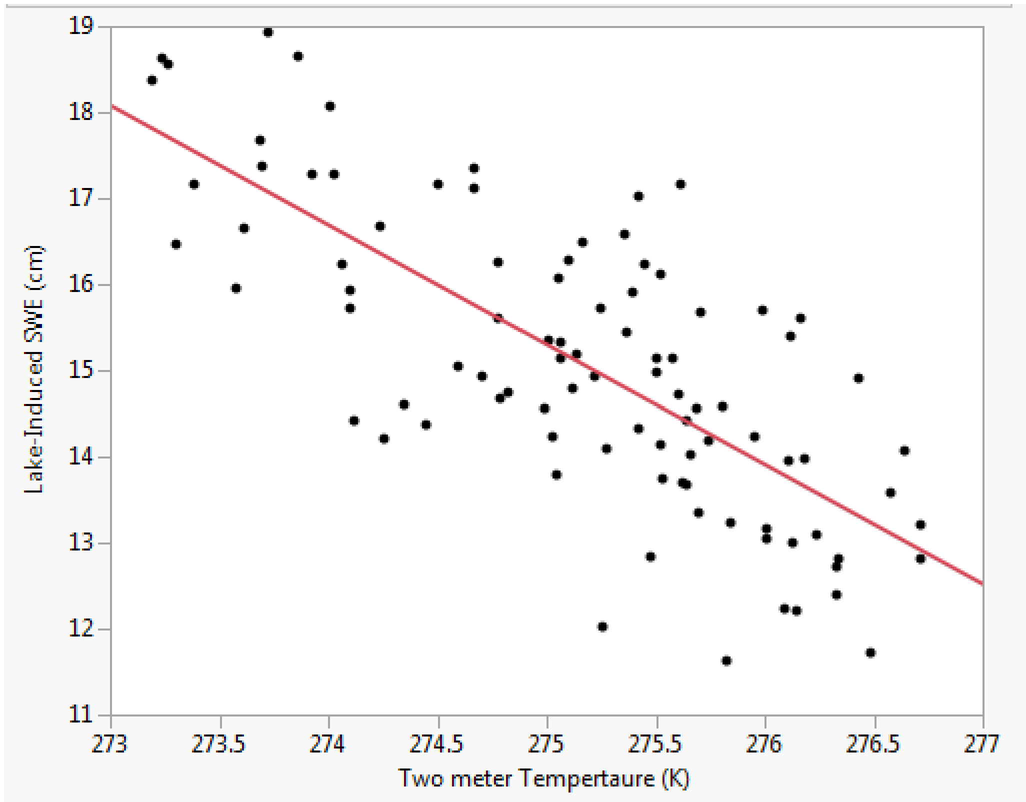

Figure 4.17. Two-meter temperature and the lake-induced belt snowfall relationship, RCP 4.5 ($R^2 = 0.55$, $p<0.0001$).

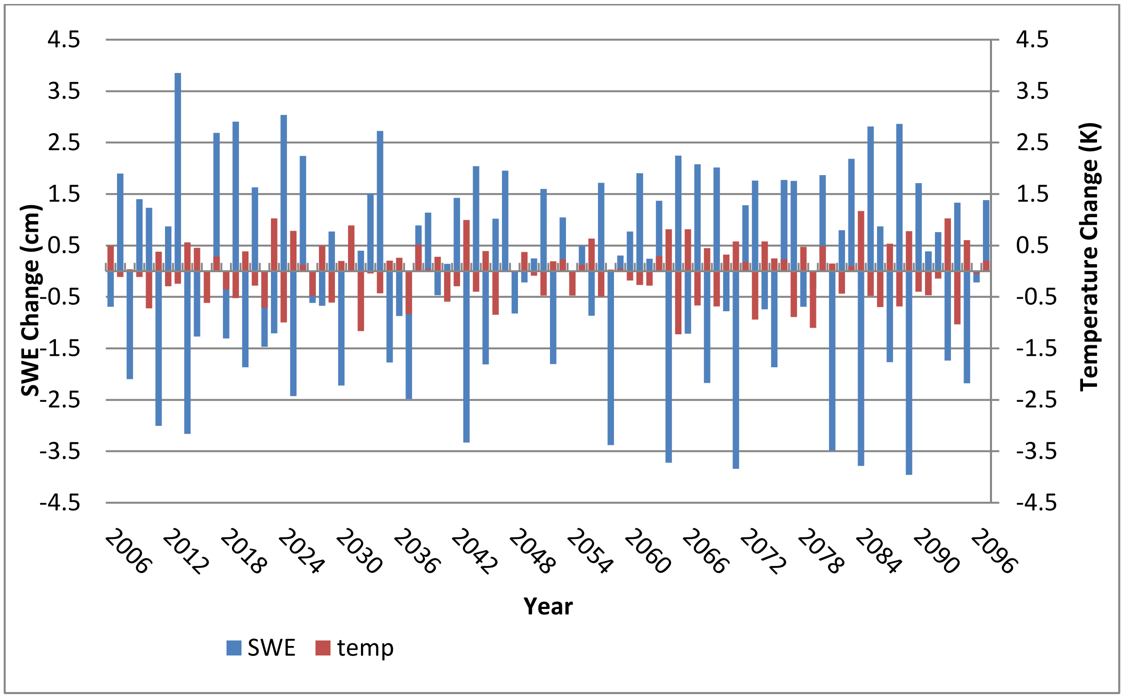

Figure 4.18. Seasonal variability of two-meter temperatures and lake-induced belt snowfall, RCP 4.5.

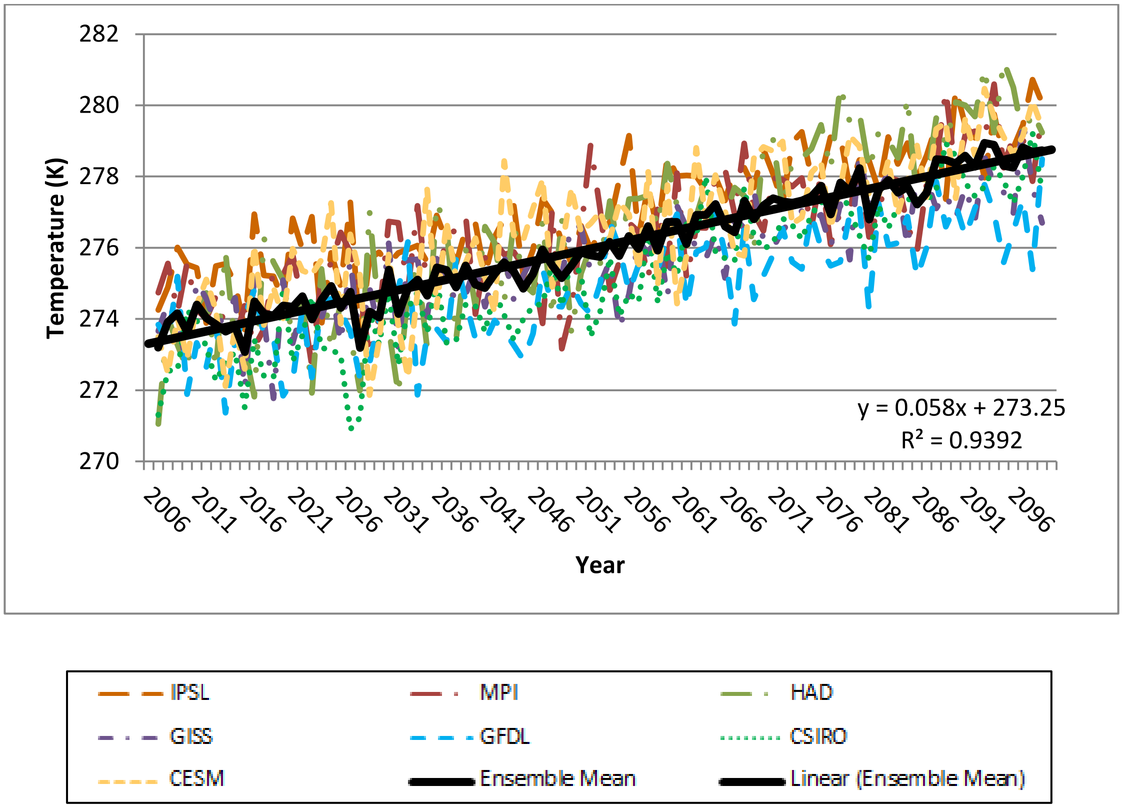

Figure 4.19. Two-meter temperatures, RCP 8.5.

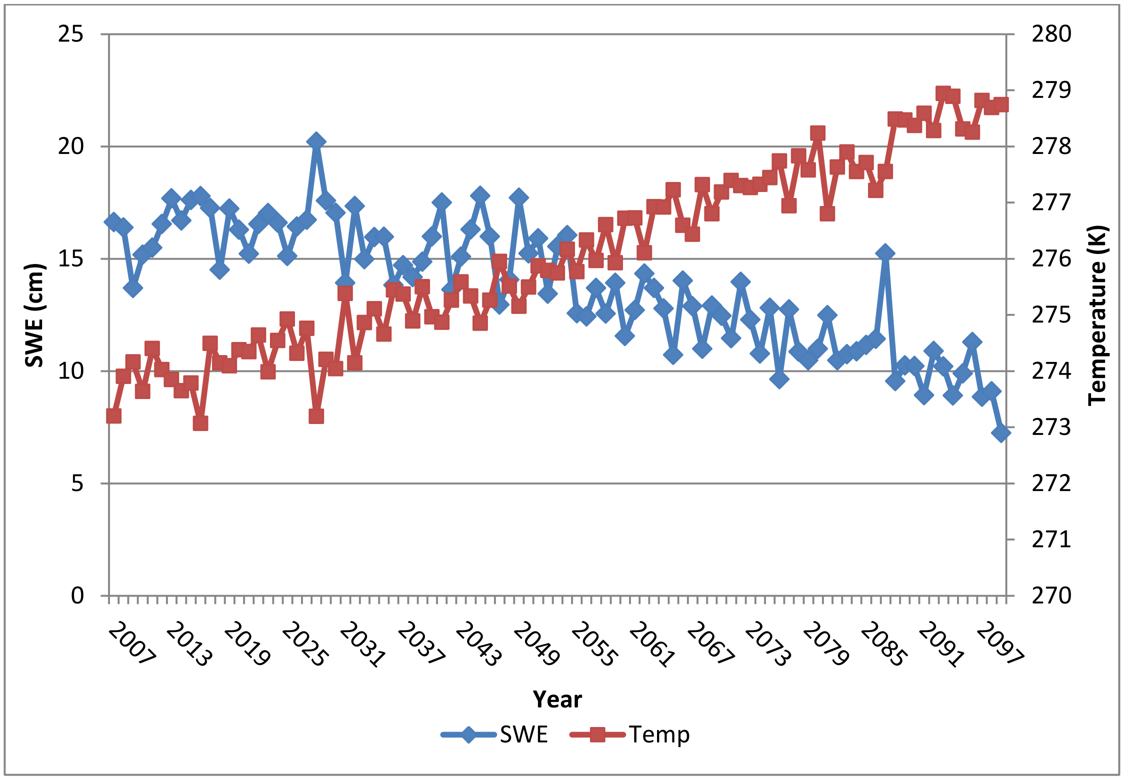

Figure 4.20. Two-meter temperature and lake-induced belt snowfall ensemble means, RCP 8.5.

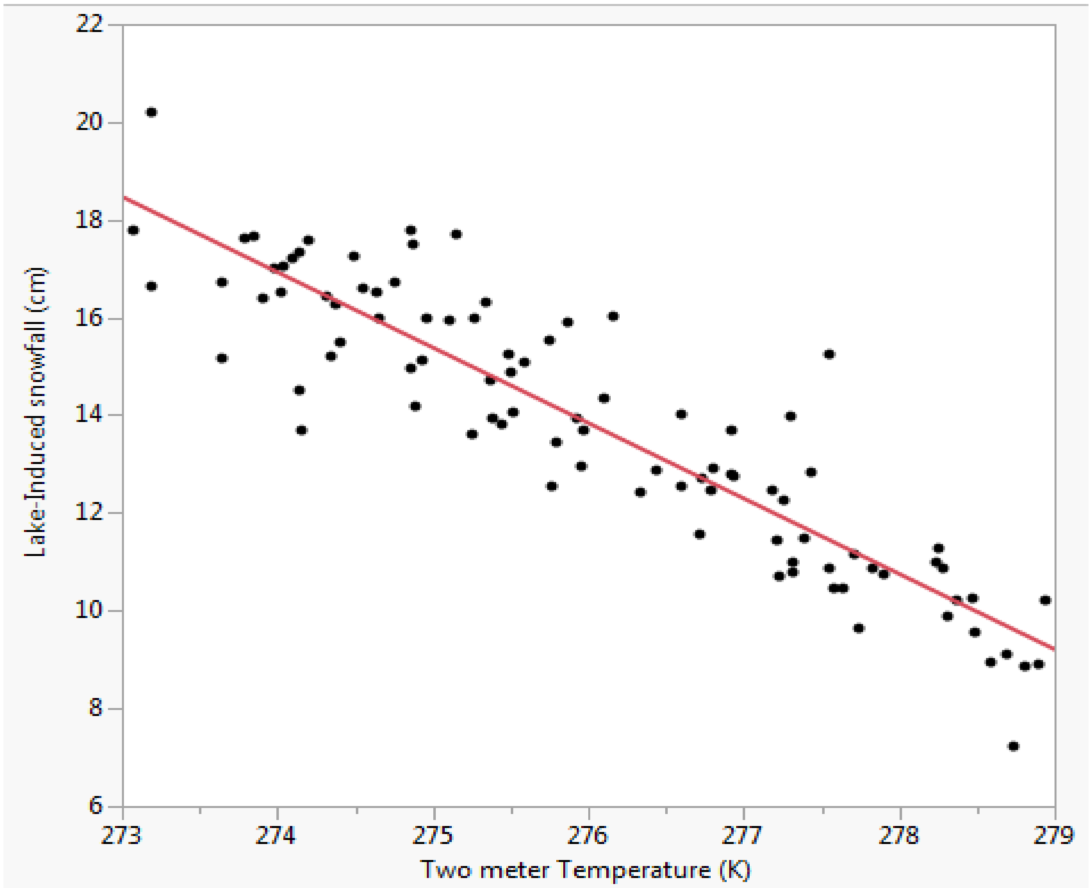

Figure 4.21. Two-meter temperature and lake-induced belt snowfall relationship, RCP 8.5 (R^2=0.83, p<0.0001).

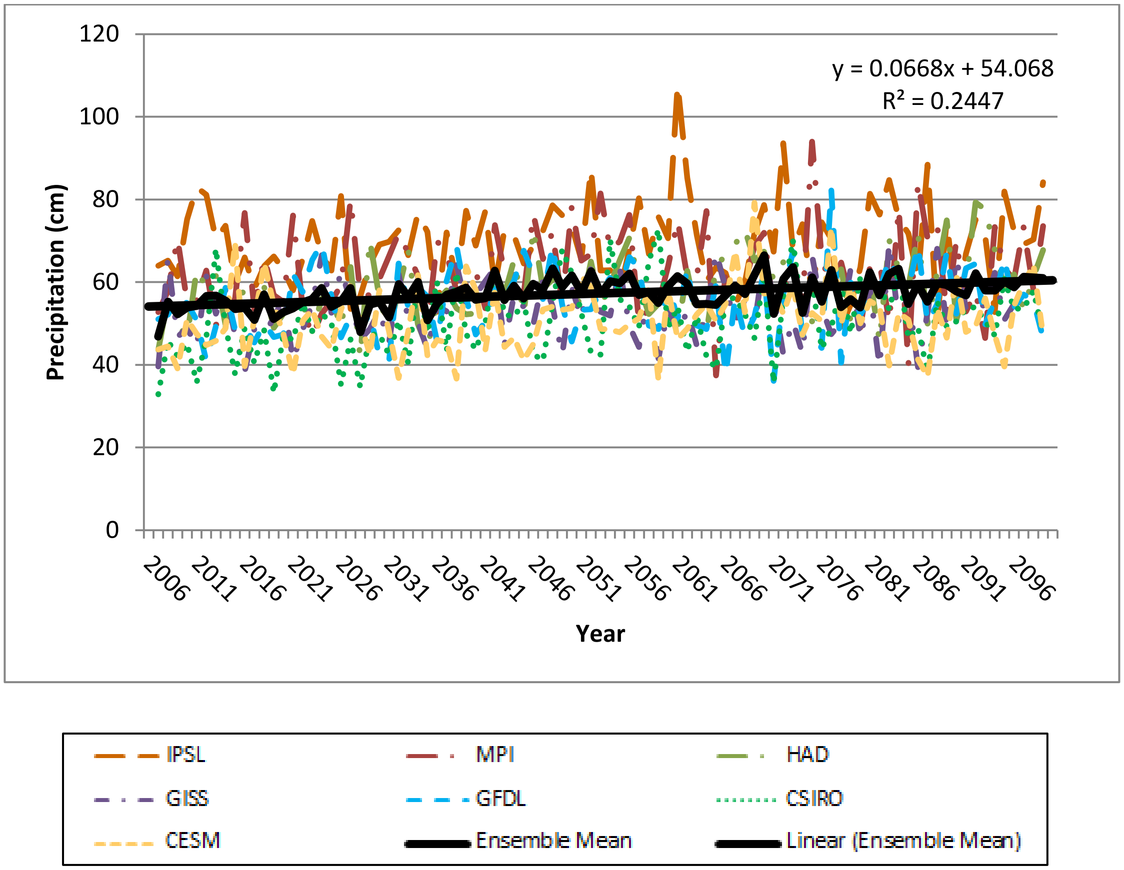

Figure 4.22. Regional precipitation total, RCP 4.5.

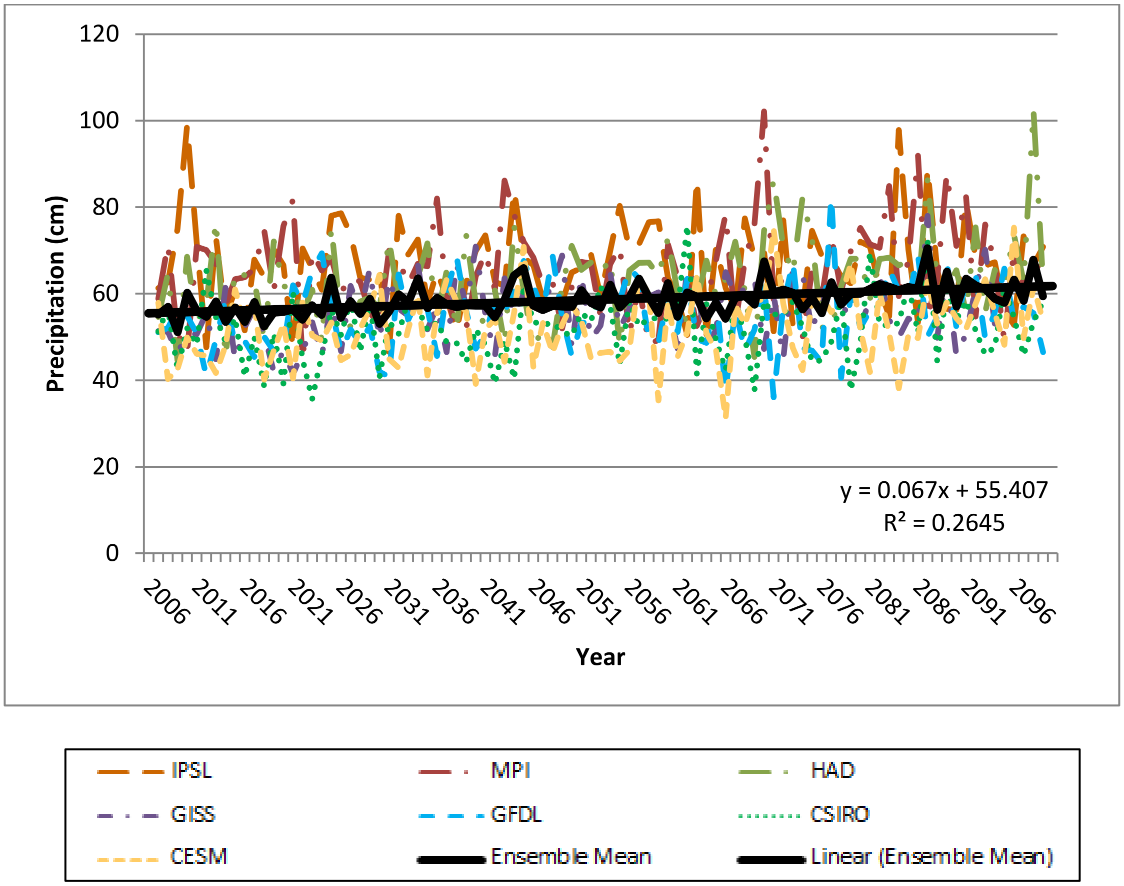

Figure 4.23. Regional precipitation total, RCP 8.5.

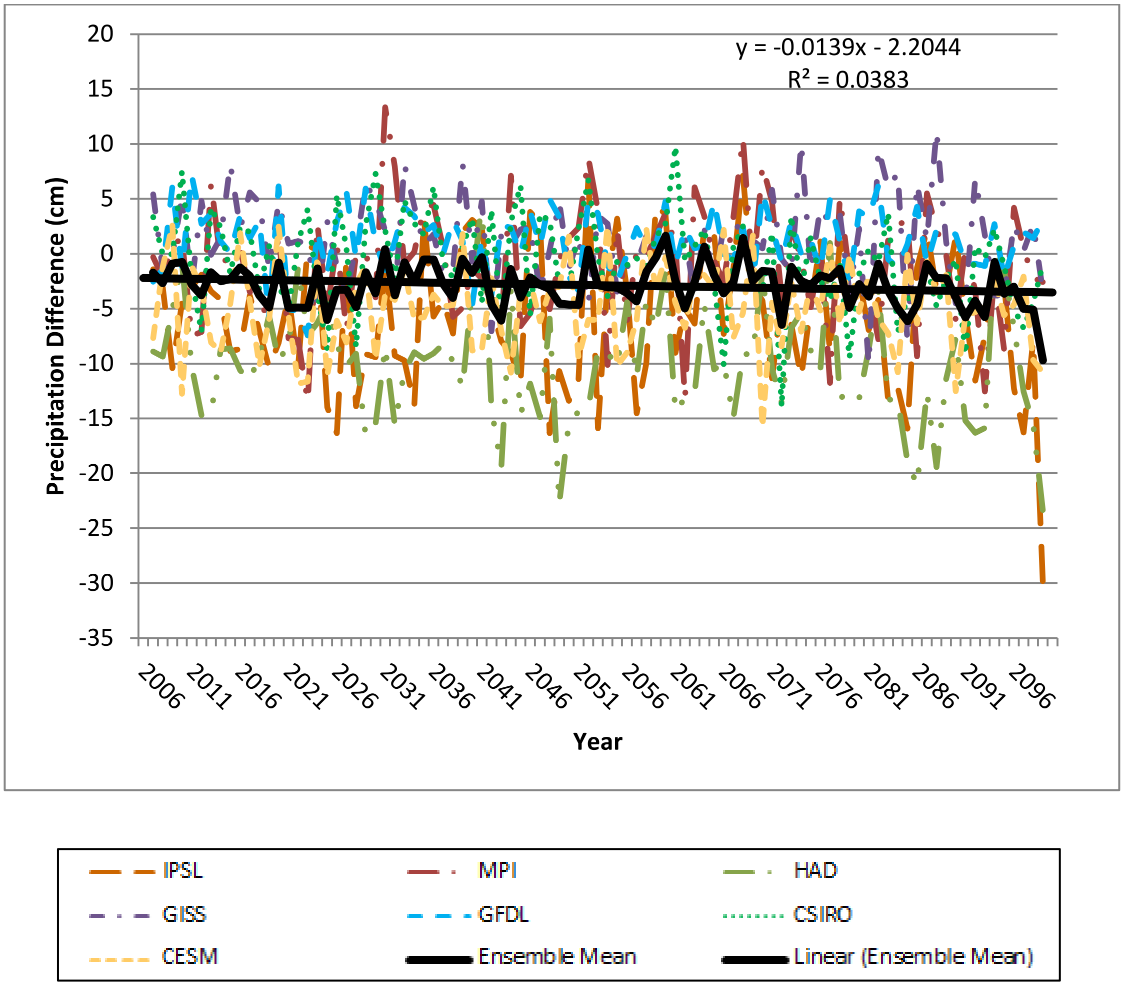

Figure 4.24. Lake-induced belt and non-lake-induced grid cell precipitation difference, RCP 4.5.

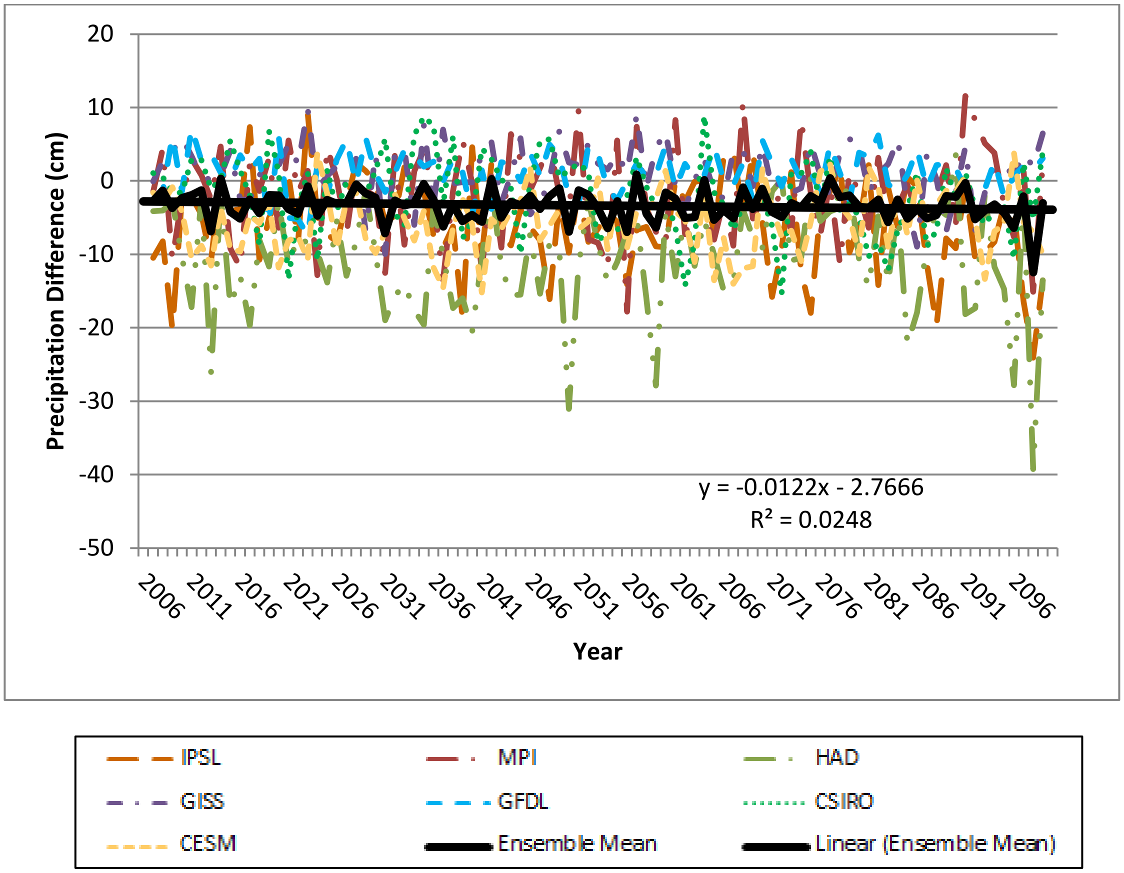

Figure 4.25. Lake-induced belt and non-lake-induced grid cell precipitation difference, RCP 8.5.

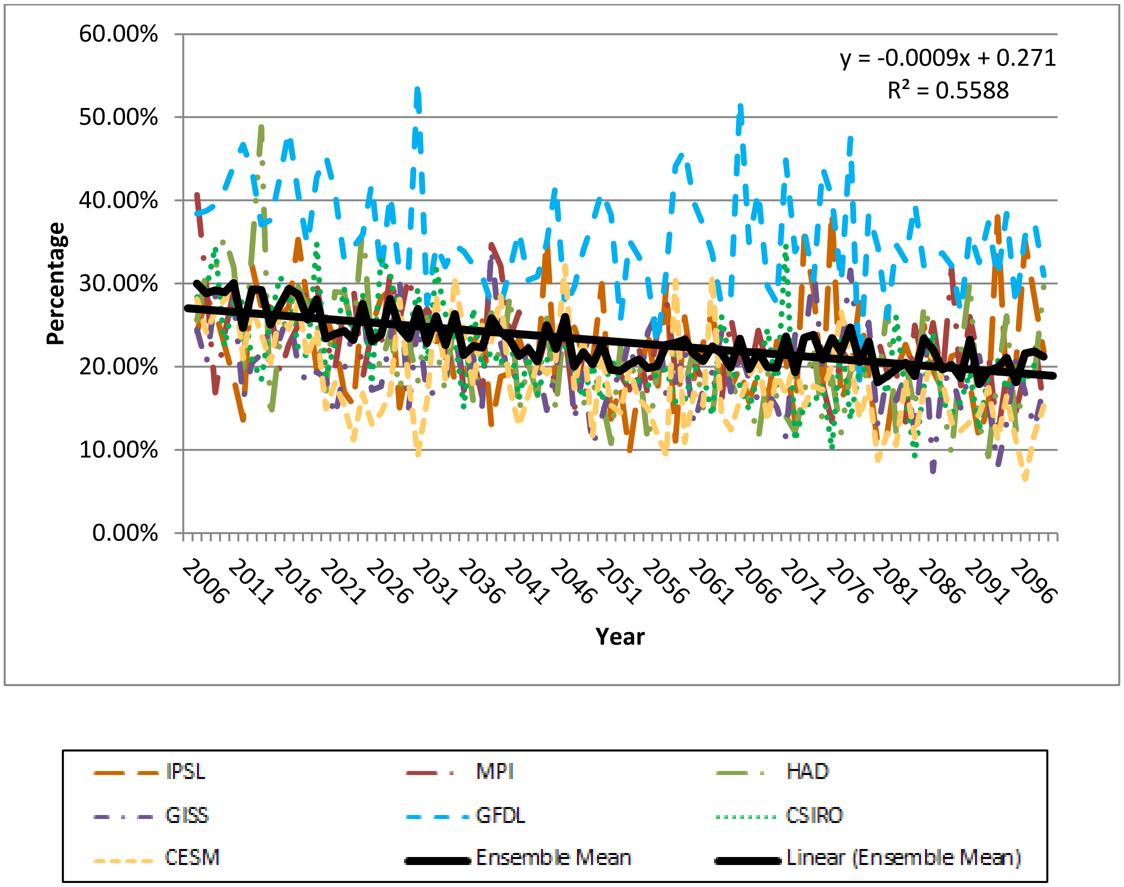

Figure 4.26. Percentage of precipitation falling as snow for non-lake-induced grid cells, RCP 4.5.

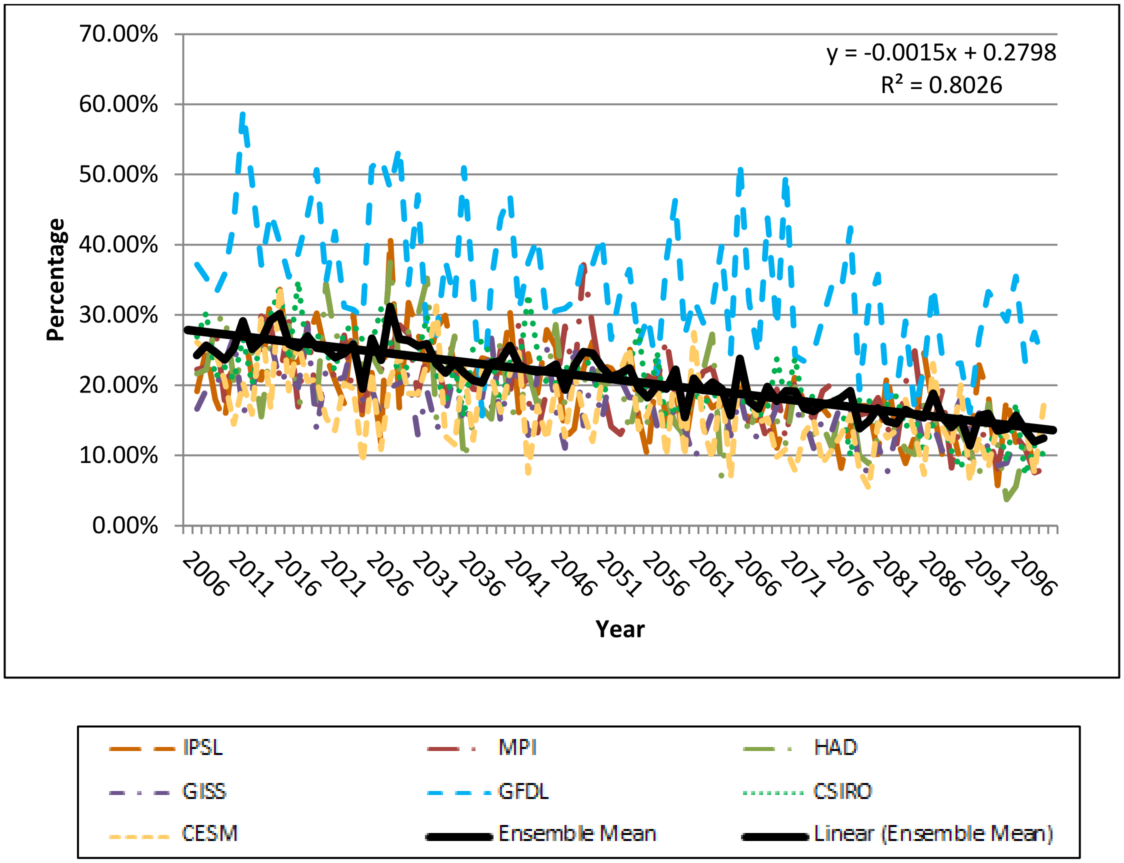

Figure 4.27. Percentage of precipitation falling as snow for non-lake-induced grid cells, RCP 8.5.

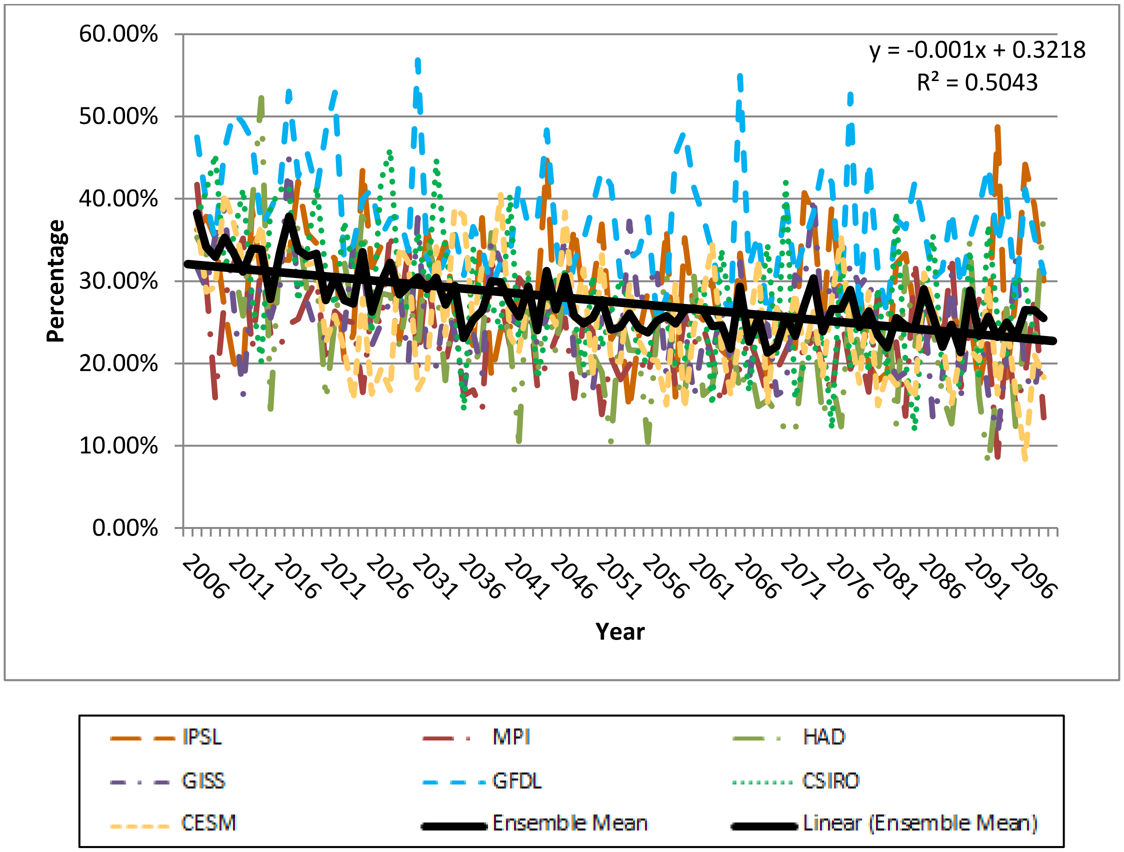

Figure 4.28. Percentage of precipitation falling as snow for lake-induced belt, RCP 4.5.

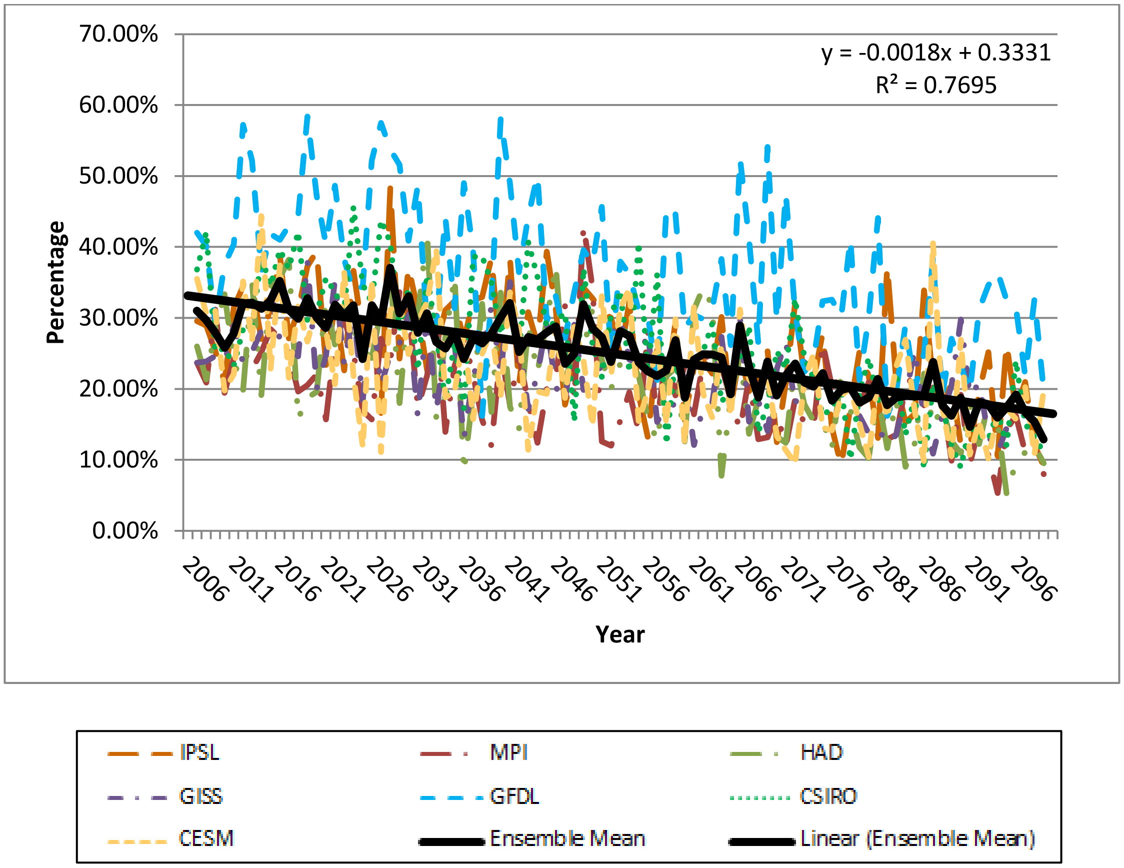

Figure 4.29. Percentage of precipitation falling as snow for lake-induced belt, RCP 8.5.

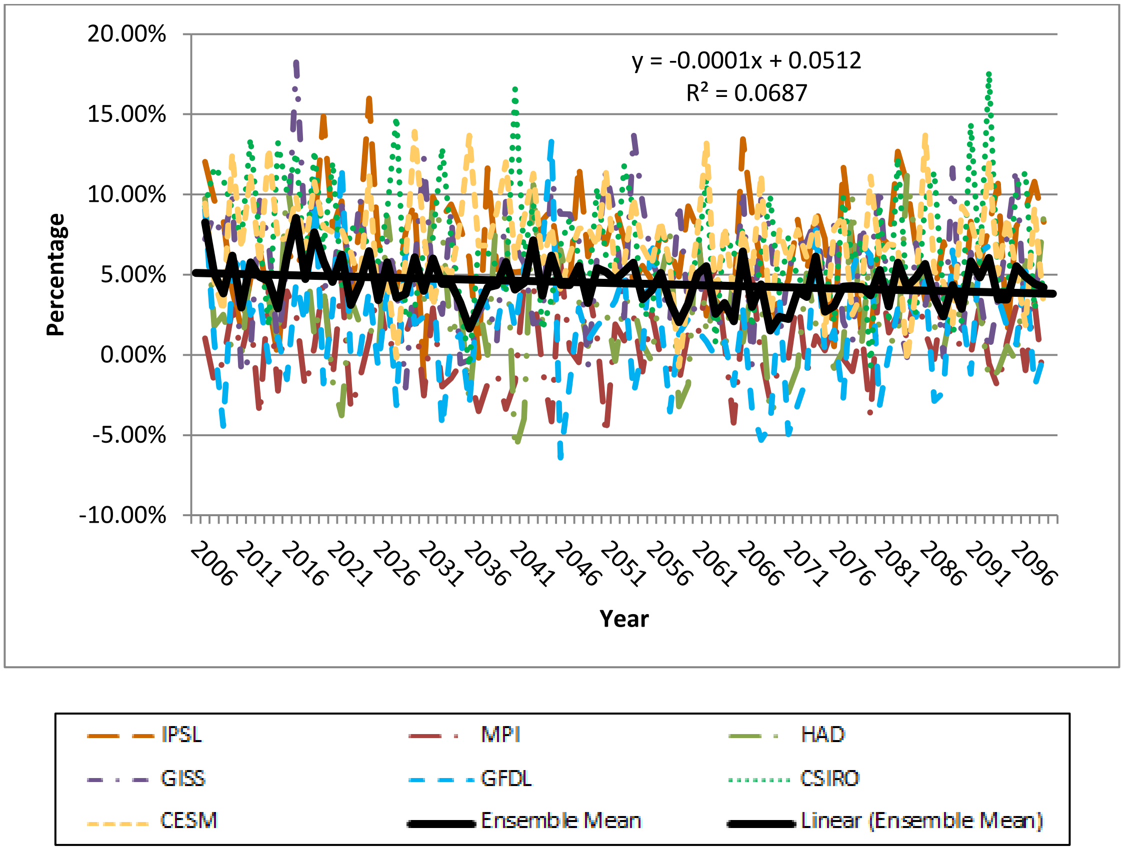

Figure 4.30. Lake-induced belt and non-lake-induced grid cell difference in percentage of precipitation falling as snow, RCP 4.5.

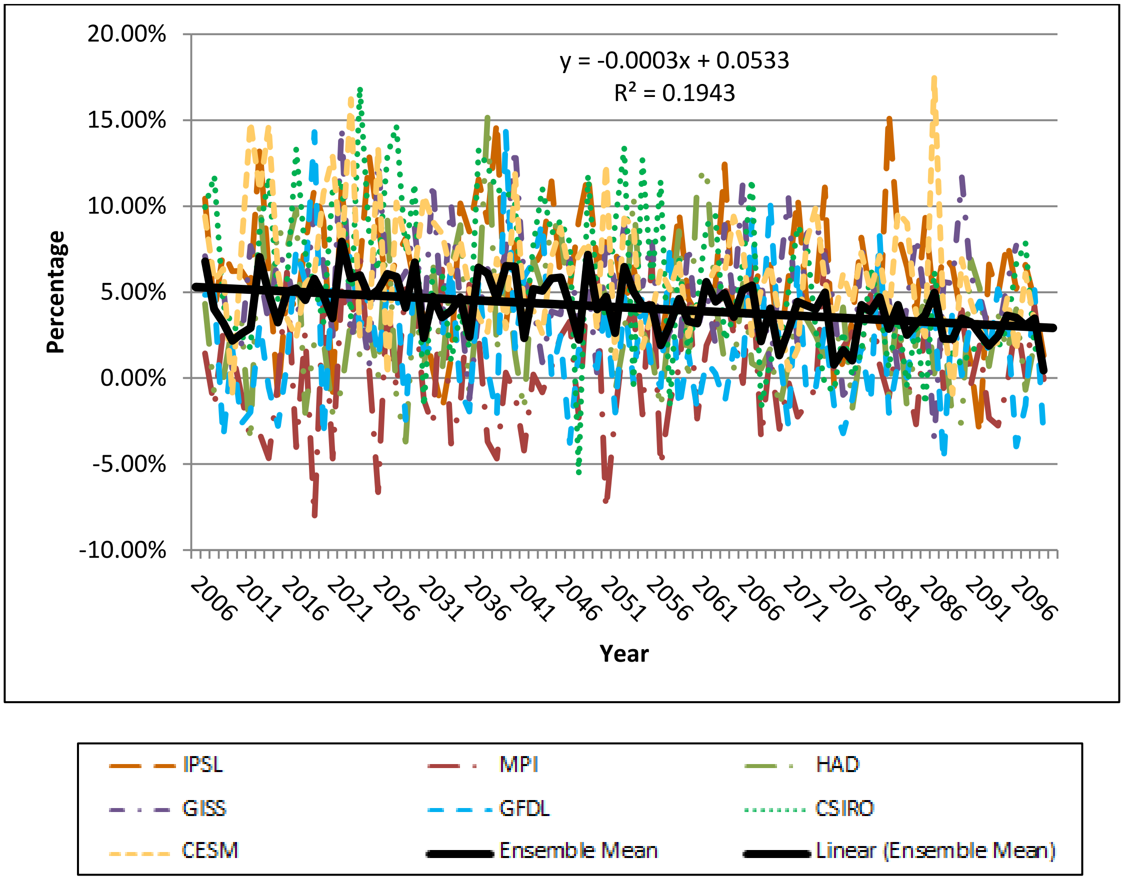

Figure 4.31. Lake-induced belt minus non-lake-induced grid cell difference in percentage of precipitation falling as snow, RCP 8.5.

Chapter 5

CONCLUSIONS

Model simulations of seasonal snowfall were obtained for seven fully coupled GCMs that are a part of the WCRP CMIP5 project. Snowfall simulations are compared to derived snowfall observations using Willmott-Matsuura monthly precipitation and temperature climatologies and Kluver's (2007) gridded snowfall observations. This comparison yielded consistencies between the climatological and simulated snowfall over the region around Lakes Erie and Ontario. While the models do not have the horizontal resolution to adequately simulate lake effect snow processes, the presence of a statistically significant lake-induced snowfall signal is apparent, on the magnitude of 1.6-1.8 cm of SWE for both RCP scenarios examined.

Trends of future snowfall in the region were examined on a seasonal (October – March) basis. Over the 94-year period from 2006-2100, a decrease of 20-45% in snowfall is observed between the two RCPs. In RCP 4.5, a decrease of 16% of snowfall occurs over the first half of the century, followed by a leveling off for the duration of the period for all grid types. Analysis of snowfall in RCP 8.5 however revealed an increase of snowfall of 12% during the first 25 years, followed by a steep 47% decline to the end of the century in the lake-induced grid cells. In the non-lake-induced grid cells, the trends were different in magnitude, with only a 4% increase during the first 25 years, followed by a 43% decrease in snowfall.

To examine the cause of the decline in regional snowfall, comparisons to lapse rates over the lakes, two-meter temperatures, precipitation totals, and snow to precipitation ratios were made. The lake lapse rates were not indicative of snowfall changes due to the failure of the models to correctly simulate observed lake surface and 850 hPa temperatures. Additionally, the averaging of lapse rates over a seasonal period effectively eliminates the potential for strong lapse rates that could be used to confirm the instability needed for lake-induced snowfall. Increased two-meter air temperatures appear to be primarily responsible for changes in snowfall with strong correlations between the two. These temperature changes do not cause a decrease in the total precipitation for the region, and in fact are related to increasing precipitation. Temperature does however result in the decrease of precipitation falling as snow in comparison to total precipitation.

While substantial results were yielded, research that may warrant further investigation can be summarized as follows:

1. Use Principle Components Analysis techniques for the gridded snowfall simulations, to see if similar grid-classifications are present including a specific lake-induced snow belt to the lee of the lakes.
2. Examine the nature of the lake-induced versus non-lake-induced snowfall in each model individually instead of through the ensemble means of all models. This would detail differences due to lake representations more completely, suggesting the best models to use for the representation of lake-induced processes.

3. Running the same analysis but with the inclusion of additional models to see if and how the results are altered.
4. Examine the lapse rates in more detail, both temporally and spatially, for each individual model.

Should the projections of climate models be accurate, changes in the hydroclimatology of the region of this magnitude would have major implications for the regional communities around Lakes Erie and Ontario. While the models do not account for all the physical mechanisms associated with lake effect snowfall, an approximate 1.7 cm of SWE lake-induced signal is present within the GCMs between the lake-induced snowfall belt and the non-lake-induced grid cells. Even if this increase in snowfall is more indicative of lake-induced enhancement of synoptically forced snowfall as opposed to true lake effect, GCMs can be useful as a preliminary tool for examining lake-induced snowfall changes within the lake-induced belt into the future. Additionally, decreases of 20-45% in snowfall depending on the RCP scenario examined will have substantial impacts on water resources and local economies, including impacts in agricultural practices, and in snow related expenses such as snow removal and in property damage.

REFERENCES

Anandhi, A., Frei, A., Pradhanang, S., Zio, M., Pierson, D., Schneiderman, E. (2011). AR4 climate model performance in simulating snow water equivalent over Catskill Mountain watersheds, New York, USA. *Hydrological Processes*. 25: 3302-3311

Assel, R., Cronk, R., Norton, D. (2003). Recent trends in Laurentian Great Lakes ice cover. *Climatic Change*. 57: 185-204

Assel, R. (2005). Classification of annual Great Lakes ice cycles: Winters of 1973-2002. *Journal of Climate*. 18: 4895-4905

Braham, R. and Dungey, M. (1984). Quantitative estimates of the effect of Lake Michigan on snowfall. *Journal of Climate and Applied Meteorology*. 23: 940-949

Burnett, A., Kirby, M., Mullins, H., Patterson, W. (2003). Increasing Great Lake-effect snowfall during the Twentieth Century: a regional response to global warming? *Journal of Climatology*. 16: 3535-3541

Byrd, G., Mestivo, M., Kraaijenbrink, G. (1992). The role of multiple lake interaction in the western New York lake-effect snowstorm of 24-26 November 1991. *Proceedings of the 49th Annual Eastern Snow Conference*. Oswego, NY, USA. Army, CRREL, 125-134

Cehak-Trock, H. (1958). Der feste niederschlag im Atlantischen klimagebiet. *Archives of Meteorological Geophysics. Bioklimatology.* 8B: 352-368

Changnon, S., Changnon, D., Karl, T. (2006). Temporal and spatial characteristics of snowstorms in the contiguous United States. *Journal of Applied Meteorology and Climatology*. 45: 1141-1155

Chuang, H. and Sousounis, P. (2003). The impact of the prevailing synoptic situation on the lake-aggregate effect. *Monthly Weather Review*. 131: 990-1010

Cohen, S., and Allsopp, T. (1988). The potential impacts of a scenario of CO_2-induced climatic change on Ontario, Canada. *Journal of Climate*. 1: 669-681

Collins, M., and Co-Authors. (2013). Long-term Climate Change: Projections, Commitments and Irreversibility. In: Climate Change 2013: The Physical Science Basis. Contribution of Working Group I to the Fifth Assessment Report of the Intergovernmental Panel on Climate Change [Stocker, T.F., D. Qin, G.-K. Plattner, M. Tignor, S.K. Allen, J. Boschung, A. Nauels, Y. Xia, V. Bex and P.M. Midgley (eds.)]. Cambridge University Press, Cambridge, United Kingdom and New York, NY, USA.

Collins, W.J. and Co-Authors. (2008). Evaluation of the HadGEM2 model. Hadley Centre technical note 74. 47pp.

Compo, G., and Co-Authors. (2011). The Twentieth Century Reanalysis Project. *Quarterly Journal of the Royal Meteorological Society.* 137: 1-28

Cox P. M., Betts, R., Bunton, C., Essery, R., Rowntree, R., Smith, J. (1999). The impact of new land surface physics on the GCM simulation of climate and climate sensitivity. *Climate Dynamics*. 15: 183-203

Dewey, K. (1979). An objective forecast method developed for Lake Ontario induced snowfall systems. *Journal of Applied Meteorology*. 18: 787-793

Donner, L., and Co-Authors. (2011). The dynamical core, physical parameterizations, and basic simulation characteristics of the atmospheric component AM3 of the GFDL global coupled model CM3. *Journal of Climate.* 24: 3484-3519

D'Orgeval, T., Polcher, J., de Rosnay, P. (2008). Sensitivity of the West African hydrological cycle in ORCHIDEE to infiltration processes. *Hydrology and Earth System Sciences*. 12: 1387-1401

Ducoudre, N., Laval, K., Perrier, A., (1993). SECHIBA, a new set of parameterizations of the hydrologic exchanges at the land-atmosphere interface within the LMD Atmospheric General Circulation Model. *Journal of Climate*. 6: 248-273

Dufresne, J. and Co-Authors. Manuscript. Climate change projections using the IPSL-CM5 Earth System Model: from CMIP3 to CMIP5. Manuscript. 53pp.

Eichenlaub, V. (1970). Lake effect snowfall to the lee of the Great Lakes: its role in Michigan. *Bulletin of the American Meteorological Society*. 51: 403-412

Eichenlaub, V. (1979). *Weather and Climate of the Great Lakes Region.* University of Notre Dame Press. Notre Dame, IN.

Ellis, A. and Johnson, J. (2004). Hydroclimatic analysis of snowfall trends associated with the North American Great Lakes. *Journal of Hydrometeorology*. 5: 471-486

Essery, R., Best, M., Betts, R., Cox, P., and Taylor, C. (2003). Explicit representation of subgrid heterogeneity in a GCM land-surface scheme *Journal of .Hydrometeorology*. 43: 530-543

Gerbush, M., Kristovich, D., Laird, N. (2008). Mesoscale boundary layer and heat flux variations over pack ice-covered Lake Erie. *Journal of Applied Meteorology and Climatology*. 47: 668-682

Gordon, H. and Co-Authors. (2002). The CSRIO Mk3 Climate System Model. CSRIO Atmospheric Research Technical Paper No. 60.

Gordon, H., O'Farrell, S., Collier, M., Dix, M., Rotstayn, L. Kowalczyk, E., Hirst, T., Watterson, I. (2010). "The CSIRO Mk3.5 Climate Model". CAWCR Technical Report No. 021, pp1-74

Gula, J. and Peltier, W.R. (2012). Dynamical Downscaling over the Great Lakes Basin of North America Using the WRF Regional Climate Models: The Impact of the Great Lakes System on Regional Greenhouse Warming. *Journal of Climate*. 25: 7723-7742

Hill, J. (1971). Snow Squalls in the lee of Lakes Erie and Ontario. NOAA Tech. Memo. NEW ER-43, 20pp.

Hjelmfelt, M. (1990). Numerical study of the influence of environmental conditions on lake effect snowstorms over Lake Michigan. *Monthly Weather Review*. 118: 138-150

Holroyd, E. (1971). Lake-effect cloud bands as seen from weather satellites. *Journal of the Atmospheric Sciences*. 28: 1165-&

Karmosky, C. (2007). Synoptic climatology of snowfall in the Northeastern United States: An analysis of snowfall amounts from diverse synoptic weather types. Master’s Thesis. University of Delaware. Newark, Delaware.

Kluver, D. (2007). Characteristics and trends in North American snowfall from a comprehensive gridded dataset. Master’s Thesis, University of Delaware, Newark, Delaware

Krasting, J., Broccoli, A., Dixon, K., Lanzante, J. (2013). Future changes in Northern Hemisphere snowfall. *Journal of Climate*. 26: 7813-7828

Krinner, G., Viovy, N., de Noblet-Ducoudre, N., Ogee, J., Polcher, J. Friedlingstein, P., Ciais, P., Sitch, S., Prentice, I. A dynamic global vegetation model for studies of the coupled atmosphere-biosphere system. *Global Biogeochemical Cycles*. 19

Kristovich, D., Laird, N., Hjelmfelt, M. (2003). Convective evolution across Lake Michigan during a widespread Lake-Effect snow event. *Monthly Weather Reviews*. 131: 643-655

Kunkel, K., Westcott, N., Kristovich, D. 2002. Assessment of potential effects of climate change on heavy lake-effect snowstorms near Lake Eric. Journal of Great Lakes Research. Vol. 28 (521-536)

Kunkel, K., Ensor, L., Palecki, M., Easterling, D., Robinson, D., Hubbard, K., Redmond, K. (2009). A new look at lake-effect snowfall trends in the Laurentian Great Lakes using a temporally homogeneous data set. *Journal of Great Lakes Research*. 35: 23-29

Lafont, S., Zhao, Y., Calvet, J. Peylin, P., Ciais, P., Maignan, F., Weiss, M. (2012). Modelling LAI, surface water and carbon fluxes at high-resolution over France: comparison of ISBA-A-ga and ORCHIDEE. *Biogeosciences*. 9: 439-56

Leathers, D., Mote, T., Kluck, D., Kuivinen, K., McFeeters, S. (1993). Temporal characteristics of USA snowfall 1945-46 through 1984-85. *International Journal of Climatology*. 13: 65-76

Leathers, D. and Ellis, A. (1996) Synoptic mechanisms associated with snowfall increases to the Lee of Lakes Erie and Ontario. *International Journal of Climatology*. 10: 1117-1135

Legates, D. (1987). A climatology of Global Precipitation. *Publications in Climatology.* 40: 85pp.

Legates, D. and Willmott, C. (1990). Mean Seasonal and spatial variability in gauge-corrected, global precipitation. *International Journal of Climatology.* 10: 111-127

Moore, P, and Orville, R. (1990). Lightning characteristics in lake effect thunderstorms. *Monthly Weather Review*. 118: 1767-1782

Moss, R., and Co-Authors. (2010). The next generation of scenarios for climate change research and assessment. *Nature*. 463: 747-756

Neale, R., and Co-Authors. (2010). Description of the NCAR Community Atmospheric Model (CAM 5.0). NCAR Technical Note 486. 283pp.

Niziol, T. (1989). Some synoptic and mesoscale interactions in a lake effect snowstorm. Postprints, Second National Winter Weather Workshop. Raleigh, NC, NOAA. 260-269

Niziol, T., Snyder, W., Waldstreicher, J. (1995). Winter Weather Forecasting throughout the Eastern United States. Part IV: Lake Effect Snow. *Weather and Forecasting*. 10: 61-77

Norton, D. and Bolsenga, S. (1993). Spatiotemporal trends in Lake Effect and continental snowfall in the Laurentian Great Lakes, 1951-1980. *Journal of Climate*. 6: 1943-1956

Notaro, M., Holman, K., Zarrin, A., Fluck, E., Vavrus, S., Bennington, V. (2013). Influence of the Laurentian Great Lakes on Regional Climate. *Journal of Climate*. 26: 789-804

Olsen, K., and Co-Authors. (2010). Technical Description of version 4.0 of the Community Land Model (CLM). NCAR Technical Note 478. 266pp.

Orlanski, L. (1975). A rational subdivision of scales for atmospheric processes. *Bulletin of the American Meteorological Society*. 56: 527-530

Rawlins, M., Willmott, C., Shiklomanov, A., Linder, E., Frolking, S., Lammers, R., Vorosmarty, C. (2006). Evaluation of trends in derived snowfall and rainfall across Eurasia and linkages with discharge to the Arctic Ocean. *Geophysical Research Letters*. 33, L07403

Roeckner, E., and Co-Authors. (2003). The atmospheric general circulation model ECHAM5: Part I, Model Description. Max-Planck_Institut fur Meteorologie Report No. 349. 120pp.

Schmidlin, T. (1993). Impacts of severe winter weather during December 1989 in the Lake Erie snowbelt. *Journal of Climate*. 6: 759-767

Schmidt, G., and Co-Authors. (2014). Configuration and assessment of the GISS ModelE2 contributions to the CMIP5 archive. *Journal of Advances in Modeling Earth Systems*. ISSN: 1942-2466, Early View Publication

Scott, R. and Huff, F. (1996). Impacts of the Great Lakes on regional climate conditions. *Journal of Great Lakes Research*. 22: 845-863

Shepard, D. (1968) A two-dimensional Interpolation function for irregularly-spaced Data. *Proceedings of the 1968 ACM National Conference*, 517-523

Stocker, T., and Co-Authors. (2013) Technical Summary. In: Climate Change 2013: The Physical Science Basis. Contribution of Working Group I to the Fifth Assessment Report of the Intergovernmental Panel on Climate Change [Stocker, T.F., D. Qin, G.-K. Plattner, M. Tignor, S.K. Allen, J. Boschung, A. Nauels, Y. Xia, V. Bex and P.M. Midgley (eds.)]. Cambridge University Press, Cambridge, United Kingdom and New York, NY, USA.

Tardy, A. (2000). *Lake Effect and Lake Enhanced Snow in the Champlain Valley of Vermont*. National Weather Service Eastern Region Technical Attachment No. 2000-05

Taylor, K., Stouffer, R., Meehl, G. (2012). An overview of CMIP5 and the experimental design. *Bulletin of the American Meteorological Society*. 93: 485-498

"Topics in Lake Effect Snow Forecasting." COMET/UCAR. 2005. [http://meted.ucar.edu/norlat/snow/lake_effect]

Trumpickas, J., Shuter, B., Minns, C. (2009). Forecasting impacts of climate change on Great Lakes surface water temperatures. *Journal of Great Lakes Research*. 35: 454-463

Willmott, C. J., C. M. Rowe and W. D. Philpot (1985). Small-Scale Climate Maps: A Sensitivity Analysis of Some Common Assumptions Associated with Grid-point Interpolation and Contouring. *American Cartographer*. 12: 5-16

Willmott, C.J. and K. Matsuura, cited 2014a, Terrestrial Air Temperature: 1900-2010 Gridded Monthly Time Series (Version 3.01). http://climate.geog.udel.edu/~climate/html_pages/Global2011/README.GlobalTsT2011.html

Willmott, C.J. and K. Matsuura, cited 2014b, Terrestrial Precipitation: 1900-2010 Gridded Monthly Time Series (Version 3.01). http://climate.geog.udel.edu/~climate/html_pages/Global2011/README.GlobalTsP2011.html

Wright, D., Posselt, D., Steiner, A. (2013). Sensitivity of lake-effect snowfall to lake ice cover and temperature in the Great Lakes region. *Monthly Weather Review*. 141: 670-689